UDK 66:54(05) CODEN HMIDA 8 ISSN 0367–598X

1

Hemijska industrija

Vol. 80

Časopis Saveza hemijskih inženjera Srbije

Chemical Industry

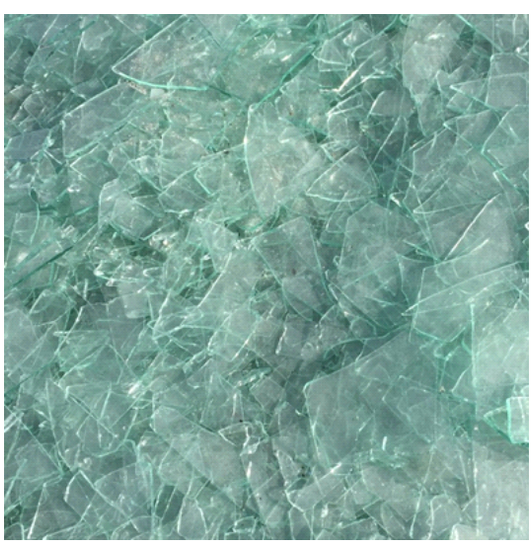

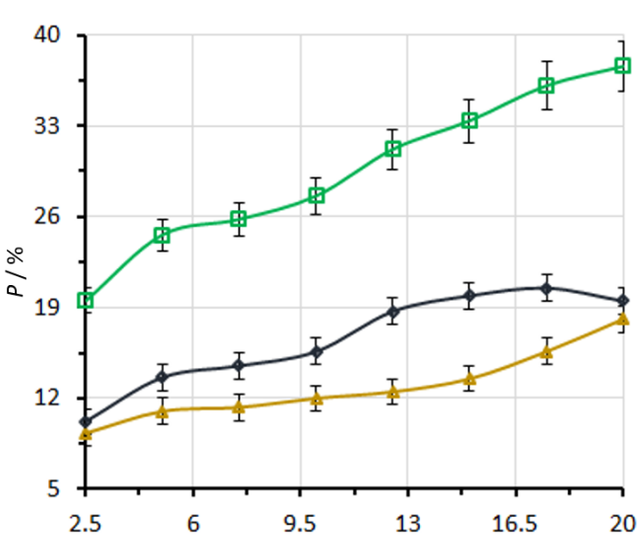

BEOGRAD, JANUAR-MART 2026. HMIDA 8, 80(1) 1-70 (2026)

Aktivnosti Saveza hemijskih inženjera Srbije pomažu:

**MINISTARSTVO NAUKE,
TEHNOLOŠKOG RAZVOJA
I INOVACIJA
REPUBLIKE SRBIJE**

Tehnološko-metalurški fakultet
Univerziteta u Beogradu

Prirodno-matematički fakultet
Univerziteta u Novom Sadu

Tehnološki fakultet
Univerziteta u Novom Sadu

Fakultet tehničkih nauka
Univerziteta u Novom Sadu

Tehnološki fakultet
Univerziteta u Nišu, Leskovac

Institut IMS, Beograd

DCP HEMIGAL
Leskovac

Barič

Elixir Prahovo

VICTORIAOIL
Šid

Chemical Industry
Химическая промышленность

Hemijska industrija

Časopis Saveza hemijskih inženjera Srbije
Journal of the Association of Chemical Engineers of Serbia
Журнал Союза химических инженеров Сербии

VOL. 80 **Beograd, januar – mart 2026.** **Broj 1**

Izdavač
Savez hemijskih inženjera Srbije
Beograd, Kneza Miloša 9/I

Glavni urednik
Bojana Obradović

Zamenica glavnog i odgovornog urednika
Emila Živković

Pomoćnik glavnog i odgovornog urednika
Ivana Drvenica

Urednici
Jelena Bajat, Dejan Bezbradica, Ivana Banković-Ilić, Dušan Mijin, Marija Nikolić, Đorđe Veljović, Tatjana Volkov-Husović

Članovi uredništva
Nikolaj Ostrovski, Milorad Cakić, Željko Čupić, Miodrag Lazić, Slobodan Petrović, Milovan Purenović, Aleksandar Spasić, Dragoslav Stoiljković, Radmila Šećerov-Sokolović, Slobodan Šerbanović, Nikola Nikačević, Svetomir Milojević

Članovi uredništva iz inostranstva
Dragomir Bukur (SAD), Jiri Hanika (Češka Republika), Valerij Meshalkin (Rusija), Ljubiša Radović (SAD), Constantinos Vayenas (Grčka)

Likovno-grafičko rešenje naslovne strane
Milan Jovanović

Redakcija
11000 Beograd, Kneza Miloša 9/I
Tel/fax: 011/3240-018
E-pošta: shi@ache.org.rs
www.ache.org.rs

Izlazi kvartalno, rukopisi se ne vraćaju

Za izdavača: Ivana T. Drvenica

Sekretar redakcije: Ksenija Kostić

Izdavanje časopisa pomaže
Republika Srbija, Ministarstvo nauke, tehnološkog razvoja i inovacija

Uplata pretplate i oglasnog prostora vrši se na tekući račun Saveza hemijskih inženjera Srbije, Beograd, broj 205-2172-71, NLB Komercijalna banka a.d., Beograd

Menadžer časopisa i kompjuterska priprema
Aleksandar Dekanski

Štampa
Razvojno-istraživački centar grafičkog inženjerstva, Tehnološko-metalurški fakultet, Univerzitet u Beogradu, Karnegijeva 4, 11000 Beograd

Indeksiranje
Radovi koji se publikuju u časopisu *Hemijska Industrija* ideksiraju se preko *Web of Science (WoS)®* servisa *Science Citation Index - Expanded™* i *Journal Citation Report (JCR)*

SADRŽAJ/CONTENTS

Numerical analysis of flow within a packed bed using computational fluid dynamics: Effects of fluid nature and regime

Soufyane Ladeg[1,2] and Nadji Moulai-Mostefa[2]

[1]FST, University of Tissemsilt, Tissemsilt, Algeria
[2]LME, University of Medea, Medea, Algeria

Abstract

This research conducts a computational fluid dynamics (CFD) analysis comparing laminar and k-epsilon turbulent models of fluid flow through a packed bed. For this, three types of fluids (water, water vapor and carbon dioxide) were examined. The CFD model was initially juxtaposed with two experimental ones reported in the literature. It was observed that the numerical model used was in reasonable agreement with the experimental data reported in literature, provided that the packed bed dimensions (column diameter and height, grain size) aligned with those used experimentally. Thus, a decrease in pressure in descending order was noticed for the three fluids studied for both regimes from the column top to the outlet. In addition, a thorough characterization of turbulence was conducted, including determination of turbulent kinetic energy (TKE) and turbulent eddy dissipation (TED). As a result, a rapid dissipation of TKE for water was observed compared to the other two fluids, where TKE decreased progressively along the column length. In contrast, the TED for water decreases gradually until the exit of the column, while for both gaseous fluids, it increases slowly along the column length. The analysis of the vapor flow included testing of two density models, namely the constant density and the Peng-Robinson model. It was observed that the PR model for vapor properties showed similar trends of TKE and TED as those predicted for carbon dioxide.

Keywords: Fixed bed, flow pattern, turbulence, modelling.

Available on-line at the Journal web address: http://www.ache.org.rs/HI/

ORIGINAL SCIENTIFIC PAPER

UDC: 544.272:551.509.313.1

Hem. Ind. **80(1)** 1-12 (2026)

1. INTRODUCTION

Due to the diminishing oil reservoirs and the completion of initial and subsequent life cycles of existing reserves, enhanced oil recovery (EOR) techniques have become crucial. Extracting oil from petroleum reservoirs in the second stage is achieved by injecting water or gas into the reservoirs [1,2]. Thus, studies of the flow of different fluids in porous soil, catalytic refining, and membrane filtration are parts of a very wide field of research [3,4].

Theory for studying single-phase laminar flow of fluids through a porous medium is based on Darcy's experiments [5]. However, its quantitative description is very complex; it moves from a saturated environment to an unsaturated one due to variations in the fluid state during flow [6,7]. There are, thus, complex relationships between the different flow parameters. Consequently, the formulation and solution of unsaturated flow problems require general analysis methods based on experimental approaches and modeling of the test results [8]. Understanding the physical phenomena linked to single- or two-phase flows at such small scales is fundamental. Indeed, interfacial phenomena and the role of intermolecular edges are still poorly understood [9]. Depending on the practical situation considered, there may exist two-phase liquid-liquid or liquid-gas flows, or even in some cases, three-phase fluid flows (liquid-liquid-gas) [10,11]. In each case, pressure loss is an important parameter to characterize the energy necessary for circulation of these fluids in a pore space. Direct measurements are difficult because experimental studies of transport mechanisms in porous media are expensive and exhibit low levels of spatial and temporal resolution. In recent years, researchers have employed numerical simulations to solve or unveil the phenomena governing the flow of fluids through a porous medium [12,13]. In this sense, computational fluid dynamics (CFD) provides possibilities to

Corresponding author: Soufiane Ladeg, Science and Technology Department, University of Tissemsilt, Tissemsilt, Algeria
E-mail: soufiane.ladeg@univ-tissemsilt.dz; https://orcid.org/0000-0003-1133-827X
Co-author: Nadji Moulai-Mostefa https://orcid.org/0000-0003-2263-025X

Paper received: 16 March 2025; Paper accepted: 21 December 2025; Paper published: 13. January 2026.
https://doi.org/10.2298/HEMIND250316001L

systematically reduce trials, integrate new functionalities, and optimize process time and calculation methods [14]. Additionally, it enables prediction of anomalies [15-17].

Several models were proposed to predict physical properties that governed the behavior of the fluid flow through a packed bed. A 3D two-phase flow transient Eulerian-Eulerian model was developed to evaluate liquid dispersion in a study of structured packing for gas-liquid reactions [18]. It was reported that elevating the inlet velocity results in broader dispersion of liquid. This implies that employing multiple liquid inlets, as opposed to a single one, caused an escalation in liquid hold-up. On the other hand, Wang *et al.* [19] conducted a study on hydrodynamic characteristics of a packed column using structured sinusoidal corrugated sheet packings. Their simulation study contributes to the evaluation and optimization of multiphase flow characteristics and the mass transfer performance of packed columns. CFD was used to evaluate axial dispersion properties of a fixed-bed reactor with various packed configurations with the aim To obtain the optimum design and scaling up of reactors with porous packed structures [20]., Also, direct numerical simulations (DEM-OpenFOAM workflow) was used to predict the accurate axial Peclet numbers and assess dispersion of single laminar phase flow in small fixed-bed reactors [21]. Pashchenko *et al.* [22] studied how a fluid moves in a fixed-bed reactor filled with porous particles by using both experiments and computer simulations. Their findings indicated that the flow through the porous medium of particles is minimal if the pore size is less than 0.5 mm, while it appears at the larger pore sizes. A comprehensive two-dimensional (2D) model was developed to simulate flow behavior in a fixed-bed reactor for production of olefins [23]. The model incorporated an exponential-function kinetic model, based on a lumped-species reaction scheme, into a commercial CFD code using user-defined functions. The simulation results demonstrated a close relationship between methanol conversion and catalytic deactivation, highlighting the significant influence of the operating conditions. In another study [24] a new wire gauze structured packing (PACK-2100) was found to improve mass transfer efficiency. These experiments and simulations showed better height equivalent to a theoretical plate value than conventional packings. DEM-CFD simulations were also used to study fluid flow and residence time distribution (RTD) in randomly packed beds [25] demonstrating that simulations could reliably replace some physical experiments.

The principal aim of the present research was to examine the hydrodynamic behavior of fluid flow through a packed bed using CFD. This study specifically concentrates on evaluating the pressure drop, kinetic energy dissipation, and turbulence characteristics associated with several fluid types *i.e*. water, water vapor, and CO_2. These fluids were chosen due to their prevalent applications in EOR, in-situ soil remediation, and diverse filtration processes. By offering comprehensive insights into flow dynamics within packed beds, this research seeks to enhance optimization of industrial operations through a more profound understanding of fluid behavior at the pore scale.

2. THEORY

2. 1. Mathematical formulations

Pressure drop as a process driving force is frequently employed in industry as a criterion because it is simple to measure in practice and depends on the fluid's velocity gradient [26]. However, this criterion does not enable local identification of the system regions with the greatest energy loss; it only indicates the system's total energy degradation. Ergun's equation presented by Eq. (1) is commonly used to model the pressure drop of a fluid flowing through a packed bed [27,28] and can be used for both liquids and gases. The first term of the equation corresponds to the Blake-Kozeny equation for laminar flow, while the second term corresponds to the Burke-Plummer Equation (1) for turbulent flow [29].

$$\frac{|\Delta P|}{L} = \frac{150\mu(1-\varepsilon)^2}{d_p{}^2\varepsilon^3}u_0 + \frac{1.75\rho(1-\varepsilon)^2}{d_p\varepsilon^3}u_0{}^2 \quad (1)$$

where ΔP is the pressure drop over the bed depth or length L, μ is the dynamic viscosity of the fluid, d_p is the mean particle diameter, ε is the void fraction and u_0 is the linear velocity related to the empty cross-section of the column.

The Darcy equation, also used for flows through porous media, is homogenous with the Blake-Kozeny equation for laminar flows. To determine the flow regime within the porous media, the Reynolds number is generally used in the form shown in Equation (2) [30].

$$\mathrm{Re} = \frac{\rho d_p u_{in}}{\mu(1-\varepsilon)} \quad (2)$$

where u_{in} is the interstitial velocity and ρ is the density of the fluid. The interstitial velocity is obtained by using the Dupuit-Forchheimer hypothesis, Equation (3), [31]:

$$u_{in} = \frac{u_0}{\varepsilon} \quad (3)$$

Consequently, Equaton (2) can be written as Equation (4):

$$\mathrm{Re} = \frac{\rho d_p u_0}{\varepsilon\mu(1-\varepsilon)} \quad (4)$$

Experimental results demonstrated that the non-Darcy flow occurs at Re = 10 to 1000 in unconsolidated porous media and at Re = 0.4 to 3 in weakly consolidated rocks, according to the Chilton and Colburn's definition of the Reynolds number [30]. The inertial loss coefficient (α) can be evaluated by Equation (5) [32]:

$$\alpha = \frac{d_p{}^2 \varepsilon^3}{150(1-\varepsilon)^2} \quad (5)$$

Moreover, the inertial resistance coefficient (C_2) is obtained by using Equation (6) [32]:

$$C_2 = \frac{3.5(1-\varepsilon)}{d_p \varepsilon^3} \quad (6)$$

In the CFD model, the viscous resistance coefficient ($(1/\alpha)$ / m^{-2}) and the inertial resistance coefficient (C_2 / m^{-1}) are specified in each direction of the packed bed. According to previous work [33], the average particle diameter and porosity of a sand bed are d_p= 0.238 mm and ε = 0.4, respectively.

2. 2. Flow regime

Fluid simulation software ANSYS Fluent (ANSYS Inc., USA) provides powerful turbulence models, such as the Reynolds-averaged Navier-Stokes (RANS) equations coupled with turbulence models like the k-epsilon or k-omega models, to accurately simulate and analyze turbulent flows [34]. In the present study, the k-epsilon model was utilized. Laminar flow is smooth and orderly, with predictable patterns and well-defined streamlines. Therefore, the appropriate flow regime depends on the application and desired accuracy level. Turbulent flow simulations capture complex phenomena like flow separation, turbulence-induced mixing, and pressure losses, while laminar flow simulations are suitable for smooth and predictable situations. Consequently, by modeling and analyzing flow regimes, engineers and researchers can gain valuable insights into fluid behavior, identify potential instabilities, and optimize designs to enhance efficiency and performance.

2. 3. Mesh and geometry

The laboratory column, shown in Figure 1, is cylindrical (150 mm in length, 25 mm in diameter), and a corresponding 3-D cylindrical shape was created in the ANSYS Fluent interface. As a result, a well-structured mesh (hexahedral dominant meshes) is obtained with cell refinements using the ANSYS-FLUENT workbench. The meshing process involves discretizing the domain into small, interconnected elements that accurately represent the geometry and capture the flow physics. A structured mesh is advantageous as it offers several benefits. Firstly, it provides better control over element size and distribution, allowing for a more precise representation of the geometry and flow characteristics [35].

Also, a structured mesh typically requires fewer elements compared to an unstructured mesh to achieve a similar level of accuracy. To gain time in finding the meshing solution, a structural mesh with 997470 elements and 1032914 nodes was selected (Table 1). It was clearly noticed that up to those numbers of nodes and mesh elements, the pressure drop remained constant, indicating stability of the solution for mesh variations. Furthermore, the same number of elements and nodes was used in several reported studies [15,36]. In addition, a mesh of 100,000 elements is considered as a coarse mesh, while that with more than 500,000 elements is a fine mesh.

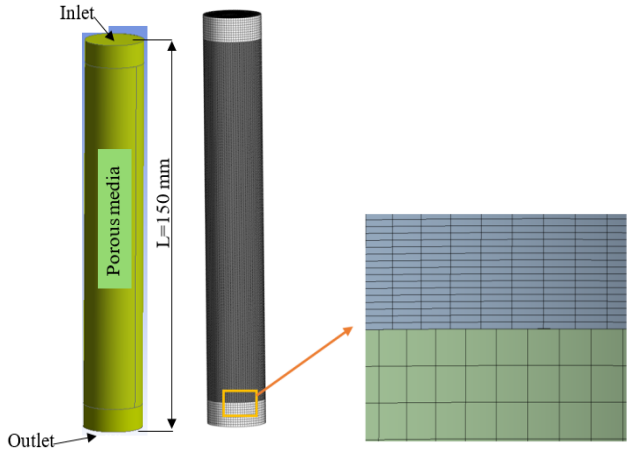

Figure 1. *Column representation showing dimensions and CFD model with meshing*

Table 1. *Mesh variation study versus pressure drop*

Run	Number of nodes	Number of mesh elements	Pressure drop, Pa
1	1032914	997470	$2.34\ 10^4$
2	1053320	1013243	$2.34\ 10^4$
3	1344520	1299180	$2.34\ 10^4$
4	2227284	2165076	$2.34\ 10^4$

The numerical solution was carried out using a pressure-based solver in ANSYS Fluent, with the simple algorithm employed for pressure-velocity coupling. For this, a second-order upwind discretization was applied to the momentum equations to enhance the accuracy of the results. Furthermore, the convergence was ensured by setting a residual tolerance of 10^{-6} and by verifying the stability and consistency of key flow parameters throughout the domain.

3. RESULTS AND DISCUSSION

3. 1. Pressure drop variation

Figure 2 compares CFD modeling results and experimental data from the literature [37,38] on pressure variation *versus* velocity. The values obtained by CFD for velocities lower or equal to 0.04 m s^{-1} are very close to the experimental results of Yang *et al.* [37]. However, for higher velocity values, there is little deviation. On the other hand, the experimental results of Erdim *et al.* [38] are well below the values predicted by CFD almost in the whole velocity range. This can be explained by the differences in column dimensions and particle sizes.

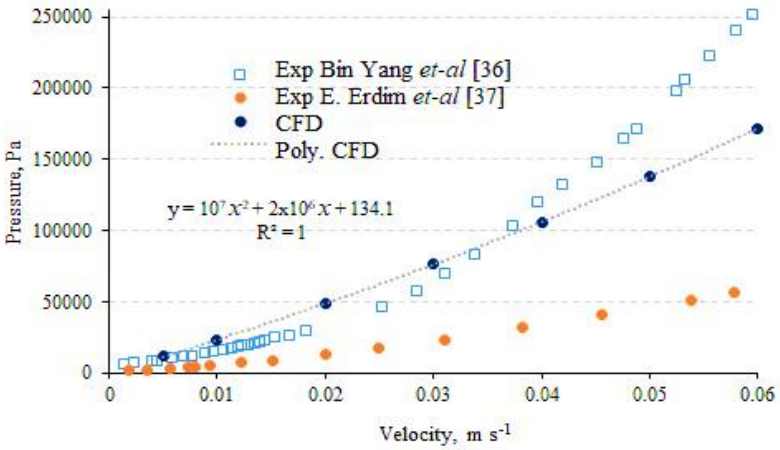

Figure 2. *Pressure vs. velocity values (symbols) obtained experimentally and by CFD modeling; line represents the best polynomial fit of the CFD data given by the presented equation; experimental data are reprinted with permission from Yang et al. [37] for 6 mm particles and 0.4 bed porosity and Edim et al. [38] for 1.18 mm glass spheres and 0.377 bed porosity*

In the first study [37], the authors used dimensions similar to the CFD model: 200 mm long column, 40 mm in diameter, with a particle diameter of 6 mm and the porosity of 0.4 . In contrast, in the second study [38] the column was 2000 mm in height and 40.14 mm in diameter, while the size of glass spheres used for the data shown in Figure 2 was 1.18 mm with the bed porosity of 0.377. Thus, the interpretation of the results indicates a relatively good agreement between CFD and experimental results at low velocities, while considerable discrepancies are observed at higher velocities due to different columns and particle dimensions. However, regardless of whether the results are obtained experimentally or through CFD simulations, the essential feature is the parabolic shape of the curve observed in all cases.

Figure 3 presents the pressure variation along the column for the three fluids. The pressure profiles across the packing are nearly linear for all fluid types. It is discernible that, at the velocity of 0.01 m s^{-1} at laminar flow conditions, due to the resistance of the porous media, there is a significant pressure drop from the top to the bottom [39]. The CFD outcomes were juxtaposed with the projections derived from the theoretical model, embodied by the Ergun equation for the laminar segment. As observed, a reasonable concurrence exists between the anticipated values from both CFD and the theoretical model. In essence, despite disparities observed in the analytical model concerning water, CO_2, and water vapor, a well-constructed mesh in the CFD model adeptly correlates with the theoretical model under laminar flow conditions. The analytical model closely corresponds with the CFD model for water while displaying a minor deviation for CO_2 and vapor. Discrepancy can be effectively resolved by adjusting the density of the modeled fluids.

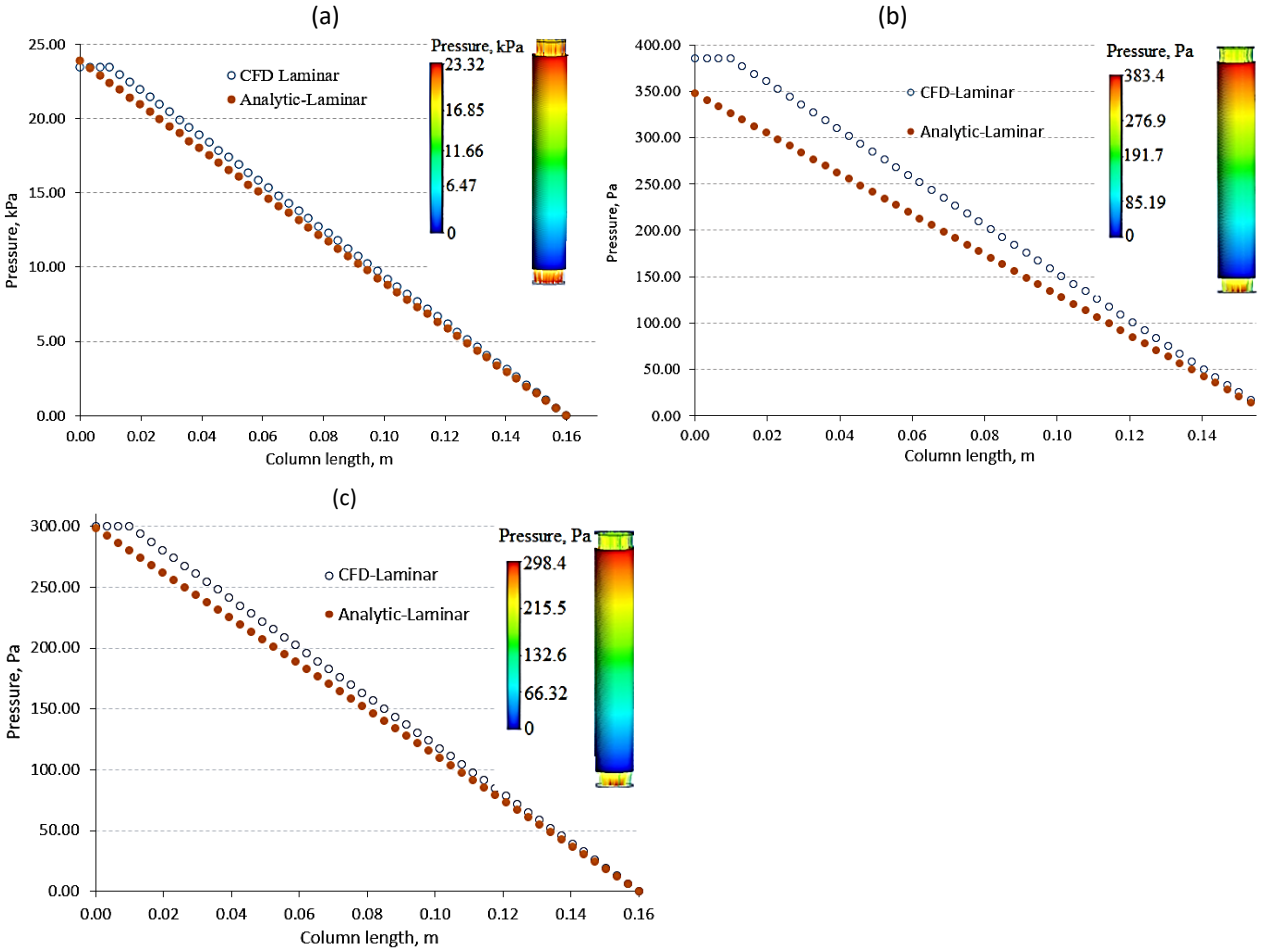

Figure 3. *Pressure variation of (a) water liquid, (b) CO_2, and (c) water vapor flowing through the cylindrical column for a velocity of* 0.01 m s^{-1}

Figure 4 illustrates the distinction in water pressure variations along the column length between laminar flow (inlet velocity of 0.01 m s^{-1}) and turbulent flow regime (inlet velocity of 0.3 m s^{-1}). In the turbulent regime, the CFD model predictions deviated somewhat from the second theoretical term of the Blake-Kozeny equation (analytical solution).

This finding was supported in literature [40] reporting a significant divergence between the numerical and experimental results when compared to empirical correlations in the turbulent regime. The notably higher pressure experienced during turbulent flow, as opposed to laminar flow, signifies that turbulent flow encounters greater resistance and obstruction as water traverses through the system. Conversely, the lower pressure in laminar flow indicates smoother water movement with reduced resistance and obstruction compared to turbulent flow. This is a well-known characteristic of the laminar regime as regular and uniform fluid motion results in a decreased momentum transfer and consequently a lower pressure. The incongruity between the theoretical model for turbulent flow and CFD outcomes suggests potential disparities or constraints within the model's assumptions. Turbulent flows entail intricate phenomena such as turbulent eddies, vortex shedding, and other complex fluid behaviors, which can pose challenges in accurately capturing them within a theoretical framework. Conversely, CFD simulations employ robust numerical techniques to solve governing equations, offering more detailed and realistic portrayals of turbulent flows. The disparity between the theoretical model for turbulence and CFD model implies potential refinements that may be necessary in the theoretical model's formulation to align with empirical observations.

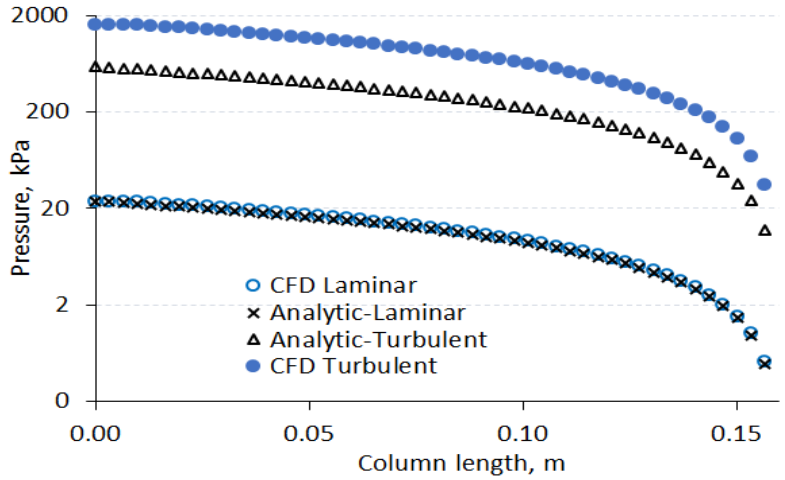

Figure 4. *Comparison of pressure variations in a logarithmic scale over the column length for water flow in laminar and turbulent regimes (inlet velocities 0.1 and 0.3 m* s^{-1}*, respectively) predicted by CFD modeling and analytical solutions*

Figure 5 illustrates the pressure variation along the column length for different fluids. Water exhibits a higher pressure compared to CO_2 and vapor, while CO_2 demonstrates a higher pressure than vapor. The increased pressure experienced by water as compared to gases is expected. Factors such as water's viscosity, density, and interaction with the packing material play significant roles in contributing to this elevated pressure.

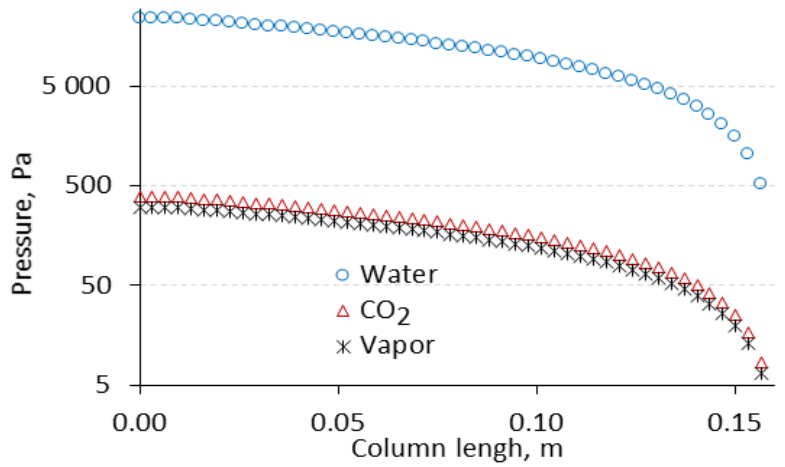

Figure 5. *Comparison of pressure variation in the laminar regime*

In contrast, the pressure for CO_2 is lower than that for water but higher than that for vapor, which registers the lowest pressure among the three fluids examined. Vapor's attributes, including lower viscosity, density, and compressibility, contribute to this diminished pressure. These outcomes underscore distinct flow characteristics and levels of resistance encountered by each fluid within the packed bed column.

3. 2. Turbulent kinetic energy evolution

The Peng-Robinson (PR) equation of state is a widely used thermodynamic model for describing fluid behavior as a function of pressure, volume and temperature, particularly in chemical and petroleum engineering. It offers significantly improved accuracy over the van der Waals equation for predicting the properties of gases and liquids such as nitrogen, carbon dioxide, and hydrocarbons. Because of its reliability and computational efficiency, PR equation is commonly applied to phase equilibrium calculations and prediction of interfacial properties [41].

Figure 6 presents the variation of turbulent kinetic energy (TKE) along the column for three different fluid models: ideal gas, real gas, and a simplified constant-density/viscosity (CD) gas model. The evolution of TKE offers critical insight into how turbulence responds to differences in fluid properties and modeling assumptions. In the initial region of the column, approximately the first third, all three models display similar TKE magnitudes. This convergence suggests that at the early stage of flow development, turbulence is not significantly influenced by thermodynamic property variations. In this zone, velocity gradients, pressure drops, and thermal effects are still moderate, resulting in comparable flow conditions across the models. As the vapor proceeds downstream, clear divergences emerge. In the CD model, a sharp increase in TKE is observed near z = 0.06 m. This spike stems from the oversimplified assumption of constant density and viscosity, which fails to capture the damping effects of compressibility and temperature-dependent viscosity.

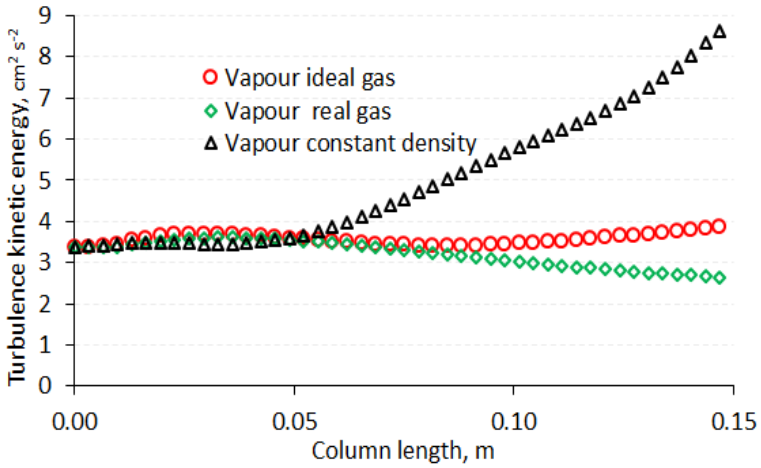

Figure 6. *Turbulent kinetic energy variations in the turbulent regime along the column length for 3 vapor models: ideal gas, real gas, and a constant-density/viscosity (CD) gas*

As a result, the model artificially sustains higher turbulence levels in response to accelerating flow, exaggerating local energy fluctuations. In contrast, the real gas model shows a gradual decrease in TKE toward the column outlet. This behavior reflects the realistic treatment of fluid properties, particularly the pressure-dependent viscosity and density. As pressure drops along the column, the fluid becomes less dense and more viscous, enhancing viscous dissipation and thus reducing turbulent intensity. This highlights the real gas model's ability to capture energy loss mechanisms more faithfully. The ideal gas model presents an intermediate behavior, maintaining relatively stable TKE values along most of the column length. A slight increase near the outlet can be attributed to mild compressibility effects and increased velocity gradients in that region. However, since this model does not account for intermolecular interactions, it underestimates both dissipative and amplifying mechanisms in turbulent transport. In conclusion, a fluid that experiences energy loss during flow is the most physically realistic scenario. Consequently, the PR model emerges as the most appropriate model for simulating real gas behavior. This final result highlights the importance of the PR model, making it the most suitable and reliable among the models considered.

Figure 7 depicts the TKE variation for the three modeled fluids in a turbulent regime along the column length. The TKE is in the following ascending order: vapor>CO_2> water. In the case of water, the TKE exhibits a progressive decline until it reaches the outlet of the column. For CO_2, TKE initially decreases slowly. However, at a column length of 0.035 m, it begins to decrease rapidly until it exits the column. In contrast, the pattern of TKE variation for vapor is markedly different. It resembles the behavior of CO_2 up to a column length of 0.015 m at the inlet, after which TKE experiences a significant increase, attaining elevated values by 0.035 m column length, before subsequently declining progressively until reaching the outlet.

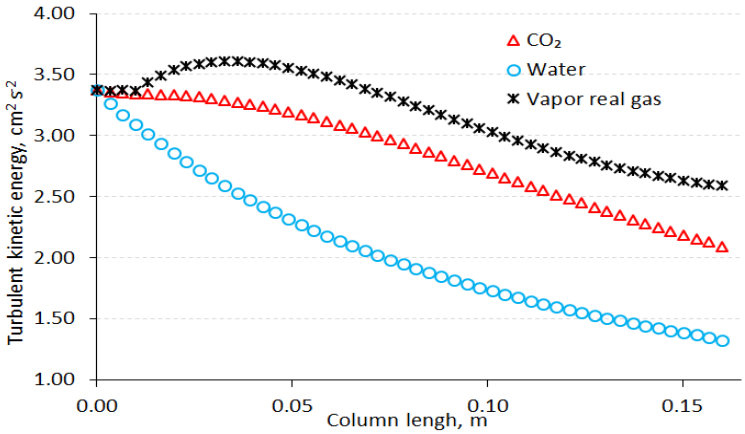

Figure 7.*Turbulent kinetic energy variations along the column length in turbulent flow regime for water, CO_2 and water vapor modeled as a real gas*

3. 3. Evolution of turbulent eddy dissipation

Variations of turbulent eddy dissipation (TED) along the column length for water, water vapor, and CO_2 are shown in Figure 8. A clear disparity in TED behavior is observed among the three fluids. Water exhibits the highest initial TED, which gradually declines along the column, reaching its lowest value at the outlet. This decreasing trend suggests a gradual attenuation of turbulence as the kinetic energy is dissipated through the densely packed porous medium. The high TED at the inlet can be attributed to water's relatively high density and viscosity, which promote stronger inertial forces and shear-induced turbulence as the fluid impinges on the solid matrix. In contrast, both vapor and CO_2 start with lower TED values that progressively increase along the column. These trends, while initially counterintuitive, can be mechanistically linked to the distinct thermophysical properties of each fluid. For vapor, the increase in TED may arise from compressibility effects and potential phase instability under pressure drop. As vapor moves through the packed bed, local pressure drops can induce partial condensation or oscillations around saturation conditions, leading to localized density gradients and transient two-phase regions. These dynamic fluctuations can enhance shear and promote eddy formation, contributing to higher energy dissipation downstream. Additionally, the release or absorption of latent heat during phase change may alter local temperature gradients, reinforcing turbulence through buoyancy-driven instabilities.

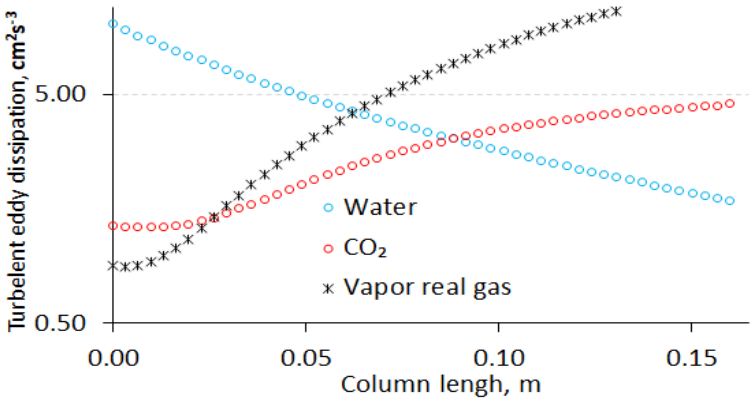

Figure 8. *TED predictions along the column length in turbulent flow regime for water, CO_2 and water vapor modeled as a real gas*

For CO_2, the gradual rise in TED along the column may be attributed to its transition toward or within the supercritical regime [42]. Supercritical CO_2 exhibits a sharp variation in key transport and thermodynamic properties such as density, specific heat capacity, and viscosity near its pseudo-critical point [43]. These elements can increase turbulence intensity by destabilizing the flow and enhancing scalar mixing. In particular, the combination of gas-like diffusivity and liquid-like density promotes efficient momentum and mass transfer, supporting the formation of eddies deeper in the column. However, the manifestation of supercritical or pseudo-critical effects strongly depends on the proximity of the operating conditions to the critical point. In the present study, the pressure distribution along the porous column shows a continuous decrease, which remains several orders of magnitude below the critical pressure of CO_2 [42,43]. Under such conditions, sharp pseudo-critical variations in thermophysical properties are not expected to be activated within the flow domain. Accordingly, the observed gradual increase in TED is more consistently explained by hydrodynamically driven mechanisms inherent to flow through porous media. As pressure decreases along the porous column due to flow resistance, CO_2 behaves as a compressible fluid. Consequently, the associated density reduction combined with pore-scale constrictions, increases the local flow velocity gradients, thereby accelerating the transfer of turbulent kinetic energy to smaller scales, which results in a smooth downstream increase in TED [44]. As a result, the initially lower TED for CO_2 may stem from its relatively low inlet density and viscosity compared to water, resulting in reduced inertial forces and weaker initial turbulence.

Overall, the TED profiles highlight how each fluid's turbulence dissipation behavior is governed by its dominant hydrodynamic characteristics within the porous medium, including momentum exchange in water, phase change induced flow variability in vapor, and compressibility-driven velocity gradients in CO_2.

4. CONCLUSION

Studies using CFD to analyze the movement of water and gases within a packed bed offer significant advantages in understanding flow dynamics, refining design variables, and improving overall system efficiency, depending on the prevailing flow conditions. In laminar flow, water exhibits a relatively constant and organized flow pattern as it passes through the packed bed. This behavior is characterized by a significant increase in pressure, increased turbulence, and maximum energy dissipation. However, CO_2 and steam exhibit relatively lower pressure in both regimes. The TED of CO_2 is relatively high, indicating that this fluid generates less turbulence during its flow through the packed column, and by the same way indicating a less energy dissipation. Vapor modeled as a real gas (Peng-Robinson model) exhibits the highest TED among the three fluids. This implies that vapor displays the lowest turbulent behavior and minimal energy dissipation. Overall, these results highlight the distinct behaviors of water, CO_2, and vapor in both laminar and turbulent flow regimes through a packed bed. Understanding these differences is crucial for designing and optimizing processes that involve these fluids in porous media, such as enhanced oil recovery.

Nomenclature

C_2 / m^{-1} - Inertial resistance coefficient
d_p / m - Mean particle diameter
L / m - Bed length
ΔP / Pa - Pressure drop
Re - Reynolds number
u_0 / m s^{-1} - Linear velocity related to an empty cross-section of the column
u_{in} / m s^{-1} - Interstitial velocity

Letter Greek

$(1/\alpha)$ / m^{-2} - Resistance coefficient
ε - Void fraction (voidage)
μ / Pa s - Dynamic viscosity
σ / kg m^{-3} - Density of the fluid

Abbreviations

CD - Constant density
CFD - Computational fluid dynamics
PR - Peng-Robinson
TED - Turbulent eddy dissipation
TKE - Turbulent kinetic energy

Acknowledgements: The authors are grateful to the staff of the Laboratory of Materials and Environment (University of Medea, Algeria), which provided support for this study.

REFERENCES

[1] Dong X, Liu H, Chen Z, Wu K, Lu N, Zhang Q. Enhanced oil recovery techniques for heavy oil and oil sands reservoirs after steam injection. *Appl Energy*. 2019; 239: 1190-1211. https://doi.org/10.1016/j.apenergy.2019.01.244

[2] Zhou X, Wang Y, Zhang L, Zhang K, Jiang Q, Pu H, Wang L, Yuan Q. Evaluation of enhanced oil recovery potential using gas/water flooding in a tight oil reservoir. *Fuel*. 2020; 272: 117706. https://doi.org/10.1016/j.fuel.2020.117706

[3] Keyvan Hosseini M, Liu L, Keyvan Hosseini P, Bhattacharyya A, Lee K, Miao J, Chen B. Review of hollow fiber (HF) membrane filtration technology for the treatment of oily wastewater: Applications and challenges. *J Mar Sci Eng*. 2022; 10(9). https://doi.org/10.3390/jmse10091313

[4] Kumar P, Brar SK, Cledon M. A computational fluid dynamics approach to predict the scale-up dimension of a water filter column. *Case Stud Chem Environ Eng*. 2022; 5: 100201. https://doi.org/10.1016/j.cscee.2022.100201

[5] Brown GO. Henry Darcy and the making of a law. *Water Resour Res*. 2002; 38(7): (11-1)-(11-12). https://doi.org/10.1029/2001WR000727

[6] Shu X, Wu Y, Zhang X, Yu F. Experiments and models for contaminant transport in unsaturated and saturated porous media-A review. *Chem Eng Res Des*. 2023; 192: 606-621. https://doi.org/10.1016/j.cherd.2023.02.022

[7] Yan C, Fan H, Huang D, Wang G. A 2D mixed fracture-pore seepage model and hydromechanical coupling for fractured porous media. *Acta Geotech*. 2021; 16(10): 3061-3086. https://doi.org/10.1007/s11440-021-01183-z

[8] Amini Y, Shadman MM, Karimi-Sabet J. CFD simulation of flow distribution in the randomly packed bed Dixon ring. *Sep Sci Technol*. 2022; 57(12): 1900-1909. https://doi.org/10.1080/01496395.2021.2009513

[9] Lagrée B, Zaleski S, Bondino I. Simulation of viscous fingering in rectangular porous media with lateral injection and two- and three-phase flows. *Transp Porous Media*. 2016; 113(3): 491-510. https://doi.org/10.1007/s11242-016-0707-x

[10] Liu S, Liu L, Gu H, Wang K. Experimental study of gas-liquid flow patterns and void fraction in prototype 5 × 5 rod bundle channel using wire-mesh sensor. *Ann Nucl Energy*. 2022; 171: 109022. https://doi.org/10.1016/j.anucene.2022.109022

[11] Alhosani A, Selem A, Foroughi S, Bijeljic B, Blunt MJ. Steady-state three-phase flow in a mixed-wet porous medium: A pore-scale X-ray microtomography study. *Adv Water Resour*. 2023; 172: 104382. https://doi.org/10.1016/j.advwatres.2023.104382

[12] Liao Y, Zheng J, Wang Z, Sun B, Sun X, Linga P. Modeling and characterizing the thermal and kinetic behavior of methane hydrate dissociation in sandy porous media. *Appl Energy*. 2022; 312: 118804. https://doi.org/10.1016/j.apenergy.2022.118804

[13] Chen X, Zhao H. A phenomenological design method of the parallel packed bed reactors for chemical looping combustion of gas fuels. *Chem Eng Sci*. 2024; 292: 119988. https://doi.org/10.1016/j.ces.2024.119988

[14] Amini Y, Nasr Esfahany M. CFD simulation of the structured packings: A review. *Sep Sci Technol*. 2019; 54(15): 2536-2554. https://doi.org/10.1080/01496395.2018.1549078

[15] Wang Y. CFD simulation of propane combustion in a porous media: application to enhanced oil recovery of heavy oil reservoirs. *Pet Sci Technol*. 2020; 38(5): 432-439. https://doi.org/10.1080/10916466.2019.1705857

[16] Jiang Y, Khadilkar MR, Al-Dahhan MH, Dudukovic MP. CFD of multiphase flow in packed-bed reactors: II. Results and applications. *AIChE J*. 2002; 48(4): 716-730. https://doi.org/10.1002/aic.690480407

[17] Gao X, Zhu YP, Luo ZH. CFD modeling of gas flow in porous medium and catalytic coupling reaction from carbon monoxide to diethyl oxalate in fixed-bed reactors. *Chem Eng Sci*. 2011; 66(23): 6028-6038. https://doi.org/10.1016/j.ces.2011.08.031

[18] Macfarlan LH, Phan MT, Eldridge RB. Methodologies for predicting the mass transfer performance of structured packings with computational fluid dynamics: a review. *Chem Eng Process - Process Intensif*. 2022; 172: 108798. https://doi.org/10.1016/j.cep.2022.108798

[19] Wang G, Cai W, Xie L, Zhang X, Wang Y. CFD modeling and simulation of the hydrodynamics characteristics of packed column with structured sinusoidal corrugated sheets packings. *Chem Eng Res Des*. 2022; 183: 56-66. https://doi.org/10.1016/j.cherd.2022.04.038

[20] Peng J, Yu B, Yan S, Xie L. CFD Modeling and simulation of the axial dispersion characteristics of a fixed-bed reactor. *ACS Omega*. 2022; 7(30): 26455-26464. https://doi.org/10.1021/acsomega.2c02417

[21] Petrazzuoli V, Rolland M, Sassanis V, Ngu V, Schuurman Y, Gamet L. Numerical prediction of Péclet number in small-sized fixed bed reactors of spheres. *Chem Eng Sci*. 2021; 240: 116667. https://doi.org/10.1016/j.ces.2021.116667

[22] Pashchenko D, Karpilov I, Mustafin R. Numerical calculation with experimental validation of pressure drop in a fixed-bed reactor filled with the porous elements. *AIChE J*. 2020; 66(5): e16937. https://doi.org/10.1002/aic.16937

[23] Zhuang YQ, Gao X, Zhu Y ping, Luo Z hong. CFD modeling of methanol to olefins process in a fixed-bed reactor. *Powder Technol*. 2012; 221: 419-430. https://doi.org/10.1016/j.powtec.2012.01.041

[24] Amini Y, Karimi-Sabet J, Nasr Esfahany M, Haghshenasfard M, Dastbaz A. Experimental and numerical study of mass transfer efficiency in new wire gauze with high capacity structured packing. *Sep Sci Technol*. 2019; 54(16): 2706-2717. https://doi.org/10.1080/01496395.2018.1549076

[25] Mohanty R, Mohanty S, Mishra BK. Study of flow through a packed bed using discrete element method and computational fluid dynamics. *J Taiwan Inst Chem Eng*. 2016; 63: 71-80. https://doi.org/10.1016/j.jtice.2016.03.025

[26] Liu X, Peng C, Bai H, Zhang Q, Ye G, Zhou X, Yuan W. A pore network model for calculating pressure drop in packed beds of arbitrary-shaped particles. *AIChE J*. 2020; 66(9). https://doi.org/10.1002/aic.16258
[27] Ergun S, Orning AA. Fluid flow through aandomly packed columns and fluidized beds. *Ind Eng Chem*. 1949; 41(6): 1179-1184. https://doi.org/10.1021/ie50474a011
[28] Koekemoer A, Luckos A. Effect of material type and particle size distribution on pressure drop in packed beds of large particles: Extending the Ergun equation. *Fuel*. 2015; 158: 232-238. https://doi.org/10.1016/j.fuel.2015.05.036
[29] Wu J, Yu B, Yun M. A resistance model for flow through porous media. *Transp Porous Media*. 2008; 71(3): 331-343. https://doi.org/10.1007/s11242-007-9129-0
[30] Zeng Z, Grigg R. A Criterion for non-Darcy flow in porous media. *Transp Porous Media*. 2006; 63(1): 57-69. https://doi.org/10.1007/s11242-005-2720-3
[31] Ziółkowska, I, Ziólkowski, D.Modelling of gas interstitial velocity radial distribution over a cross-section of a tube packed with a granular catalyst bed. *Chem Eng Sci*. 1993; 48(18): 3283-3292. https://doi.org/10.1016/0009-2509(93)80212-9
[32] Zou Y, Gu H, Huang A, Zhang M, Ji C. Effects of MgO micropowder on microstructure and resistance coefficient of Al2O3-MgO castable matrix. *Ceram Int*. 2014; 40(5): 7023-7028. https://doi.org/10.1016/j.ceramint.2013.12.030
[33] Khalladi R, Benhabiles O, Bentahar F, Moulai-Mostefa N. Surfactant remediation of diesel fuel polluted soil. *J Hazard Mater*. 2009; 164(2-3): 1179-1184. https://doi.org/10.1016/j.jhazmat.2008.09.024
[34] Matsson JE. An introduction to ANSYS fluent 2022. SDC Publications; 2022. https://www.sdcpublications.com/Textbooks/Introduction-ANSYS-Fluent-2022/ISBN/978-1-63057-569-4/
[35] Baker TJ**.** Mesh generation: art or science?. *ProgAerosp Sci.* 2005; 41(1):29-63. https://doi.org/10.1016/j.paerosci.2005.02.002
[36] Hossain MA, Nabavi SA, Ranganathan P, Könözsy L, Manovic V. 3D CFD modeling of liquid dispersion in structured packed bed column for CO_2 capture. *Chem Eng Sci*. 2020; 225: 115800. https://doi.org/10.1016/j.ces.2020.115800
[37] Yang B, Yang T, Xu Z, Liu H, Yang X, Shi W. Impact of particle-size distribution on flow properties of a packed column. *J Hydrol Eng*. 2019; 24(3). https://doi.org/10.1061/(asce)he.1943-5584.0001735
[38] Erdim E, Akgiray Ö, Demir I. A revisit of pressure drop-flow rate correlations for packed beds of spheres. *Powder Technol*. 2015; 283: 488-504. https://doi.org/10.1016/j.powtec.2015.06.017
[39] Linsong J, Hongsheng L, Shaoyi S, Maozhao X, Dan W, Minli B. Pore-scale simulation of flow and turbulence characteristics in three-dimensional randomly packed beds. *Powder Technol.* 2018; 338: 197-210. https://doi.org/10.1016/j.powtec.2018.06.013
[40] Papkov V, Shadymov N, Pashchenko D. Gas flow through a packed bed with low tube-to-particle diameter ratio: Effect of pellet roughness. *Phys Fluids*. 2024; 36(2): 027127. https://doi.org/10.1063/5.0183475
[41] Lopez-Echeverry JS, Reif-Acherman S, Araujo-Lopez E. Peng-Robinson equation of state: 40 years through cubics. Fluid Phase Equilib. 2017; 447: 39-71. https://doi.org/10.1016/j.fluid.2017.05.007
[42] Paterson L, Lu M, Connell L, Ennis-King JP. Numerical modeling of pressure and temperature profiles including phase transitions in carbon dioxide wells. SPE Annual Technical Conference and Exhibition, Denver, Colorado, USA: Society of Petroleum Engineers, 2008, paper SPE-115946-MS. https://doi.org/10.2118/115946-MS
[43] Lv J, Chi Y, Zhao C, Zhang Y, Mu H. Experimental study of the supercritical CO2 diffusion coefficient in porous media under reservoir conditions. R Soc Open Sci. 2019; 6(6). https://doi.org/10.1098/rsos.181902
[44] Skjetne E, Auriault JL. High-velocity laminar and turbulent flow in porous media. *Transp Porous Media*. 1999; 36(2): 131–47. https://doi.org/10.1023/A:1006582211517

Numerička analiza strujanja unutar pakovanog sloja korišćenjem računske dinamike fluida: efekti karakteristika fluida i režima strujanja

Soufiane Ladeg[1,2] i Nadji Moulai-Mostefa[2]

[1]FST, University of Tissemsilt, Tissemsilt, Algeria
[2]LME, University of Medea, Medea, Algeria

(Naučni rad)

Izvod

U ovom istraživanju primenjena je računska dinamika fluida (engl. computational fluid dynamics - CFD) za poređenje modela strujanja fluida u laminarnom i turbulentnom režimu kroz pakovani sloj. Ispitane su tri vrste fluida (voda, vodena para i ugljen-dioksid). Predviđanja CFD modela su prvobitno upoređena sa dve serije eksperimentalnih podataka objavljene u literaturi. Primećeno je da je korišćeni numerički model u dobroj saglasnosti sa eksperimentalnim podacima, pod uslovom da su dimenzije pakovanog sloja (prečnik i visina kolone, i veličina čestica) u skladu sa onima koje su eksperimentalno korišćene. Model je zatim predvideo opadanje pritiska od vrha kolone do dna u opadajućem redosledu za tri proučavana fluida, za oba režima strujanja. Pored toga, sprovedena je temeljna karakterizacija turbulencije, uključujući određivanje turbulentne kinetičke energije (TKE) i turbulentne disipacije vrtloga (eng.turbulent eddy dissipation - TED). U slučaju vode dobijena je brza disipacija TKE u poređenju sa druga dva fluida, gde se TKE progresivno smanjivala duž kolone. Nasuprot tome, TED za vodu postepeno opada do izlaza iz kolone, dok se za oba gasovita fluida polako povećava duž kolone. Analiza strujanja pare obuhvatila je testiranje dva modela gustine, naime konstantne gustine i Peng-Robinsonovog (PR) modela. Dobijeno je da PR model za svojstva pare pokazuje slične trendove TKE i TED kao u predviđanjima za ugljen-dioksid.

Ključne reči: Pakovani sloj, strujanje fluida, turbulencija, modelovanje

Polymer waste utilization in the manufacturing of facing ceramics produced using glass cullet

Anastasiya S. Akimova, Evgeniy S. Pikalov and Oleg G. Selivanov

Vladimir State University, Vladimir, Russia

Abstract

The paper presents results on the development of a facing ceramic material produced from the low-plasticity clay with the addition of boric acid and flat window glass cullet, which serve for liquid-phase sintering and achieving a surface self-glazing effect. Additionally, polymer waste, in particular, waste from consumed non-plasticized PVC products, was introduced as a combustible additive. The research results show how the basic properties of the produced ceramics depend on the polymer waste amount added to the batch, with boric acid and cullet included in quantities that provide the maximum possible strength and frost resistance. The optimal polymer waste amount was determined, enabling production of a material that meets the requirements for ceramic facing products and qualifies as conditionally effective in terms of thermal engineering characteristics. The resulting batch composition enables the joint utilization of polymer and glass waste, while simultaneously expanding the raw material base and product range for facing ceramics production.

Keywords: Low-plasticity clay; self-glazing; liquid-phase sintering; energy efficiency.

Available on-line at the Journal web address: http://www.ache.org.rs/HI/

TECHNICAL PAPER

UDC 666.1.037.6:678.743.2: 666.3.017

Hem. Ind. **80(1)** 13-20 (2026)

1. INTRODUCTION

The problem of waste recycling is becoming extremely urgent in modern society. Waste recycling, on the one hand, prevents pollution and environmental degradation, and on the other, promotes rational utilization of natural resources and reduces economic expenditure of raw materials.

An effective solution for improving waste recycling is to utilize waste materials in the production of construction materials. This approach allows for the separate and complex processing of most waste types in large quantities, utilizing relatively simple and inexpensive technologies and processes. The most effective and promising utilization methods enable the joint processing of various waste types, using them as quality-improving additives and property-modifying agents in new products [1-3].

When using waste, it is important to consider the amount generated and accumulated, as well as its potential use as a secondary resource. This paper examines batch compositions that enable comprehensive utilization of polymer waste, in particular non-plasticized polyvinyl chloride (NPVC), and sheet glass cullet. Polymer waste currently ranks among the highest-volume waste types, and its utilization is an urgent task [4-6]. Polymer waste characterized by high purity and low degradation degree is successfully processed into an additive to primary raw materials for manufacturing plastic products, while low-quality waste with many impurities is practically unclaimed [5,7,8]. A similar trend is seen with glass waste: production waste is recycled by glass manufacturers, while post-consumer waste, amounting up to 10 % of the total waste amount, is instead accumulated at disposal sites and landfills [9-11].

Previous studies explored the utilization of polymer and glass waste in developing batch compositions based on low-plastic clay, with boric acid added as a melt, window glass cullet as a fluxing and strengthening additive, and NPVC waste as a combustible additive to improve the product energy efficiency. It was found that adding 2.5 wt.% boric acid and 12.5 wt.% cullet yielded the highest strength and the lowest water absorption, which could be achieved with NPVC waste additions ranging from 2.5 to 20 wt.% [1].

Corresponding author: Oleg Selivanov, Vladimir State University, Vladimir, Russia;
E-mail: selivanov6003@mail.ru; http://orcid.org/0000-0003-3674-0660
Co-authors: Evgeniy Pikalov https://orcid.org/0000-0001-9380-8014 and Anastasiya Akimova https://orcid.org/0000-0003-3169-5944

Paper received: 17 March 2025; Paper accepted: 13 January 2026; Paper published: 2 February 2026.
https://doi.org/10.2298/HEMIND250317002A

The objectives of the present work were to study the effect of polymer waste on the basic properties of self-glazing ceramics produced using cullet, and to determine the optimal amount of polymer waste in the batch so that the manufactured products meet regulatory requirements for facing ceramics while also providing enhanced energy efficiency.

2. MATERIALS AND METHODS

The basic component of the considered batch was the clay from Suvorotskoe deposit in the Vladimir region characterized by 5.2 clay plasticity in compliance with the standard method testifying of its low-plasticity and thus indicating the reason for the poor strength and high-water absorption of the products [4,12]. Therefore, introduction of special additives is required to improve the products quality. The used clay is characterized by the following composition: 67.5 wt.% SiO_2; 10.75 wt.% Al_2O_3; 5.85 wt.% Fe_2O_3; 2.8 wt.% CaO; 1.7 wt.% MgO; 2.4 wt.% K_2O; 0.7 wt.% Na_2O and loss on ignition of 8.3 wt.% [4,13].

The strengthening additive was sheet window glass cullet (Figure 1), due to its liquid-phase sintering, obtained after crushing the glass waste of the following composition: 73.5 wt.% SiO_2; 7.4 wt.% CaO; 1.9 wt.% MgO; 11.1 wt.% Na_2O; 5.1 wt.% K_2O and 0.9 wt.% Al_2O_3[1, 8].

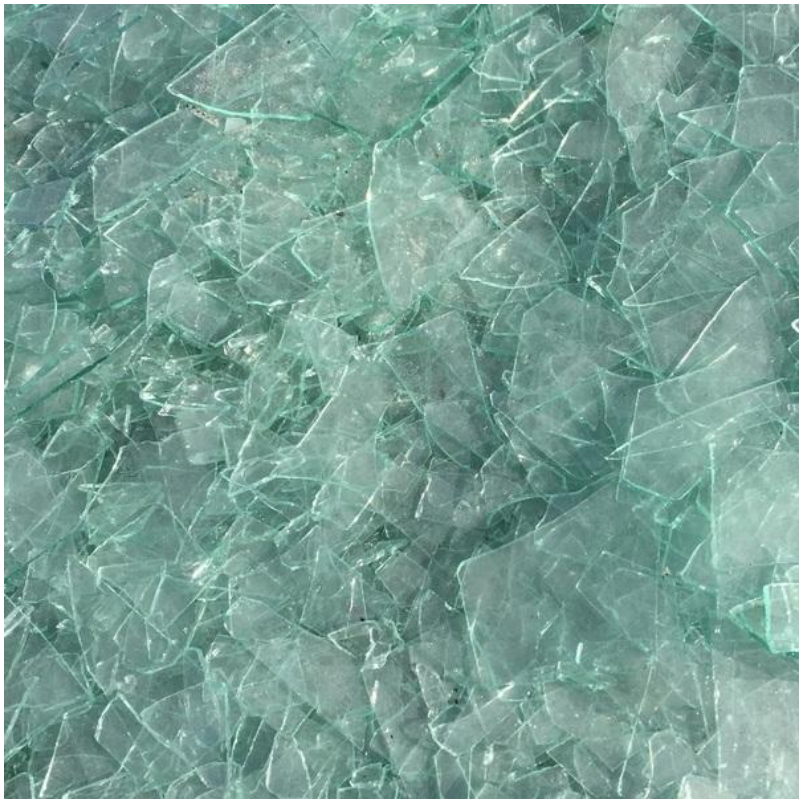

Figure 1. *Sheet window glass cullet*

NPVC waste (Figure 2), in particular building profiles waste (docking profiles and plinths) and finishing panels, was introduced into the developed batch composition as a combustible additive. It should be noted that the NPVC combustion products are highly toxic, primarily hydrochloric acid vapors and various organochlorine compounds, including dioxins. To neutralize these substances, afterburning chambers are required to decompose the combustion products at 1200 and 1400 °C. The most effective method for eliminating hydrochloric acid vapors is dry purification, which involves introducing quicklime, magnesium oxide, or sodium hydroxide into the flue gases, where they react with hydrochloric acid to form harmless compounds [4].

Both used waste types are accumulated in sufficiently large quantities because of construction and repair, justifying the relevance of their application in the studied batch composition.

Figure 2. *NPVC waste*

Boric acid brand B grade 2 in compliance with standard GOST 18704-78 [14], containing basic substance of at least 98.6 wt.%, was additionally introduced into the batch. The boric acid introduction reduces the liquid-phase sintering temperature and, alongside the cullet, provides self-glazing effect and product vitrification [1].

In accordance with previous results to ensure high-quality ceramics, 12.5 wt.% glass cullet, 2.5 wt.% boric acid and 2.5 to 20 wt.% NPVC were added to the batch in this work. Adding smaller amounts of NPVC waste does not induce significant changes in thermal conductivity and other material properties. However, incorporating more than 20 wt.% NPVC results in a substantial decrease in strength and an increase in water absorption, which together reduce frost resistance. Additionally, if excessive amounts of NPVC waste are added, traces of additive burnout remain visible both within the material depth and on its surface [1].

Before using the clay, NPVC waste and cullet intended as batch components were separately crushed to a maximum particle size of 0.63 mm and then dried to a constant weight. Also, all the batch components were initially mixed dry in accordance with the intended batch compositions, followed by mixing with water at the concentration of 8 wt.% to achieve uniform molding mass. The mixing period at each stage lasted 5 min. Ceramic samples were made from the molding mass by one-sided pressing at 15 MPa, followed by firing in an oxidizing atmosphere at a heating rate of 5 °C·min^{-1}, with a 30 min hold at 1050 °C.

The samples (Figure 3) were shaped like cubes with 50 mm sides, prepared in sets of three for each batch composition, and the results were averaged for each set. For the bending strength measurements, parallelepiped samples measuring 10×10×70 mm were prepared.

Compressive strength (σ_{cmp} / MPa) has been determined by continuous and uniform load impact on the sample until its destruction with maximum load fixation. When determining the bending strength (σ_{bnd} / MPa), the sample was mounted on the supports on both sides at 25 mm middle from the center. The bending load was applied continuously and evenly through the third support installed in the sample middle. To determine the strength characteristics, a hydraulic press P6326B (JSC Gidropress, Russia) was used.

Figure 3*. Sample of the developed ceramic material*

Water absorption (WA, %) has been determined by measuring the sample mass increase from the dry state till saturation with water at the atmospheric pressure of 48 h.

Frost resistance (FR, cycles) of the samples has been determined after the water absorption experiment. For this purpose, water-saturated samples were kept in a KM-0,15 freezer (LLC Mayak, Russia) at -15 to -20 °C for 4 hours, then placed in water at room temperature for 2 hours and examined for cracks. If the cracks were not found, the sample underwent another freeze-thaw cycle.

The density (ρ / kg/m^3) was calculated from the measured mass and volume of the air-dry sample.

To determine the total porosity (P_{tl} / %), the true density (ρ_{true} / kg m^{-3}) has been determined by the pycnometric method, and then calculated according to the Equation (1):

$$P_{tl} = (\rho_{true} - \rho)100 / \rho_{true} \quad (1)$$

Open porosity (P_{opn} / %) was calculated by the Equation (2):

$$P_{opn} = WA\rho \quad (2)$$

Closed porosity (P_{clsd} / %) was calculated by the equation (3):

$$P_{clsd} = P_{tl} - P_{opn} \quad (3)$$

Thermal conductivity (λ / W m^{-1}·°C^{-1}) was determined by using MIT-1 mobile thermal conductivity meter (LLC NPP Interpribor, Russia). For this purpose, 4 cubic samples with 50mm sides were placed on top of each other. The samples' touching surfaces were thoroughly polished, and then a hole was drilled through the centers of the samples. The device's measuring probe was placed into the hole, and the expected range of thermal conductivity was set. The device was then left for 2 hours to adjust the heating power and stabilize the heat flow. Afterward, readings were recorded, ensuring that the ambient temperature was maintained between 20 to 30 °C.

3. RESULTS AND DISCUSSION

The results obtained in this research show that the overall porosity of the developed material increases rapidly and almost linearly with increasing waste content in the batch. This is due to the burnout of the waste during firing, which leads to the formation of pores and voids formation within the samples (Figure 4).

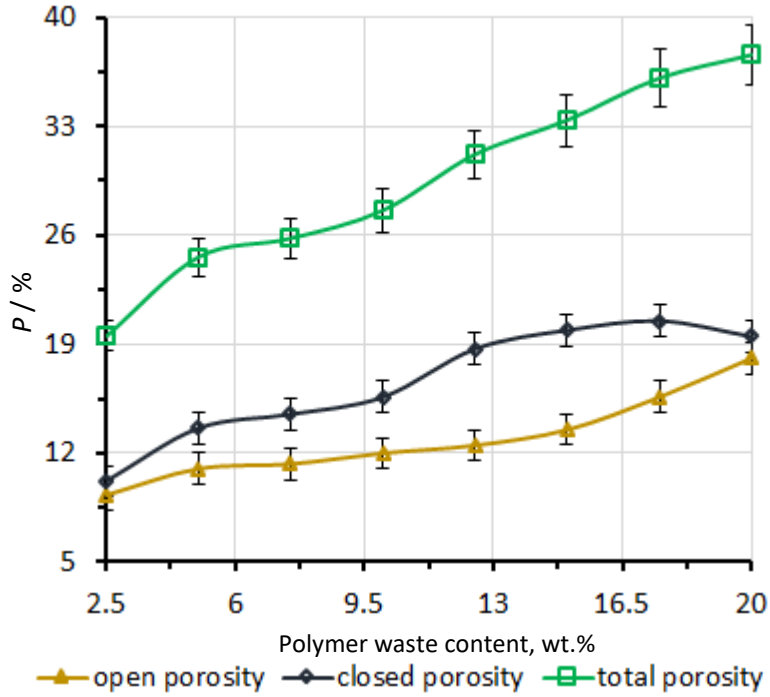

Figure 4. *Porosity of the developed ceramics as a function of the polymer waste content*

Open porosity also increases linearly, but when more than 10 wt.% NPVC waste is added, the rate of open pore formation accelerates. At the same time, closed porosity increases with NPVC content up to 17.5 wt.%, but higher amounts of polymer waste led to a decrease in closed porosity.

The observed increase in open porosity and decrease in closed porosity at NPVC contents above 17.5 wt.% NPVC can be attributed to the development of a porous structure, during which pores begin to connect at both the surface and within the depth of the ceramics once a certain amount of additive is reached.

The results also revealed an almost linear decrease in ceramics compressive and bending strengths with the increase in polymer waste content (Figure 5).

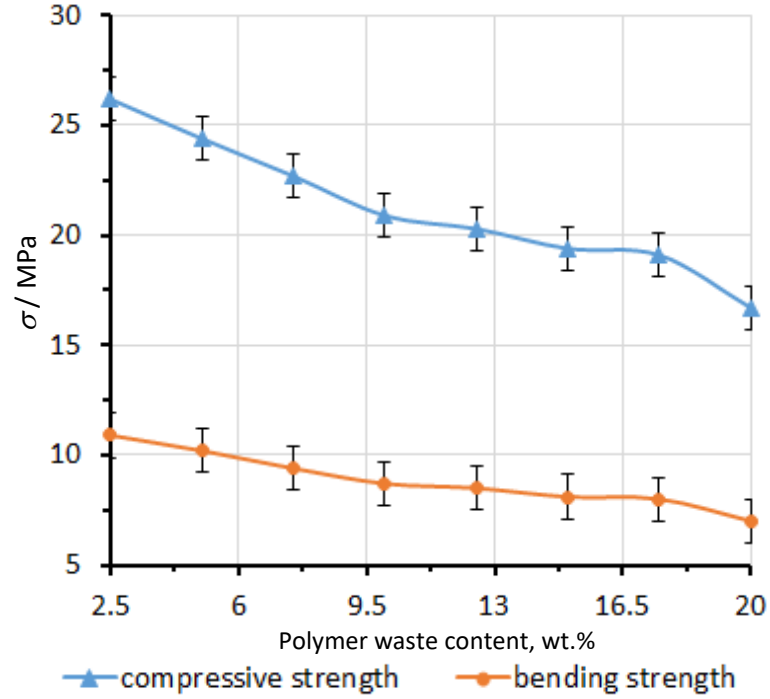

Figure 5. *Dependence of the ceramic strength on the polymer waste content*

Such dependence is related to the formation of pores during NPVC combustion causing a decrease in the contact area between the crystalline and vitreous phases throughout the entire material volume. As a result, the framework of ceramic particles within the glassy phase layer is disrupted. At the same time, a more significant decrease in material strength characteristics occurs as the NPVC waste content increases from 2.5 to 10 wt.%, likely due to greater disruption of the ceramic particle framework.

The ceramics water absorption increased almost linearly with the increase in the NPVC waste content, which in turn causes a similar linear decrease in the frost resistance (Figure 6). This relationship can be explained by the increase in material porosity and the higher fraction of open pores resulting from the formation of a developed porous structure. Figure 7 shows dependences of density and thermal conductivity of the developed ceramics on the NPVC waste content. Both properties are found to decrease rapidly as the NPVC waste content is increased, which corresponds again to the formation of an open porous material structure.

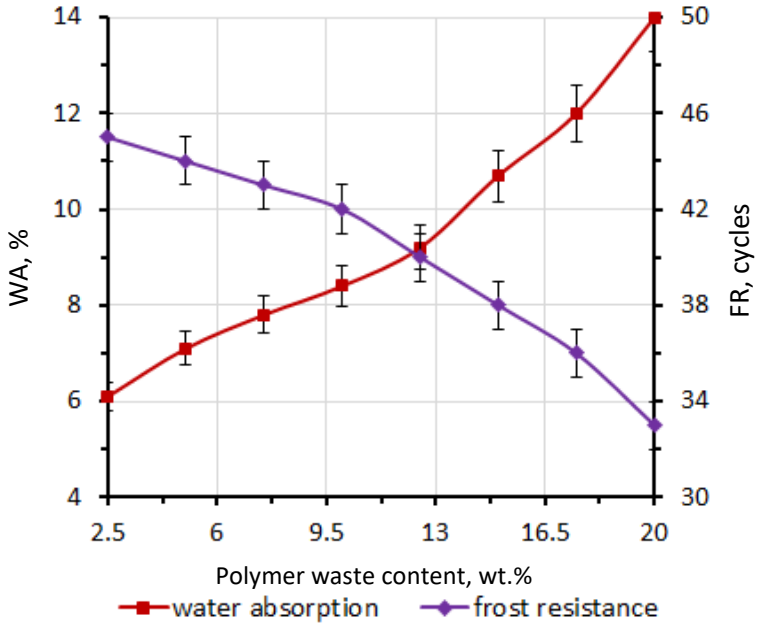

Figure 6. *Water absorption and frost resistance of the developed ceramics as functions of the polymer waste content*

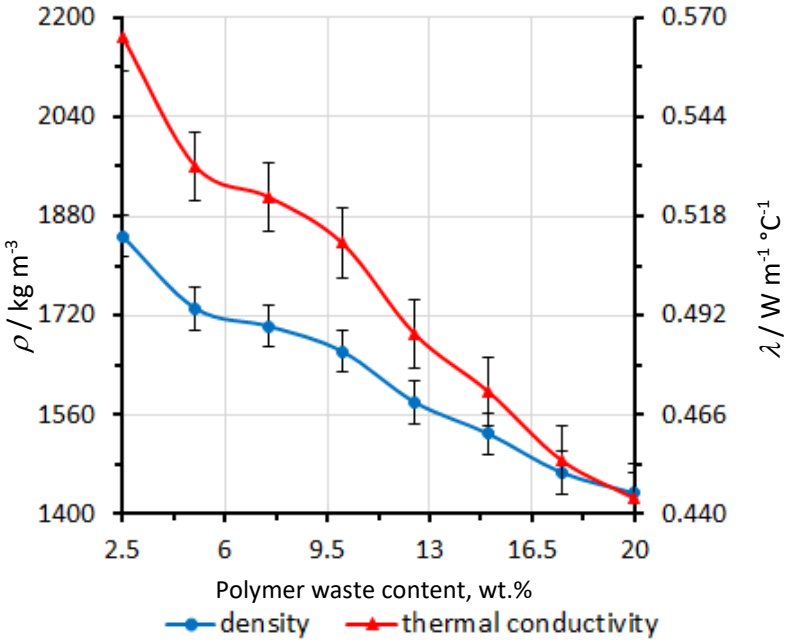

Figure 7. *Dependence of the developed ceramics density and thermal conductivity on the polymer waste content*

Overall, the results obtained in the research revealed that the pore-forming effect of NPVC waste burning during the ceramics firing negatively affects certain material properties such as strength, water absorption and frost resistance. At the same time, the material's density and thermal conductivity decrease, resulting in a lighter product with improved energy efficiency. Because all properties change almost linearly with increasing NPVC waste content in the batch, it is recommended to limit the amount of this additive to achieve sufficient energy efficiency.

According to the standard GOST 530-2012, energy efficiency is achieved when thermal conductivity does not exceed 0.46 W m^{-1}·°C^{-1}. Introducing 17.5 wt.% of NPVC waste into the batch results in a thermal conductivity of λ = 0.454 W m^{-1}·°C^{-1} allowing the final products to be classified as conditionally effective. Increasing the NPVC content further is not rational, since it significantly worsens the basic performance properties of the developed ceramics. Conversely, lower polymer waste content leads to thermal conductivity above the required level for energy-efficient materials.

4. CONCLUSION

This study contributed to developing a batch composition based on low-plasticity clay with additions of 2.5 wt.% boric acid, 12.5 wt.% cullet and 17.5 wt.% polymer waste. This batch composition enables the production of a ceramic material that can be classified as conditionally effective (λ < 0.46 W m^{-1} °C^{-1}) in compliance with the standard GOST 530-2012 [15]. In terms of compressive and bending strength values (19.1 and 8 MPa, respectively), the resulting ceramics is comparable to facing bricks and stones of the M175 brand (σ_{cmp} > 17.5 MPa). However, in terms of frost resistance it corresponds to the F35 brand (FR > 35), which is used for manufacturing facing construction products.

Thus, the developed batch composition ensures the combined processing of glass and polymer waste as functional additives in the production of high-quality facing ceramics. This approach, on the one hand, provides the solution to the problem of waste accumulation, while on the other, it expands the range of construction materials, products, and available raw materials.

REFERENCES

[1] Vitkalova I, Torlova A, Pikalov E, Selivanov O. The Use of Polymer and Glass Waste to Obtain a Self-Glazing Facing Ceramic. *Ecol Ind Russ*. 2019; 23(11): 38-42. https://doi.org/10.18412/1816-0395-2019-11-38-42

[2] Krishnan AK, Wong YC, Zhang Z, Arulrajah A. A transition towards circular economy with the utilisation of recycled fly ash and waste materials in clay, concrete and fly ash bricks: A review. *J Build Eng*. 2024; 98: 111210. https://doi.org/10.1016/j.jobe.2024.111210

[3] Shi X, Liao Q, Chen K, Wang Y, Liu L, Wang F, Zhu H, Zhang L, Liu C. Foaming process and thermal insulation properties of foamed glass-ceramics prepared by recycling muti-solid wastes. *Constr Build Mater*. 2025; 466: 140270. https://doi.org/10.1016/j.conbuildmat.2025.140270

[4] Vitkalova I, Torlova A, Pikalov E, Selivanov O. Energy Efficiency Improving of Construction Ceramics, Applying Polymer Waste. *Adv Intell Syst Comput*. 2019; 983: 786-794. https://doi.org/10.1007/978-3-030-19868-8_77

[5] Martínez-Narro G, Hassan S, Phan AN. Chemical recycling of plastic waste for sustainable polymer manufacturing. *J Environ Chem Eng*. 2024; 12(2): 112323. https://doi.org/10.1016/j.jece.2024.112323

[6] Al-Mansour A, Xu C, Yang R, Dai Y, Dang N, Lan Y, Zhang M, Fu C, Gong F, Zeng Q. Unleashing high-volume waste plastic recycling in sustainable cement mortar with synergistic matrix enabled by in-situ polymerization. *Constr Build Mater*. 2024; 447: 138031. https://doi.org/10.1016/j.conbuildmat.2024.138031

[7] Sánchez-Rivera KL, Zhou P, Radkevich E, Sharma A, Bar-Ziv E, Van Lehn RC, Huber GW. A solvent-targeted recovery and precipitation scheme for the recycling of up to ten polymers from post-industrial mixed plastic waste. *Waste Manage*. 2025; 194: 290-297. https://doi.org/10.1016/j.wasman.2025.01.022

[8] Anuar SZK, Nordin AH, Husna SMR, Yusoff AH, Paiman SH, Noor SFM, Nordin ML, Ali SN, Ismail YMNS. Recent advances in recycling and upcycling of hazardous plastic waste: A review. *J Environ Manage*. 2025; 380: 124867. https://doi.org/10.1016/j.jenvman.2025.124867

[9] Vitkalova I, Torlova A, Pikalov E, Selivanov O. The Development of Energy Efficient Facing Composite Material Based on Technogenic Waste. *Adv Intell Syst Comput*. 2019; 983: 778-785. https://doi.org/10.1007/978-3-030-19868-8_76

[10] Liu X, Ye Z, Lu J-X, Xu S, Hsu S-C, Poon CS. Comparative LCA-MCDA of high-strength eco-pervious concrete by using recycled waste glass materials. *J Clean Prod*. 2024; 479: 144048. https://doi.org/10.1016/j.jclepro.2024.144048

[11] Yuan X, Wang J, Song Q, Xu Z. Integrated assessment of economic benefits and environmental impact in waste glass closed-loop recycling for promoting glass circularity. *J Clean Prod*. 2024; 444: 141155. https://doi.org/10.1016/j.jclepro.2024.141155
[12] Pavlycheva EA, Pikalov ES, Selivanov OG. Glazing effect for producing environmentally friendly ceramics for cladding applications. *Hem Ind.* 2021; 75: 167-173. https://doi.org/10.2298/HEMIND210112017
[13] Filippova LS, Akimova AS, Pikalov ES. Application of Cryolite for Liquid-Phase Sintering of Facing Ceramic Based on Low-Plasticity Clay. *Inorg Mater: Appl Res*. 2025; 16(1): 98-102. https://doi.org/10.1134/S2075113324701405
[14] GOST 18704-78 Boric acid. Technical conditions. Reissue (April 1993) with changes No. 1, 2, 3. 1993. https://meganorm.ru/Data2/1/4294834/4294834571.pdf (In Russian)
[15] GOST 530-2012 Brick and stone ceramic General technical conditions. 2013. https://files.stroyinf.ru/Data2/1/4293782/4293782555.pdf (In Russian)

Korišćenje polimernog otpada u proizvodnji keramike za oblaganje napravljene od staklene šljake

Anastasiya S. Akimova, Evgeniy S. Pikalov i Oleg G. Selivano

Vladimir State University, Vladimir, Russia

(Stručni rad)

Izvod

U radu su predstavljeni rezultati razvoja keramičkog materijala za oblaganje proizvedenog od gline niske plastičnosti uz dodatak borne kiseline i staklene šljake poreklom od ravnog prozorskog stakla, za primenu za sinterovanje u tečnoj fazi i postizanje efekta samoglaziranja površine. Dodatno je kao zapaljivi aditiv uveden polimerni otpad, otpad od potrošenih neplastificiranih PVC proizvoda. Rezultati istraživanja pokazuju da osnovna svojstva proizvedene keramike zavise od količine polimernog otpada dodatog u smesu, pri čemu su borna kiselina i staklena šljaka dodati u količinama koje obezbeđuju maksimalnu moguću čvrstoću i otpornost na mraz. Određena je optimalna količina polimernog otpada, što omogućava proizvodnju materijala koji ispunjava zahteve za keramičke proizvode za oblaganje i kvalifikuje se kao uslovno efikasan u pogledu termotehničkih karakteristika. Dobijeni sastav smese omogućava zajedničko korišćenje polimernog i staklenog otpada, uz istovremeno proširenje sirovinske baze i asortimana proizvoda za proizvodnju keramike za oblaganje.

Ključne reči: Glina niske plastičnosti; samoglaziranje; sinterovanje u tečnoj fazi; energetska efikasnost.

Assessment of the efficiency of innovative reagents for purification of water from the Sava River (Belgrade)

Evgenii Nikolaevich Kuzin

Department of Industrial Ecology, D. Mendeleev University of Chemical Technology of Russia, Moscow, Russia

Abstract

There is a growing focus on enhancing environmental safety in Serbia. The development of hydrosphere protection technologies is one of the priority tasks, the solution of which will considerably improve the quality of life for the population and bring the country closer to the EU standards. The Sava River is one of the largest waterways running through Belgrade. In this work it was shown that the use of complex titanium-containing coagulants allows not only for the efficient removal of dispersed particles from water and a 70 % reduction in organic compound content, but also a 66 % decrease in the level of microbiological contamination. The use of sodium ferrate, a coagulant and bactericide, allows for a significant reduction of pollutant content in water as well as complete water decontamination. It was demonstrated that the use of a complex titanium-containing reagent considerably increases the sedimentation rate of coagulation sludge by 20 to 30 % and the filtration rate by 10 to 20 %.

Keywords: Water treatment, titanium-containing coagulant, sodium ferrate.

Available on-line at the Journal web address: http://www.ache.org.rs/HI/

ORIGINAL SCIENTIFIC PAPER

UDC 628.161.3:628.16:66.065.2-926

Hem. Ind. **80(1)** 21-28 (2026)

1. INTRODUCTION

Serbia is a beautiful, small country located in Southeast Europe, at the heart of the Balkan region. Currently, the country is preparing to accede to the European Union, which means it should fulfil several conditions (environmental, economic, political, *etc*.) imposed on all potential and current members. One of the most important requirements set for Serbia is to increase the level of environmental safety. The list of the main trends includes improving the quality of atmospheric air, constructing and operating waste treatment facilities, and organizing systems for the collection, sorting and recycling (or incineration) of waste. An equally important area is the prevention of microbiological contamination of drinking water and wastewater (The Drinking Water Directive 2020 (2020/2184) [1]. The implementation of these measures will not only allow meeting the EU requirements, but also achieving the 3, 6, 11 and 14 sustainable development goals.

Unfortunately, at present, these trends are not being implemented in practice, and the main environmental protection measures are only at the elaboration stage (except for Vojvodina). Currently, most of household and industrial wastewater flows into the rivers either after minimal treatment or without it. Large cities are provided with drinking water from ground (alluvial) sources, with 45 % spent for the needs of population, 25 % for industrial purposes, and 30 % for other uses (including agriculture) [2-5].

Industrial and sewage wastewater as well as water of surface runoff from agricultural sites is transported *via* a system of pipes into rivers downstream the flow course or is used as irrigation water for aeration fields. The major pollutants in such natural and wastewater streams nitrogen (nitrate/ammonium), phosphorus, and dissolved organic compounds that can serve as nutrients for sludge microorganisms or plants, and their concentrations and suitability for such purposes are indicated by chemical oxygen demand (COD) and by biochemical oxygen demand (BOD).

Basic physicochemical purification methods are used to remove the above pollutants from water, often in combination with filtration/sorption processes and reverse osmosis, followed by decontamination. Coagulants based on aluminium or iron salts are employed as the main consumable reagents. Although traditional reagents are highly efficient and moderately priced, they are not always suitable for treating wastewater with complex compositions [6].

Corresponding author: Evgenii Nikolaevich Kuzin, Department of Industrial Ecology, D. Mendeleev University of Chemical Technology of Russia, Moscow, Russia; E-mail: kuzin.e.n@muctr.ru; https://orcid.org/0000-0003-2579-3900

Paper received: 2 June 2025; Paper accepted: 4 February 2026; Paper published: 24 February 2026.
https://doi.org/10.2298/HEMIND250602003K

The need to use filtration/sorption arises from the presence of xenobiotics and dissolved organic compounds such as pharmaceutical substances, pesticides, and petroleum products, in the water. Reverse osmosis is necessary when concentrations of salts or heavy metals significantly exceed safe limits. To ensure bacteriological safety, chlorine-containing reagents (such as hypochlorite) are commonly used; in some cases, ozone or ultraviolet radiation is also employed.

To address these challenges, innovative reagents such as coagulants based on titanium compounds [7-10] or the coagulant-bactericide sodium ferrate [11-12] can be used. The advantages of ferrates over traditional regents are widely noted by researchers and scientists. It has been demonstrated that, due to their pronounced oxidizing effect, ferrates are less prone to form organic iron-containing complexes. Equally important is their ability to reduce the content of dissolved organic compounds such as phenols, pesticides and xenobiotics, thereby improving organoleptic quality indicators (taste, UV 254, and odour) of water. The use of ferrates requires significantly lower reagent costs for pH correction of the treated water, and the resulting coagulation sludge settles more easily and rapidly than that produced by pure aluminium or iron salts [13-15].

Titanium-containing reagents, in turn, can reduce coagulant consumption by a factor of 2 or more and significantly improve the removal efficiency of suspended solids as well as suspended and dissolved organic compounds [16-18]. These reagents are weakly bactericidal, while the resulting sludge is easier to filter and is less toxic as compared to aluminium sludge [19-20].

Summarizing the above, we can conclude that ferrate and titanium-containing coagulants are highly promising for use in the treatment of surface water sources. The main objective of this work was to assess the quality of surface water in the Sava River and to develop a process flow diagram for water treatment/purification using innovative reagents, specifically titanium-containing and ferrate coagulants.

2. MATERIALS AND METHODS

The research was conducted in the wastewater treatment laboratory at the Department of Industrial Ecology, Faculty of Biotechnology and Industrial Ecology, D. Mendeleev University of Chemical Technology of Russia (Moscow, Russia).

Water samples (5 dm^3) were taken from the "Savska Promenade" area of Belgrade between July 8 and 25, 2024. This sampling point was chosen because the low water flow rate at this location (resulting in minimal turbidity) and the absence of man-made sources of domestic wastewater discharge in the immediate vicinity (only storm drains are present).

Jar-tests were performed in 5 repetitions for each dose of reagent and were conducted on a JLT 4 laboratory flocculator (VELP, Italy) using the standard procedure [9-10,21]. The rapid coagulation phase (intensive mixing of the coagulant in water) lasted 120 s, the flocculation phase (slow coagulation) is 480 s, and the sedimentation time was 20 min.

Coagulant samples were aqueous solution of aluminum sulphate Kemira ALS – 8.0 wt.% and polyaluminium chloride Kemira PAX-XL-18 – 18 wt.% produced by Kemira (Kemira, Finland) and a sample of innovative complex titanium-containing coagulant obtained according to the previously described method (95 wt.% aluminum sulphate + 5 wt.% TiO_2) [10].

Sodium ferrate (synthesized by electrochemical method at department industrial ecology Mendeleev University of Chemical technology, Russia, Moscow), a coagulant-oxidizer (bactericide) obtained in the steam process of anodic dissolution of iron in alkalis (11.2 g dm^{-3} by Fe^{6+}), was also tested as an unconventional reagent. This reagent has appeared on the market quite recently but has proven itself well in the processes of cleaning wastewater of complex composition (for example, landfill leachate) [12, 22].

The following equipment was used to determine the quantitative and qualitative characteristics of wastewater samples.

The concentration of heavy metals was determined by atomic -emission spectroscopy with magnetic plasma by a Spectrosky device (Skygrad, Russia) and by a spectrophotometer DR 6000 (HACH, USA). To determine the particle size

of coagulation sludge, a digital meter Analysette 22 NanoTec Fritsch (Germany) was used. pH was measured using a digital meter (pHHQ11B, HACH, USA). The content of suspended solids and sedimentation rate were determined using a portable turbidimeter (HANNA 98703, HACH, USA), as the suspended solids content serves as a rapid indicator of water pollution and reagent treatment effectiveness.

To determine individual parameters of the river water samples before and after the reagent treatment, the following analytical control methods were used.

Oxidisability was determined by the reference methods (Dichromate oxidizability) [23]. The content of oils (gasoline, diesel) was determined by the Soxhlet method based on extraction with carbon tetrachloride followed by IR spectrophotometry using a KN-2N device (Sibecopribor, Russia). The content of dissolved salts (mineralization) was determined gravimetrically. The degree of microbiological contamination of the water was determined using test kits [24].

The selected indicators are highly significant and enable evaluation of both source water quality and the efficiency of reagent-based purification.

The filtration rate was determined by passing a specified volume of pre-coagulated water through a 15 μm filter for 60 s and then measuring the volume of filtrate collected.

The error in the results of analyses for the main pollutants did not exceed 15 % (calculated error + measurement error of the device).

3. RESULTS AND DISCUSSION

At the first stage of research, the composition of water was determined by chemical and bacteriological indicators. Data on the content of pollutants and the maximum concentrations established by the regulatory framework for household water [1] are presented in Table 1.

Table 1. *Results of studying water quality in the Sava River*

Indicator	In water	Standard [1]
pH	7.3	6.5 to 9.5
Turbidity, NTU	49.8	1.0
Oxidisability, mg(O) dm^{-3}	14.8	5.0
Content of NO_3, mg dm^{-3}	4.4	50
Content of NH_4, mg dm^{-3}	0.2	0.5
Content of PO_4, mg dm^{-3}	0.85	0.05*
Content of Al, mg dm^{-3}	0.3	0.2
Content of Fe, mg dm^{-3}	0.45	0.2
Content of oil, mg dm^{-3}	0.12	0.05*
Mineralization (salinity), mg dm^{-3}	212	500
Number of *Klebsiella pneumoniae, c*ells *per* mL	500	0
Number of *Enteroccocus faecalis* cells *per* mL	1,500	0
Number of *Escherichia coli* cells *per* mL	1,000	0
Number of *Staphylococcus aureus* cells *per* mL	5,500	0
Colony forming unit (CFU), cells *per* mL**	12,800	0

*The indicator is not standardized for water in the Republic of Serbia, but is currently used in Russia and the Asian region (Sanitarian rules 1.2.3685-21 and WHO/SDE/WSH/05.08/123, respectively).

**Not found in water samples: *Citrobacter freundii; Salmonella Enteritidis; Salmonella flexneri; Proteus mirabilis; Aspergillus niger; Saccharomces cerevisiae; Candida albicans; Pseudomonas aeruginosa*

Data in Table 1 show that water in the Sava River contains phosphate anion, nitrates and chemical oxygen demand in considerable excesses. Impurities of metals such as Zn and Cu were found in water in concentrations not exceeding the current standards (<0.2 mg dm^{-3}). Data in Table 1 also show that the selected sample is characterized by microbiological contamination with pathogenic microorganisms such as *Staphylococcus aureus* as well as a significant water contamination with *Klebsiella pnemoniae*, *Enterococcus* and *E. coli*. A high level of biological contamination can lead to outbreaks of various diseases and the active growth of biofilms on the surfaces of pipeline equipment [25].

The next stage of the research involved assessing the efficiency of reagent treatment for reducing turbidity and the content of dissolved organic compounds in the water. The results of the experiment are presented in Figures 1 and 2.

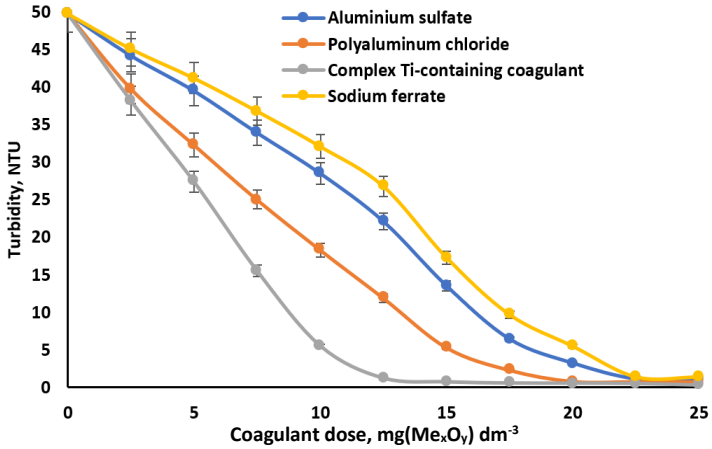

Fig. 1. *Effect of coagulant type and dose on turbidity index. Me_XO_Y stand for aluminium sulphate and polyaluminium chloride Al_2O_3, for sodium ferrate Fe_2O_3 and for complex Ti-containing coagulant - Al_2O_3+TiO_2*

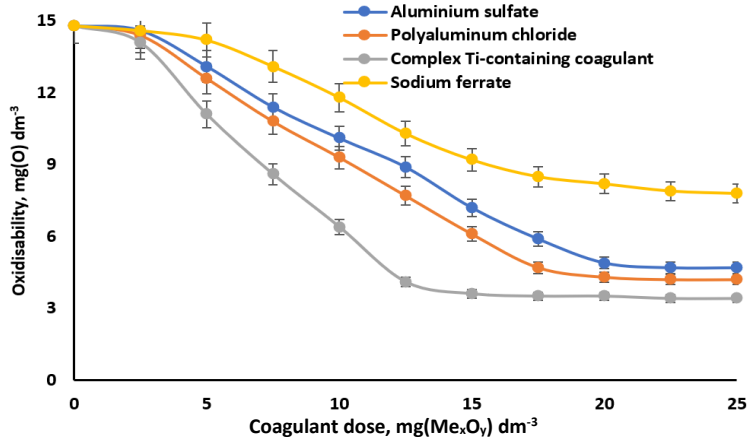

Fig. 2. *Effect of coagulant type and dose on oxidisability index. Me_XO_Y stand for aluminium sulphate and polyaluminium chloride Al_2O_3, for sodium ferrate Fe_2O_3 and for complex Ti-containing coagulant - Al_2O_3+TiO_2.*

Data from Figures 1 and 2 show that the complex titanium-containing coagulant was the most efficient, achieving the lowest residual turbidity and oxidizability values at a dosage of 12.5 to 15.0 mg dm^{-3}. High efficiency of the complex reagent is due to the parallel processes of primary nucleation (neutralization coagulation) of positively charged hydrolysis products of aluminium compounds and negatively charged hydrolysis products of titanium salts, as well as polycondensation/polymerization processes (flocculation) of meta- and orthotitanic acids being formed during hydrolysis [26-28]. The size of dispersed titanium particles in purified water was 0.8 to 0.9 µm, which, according to literary data, indicates the safety of the reagent for humans (absence of cytotoxicity) [29].

To achieve a similar residual turbidity for the traditional aluminium-containing reagents, dosages were 20 and 22.5 mg dm^{-3} for polyoxychloride and aluminium sulphate, respectively. These dosages are standard for purification of slightly turbid waters for drinking purposes.

Sodium ferrate demonstrated the lowest efficiency in reducing turbidity (residual value of 1.4 NTU exceeds the standard), but the effect of complete water decontamination was achieved during treatment (Table 3). Low efficiency of ferrate in reducing turbidity can be attributed to the formation of iron complexes with organic humic acids.

For all coagulant samples, a decrease in the content of dissolved organic matter (indicated by oxidisability and colour) was recorded; 70 % for the complex reagent, 40 to 50 % for the reagents containing aluminium, and 30 % for sodium ferrate.

The sediments (sludge) obtained using ferrate and the complex titanium-containing reagent differed from those formed with the traditional coagulants based on aluminium salts used in this study. Data on the technological parameters for sediment separation (precipitation/filtration) are presented in Table 2.

Table 2. *Technological parameters for sludge separation for different reagent types*

Reagent type	Particle size range, μm	Sludge sedimentation time, min	Filtration rate, mL min^{-1}
Aluminium sulphate	340 to 430	6.5	53
Polyaluminium chloride	400 to 490	5.5	59
Complex Ti-containing coagulant	480 to 550	4.0	67
Sodium ferrate	640 to700	4.5	42

Data in Table 2 clearly show that the coagulation sludge forming when the complex titanium-containing coagulant and sodium ferrate are used has an increased sedimentation and filtration rate, which will improve the efficiency of the treatment facilities. Sludge sedimentation time was decreased by 20 to 30 % and filtration rate by 10 to 20 % compared to the traditional reagents.

So, the optimal dosages of reactants were determined as: 12.5 mg dm^{-3} for Complex Ti-containing coagulant and 22.5 mg dm^{-3} for all another reagent. Residual concentrations of pollutants and microbiological contaminants obtained with optimal doses of reagents are presented in Table 3.

Table 3. *Residual concentrations of pollutants at optimal dosages of reactants:*

Indicator	Source value	Complex titanium-containing coagulant	Aluminium sulphate	Polyaluminium chloride	Sodium ferrate	Standard
pH	7.3	7.1	6.9	7.1	8.1	6.5-9.5
Turbidity, NTU	49.8	0.45	0.9	0.74	1.2	1.0
Oxidisability, mg(O) dm^{-3}	14.8	3.6	4.9	4.3	7.9	5.0
Content of NO_3, mg dm^{-3}	4.4	4.1	4.1	4.1	4.1	50
Content of NH_4, mg dm^{-3}	0.2	0.2	0.2	0.2	0.2	0.5
Content of PO_4, mg dm^{-3}	0.85	0.03	0.07	0.04	0.2	0.05
Content of Al, mg dm^{-3}	0.3	0.05	0.07	0.06	0.1	0.2
Content of Fe, mg dm^{-3}	0.45	0.1	0.12	0.1	0.28	0.2
Content of Ti, mg dm^{-3}	0	0.07	0	0	0	0.1
Content of oil, mg dm^{-3}	0.12	0.03	0.05	0.04	0.05	0.05*
Mineralization (Salinity), mg dm^{-3}	212	219	225	223	227	500
Number of *Klebsiella pneumoniae,* cells *per* mL	500	145	470	450	0	0
Number of *Enteroccocus faecalis* cells *per* mL	1,500	480	1,400	1,400	0	0
Number of *Escherichia coli* cells *per* mL	1,000	350	950	920	0	0
Number of *Staphylococcus aureus* cells *per* mL	5,500	1,250	4,800	4,500	0	0
Colony forming unit (CFU), cells *per* mL**	12,800	3,900	11,650	10,500	0	0

Table 3 shows that, despite its high efficiency, the complex titanium-containing coagulant does not meet the standard for microbiological safety. It should be noted that water treatment with the titanium-containing reagent made an almost 3-fold reduction in the level of biological contamination of water. Sodium ferrate was the least efficient in terms of removing suspended solids (turbidity) and other indicators, while providing complete water decontamination/disinfection.

The sludge produced by the coagulation treatment process is classified, based on its chemical composition, as low-hazard (non-toxic) waste and can be disposed of in solid municipal waste landfills.

The cost of titanium-containing reagents and ferrates is, on average, 10 to 15 % higher than that of aluminium sulphate, but about 50 % lower than that of PAX. However, their increased cleaning efficiency, faster sedimentation and filtration processes, and disinfectant effect are expected to improve the performance of treatment facilities and reduce operating costs.

Analysis of the obtained results indicates that reagent treatment enables efficient purification of water from the Sava River. The residual concentrations of almost all analysed pollutants are within the established standards.

The obtained results are in good agreement with the results reported for the use of pure titanium salts, while the cost of the innovative complex reagent (synthesized for the first time) was 2-3 times lower [7-8].

Physicochemical purification by coagulation/flocculation and sedimentation cannot be used as the sole treatment process but should be incorporated into a comprehensive water treatment system such as the one presented in Figure 3.

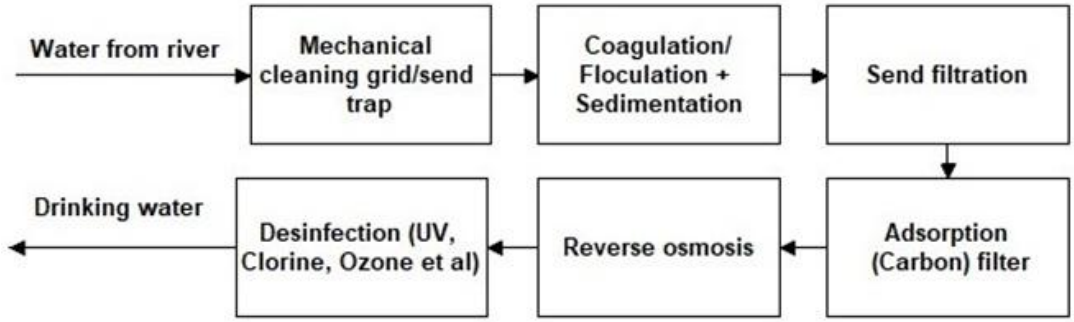

Figure 3. *Scheme of a proposed complex purification system of water from the Sava River (Belgrade)*

The proposed process flowsheet (Figure 3) enables the production of high-quality clean water from portions of the Sava river that receive primarily surface runoff. The key area of using the treated water will be to meet the needs of industrial enterprises (*e.g.* paint and varnish, petrochemical industries).

The adsorption and reverse osmosis purification stages (standard drinking water purification methods) are required because of possible fluctuations in pollutant concentrations depending on the season, while these units can be in the form of bypass lines and be connected as needed.

4. CONCLUSION

In this work, the quality of surface water from the Sava River (Belgrade, Serbia) was assessed first. The results showed that the primary pollutants in the water were suspended solids (turbidity), phosphates, dissolved organic compounds (as indicated by oxidizability and colour), and an extremely high level of microbiological contamination, including pathogenic *Staphylococcus aureus.*

In the next step, it was demonstrated that using a complex titanium-containing coagulant enables highly efficient removal of most undissolved impurities (suspend solids) from water, as well as a 70 % reduction in organic impurity content. Achieving equivalent purification efficiency with traditional aluminium-containing coagulants required an effective dose that was, on average, 1.5 to 2.0 times higher.

The use of sodium ferrate enabled complete elimination of microorganisms; however, the residual turbidity and organic matter content remained much higher compared to treatments with aluminium salts or the complex reagent.

It was demonstrated that the use of the innovative, complex titanium-containing coagulant significantly intensifies the formation and settling of coagulation sludge. Based on the obtained data, a process flow diagram was developed for purification of water from the Sava River for household use, in accordance with the Drinking Water Directive 2020 (2020/2184) [1].

Funding: *This research received no external funding.*

Data availability statement: *The original contributions presented in this study are included in the article. Further inquiries can be directed to the corresponding author.*

Acknowledgments: *The author expresses his deep gratitude to his scientific supervisor, Natalia Kruchinina, Department of Industrial Ecology, Mendeleev University of Chemical Technology of Russia.*

Conflicts of Interest: *The author declares no conflicts of interest.*

REFERENCES

[1] Dettori M, Arghittu A, Deiana G, Castiglia P, Azara A. The revised European Directive 2020/2184 on the quality of water intended for human consumption. A step forward in risk assessment, consumer safety and informative communication. *Environ Res*. 2022; 20: 112773. https://doi.org/10.1016/j.envres.2022.112773

[2] Marković M, Zuliani T, Simić SB, Mataruga Z, Kostić O, Jarić S, Vidmar J, Milačič R, Ščančar J, Mitrović M, Pavlović P. Potentially toxic elements in the riparian soils of the Sava River. *J Soil Sediments.* 2018; 18: 3404-3414. https://doi.org/10.1007/s11368-018-2071-7

[3] Babić G, Vuković M, Voza D, Takić L, Mladenović-Ranisavljević I. Assessing Surface Water Quality in the Serbian Part of the Tisa River Basin. *Polish J Environ Stud*. 2019; 28(6); 4073-4085. https://doi.org/10.15244/pjoes/95184

[4] Kašanin-Grubin M, Gajić V, Veselinović G, Stojadinović S, Antić N, Štrbac S. Provenance and Pollution Status of river Sediments in the Danube Watershed in Serbia. *Water.* 2023; 15(19): 3406. https://doi.org/10.3390/w15193406

[5] Stevanović SD, Krstić J., Stojanović BT, Paunović DĐ, Dimitrijević DS, Veličković JM, Stanković NJ. Monitoring of drinking water from the karst springs of the Ljuberadja-Niš water supply system (Serbia). *SN Appl Sci*. 2020; 2: 1847. https://doi.org/10.1007/s42452-020-03674-2

[6] Han SW, Kang June LS. Comparison of Al(III) and Fe(III) Coagulants for Improving Coagulation Effectiveness in Water Treatment. *J Korean Soc Env Eng.* 2015; 37: 325-331. https://doi.org/10.4491/KSEE.2015.37.6.325

[7] Gan Y, Li J, Zhang L, Bi W, Huang W, Li H, Zhang S. Potential of titanium coagulants for water and wastewater treatment: Current status and future perspectives. *Chem Eng J.* 2021; 406: 126837. https://doi.org/10.1016/j.cej.2020.126837

[8] Thomas M, Bąk J, Królikowska J. Efficiency of titanium salts as alternative coagulants in water and wastewater treatment. *Desalin Water Treat.* 2020; 208: 261-272. 10.5004/dwt.2020.26689

[9] Kuzin EN, Krutchinina NE. Evaluation of effectiveness of use of complex coagulants for wastewater treatment processes of mechanical engineering. *ChemChemTech*. 2019; 62 (10): 140-146. https://doi.org/10.6060/ivkkt.20196210.5939

[10] Kuzin E. Synthesis and Use of Complex Titanium-Containing Coagulant in Water Purification Processes. *Inorganics*. 2025; 13 (1): 9. https://doi.org/10.3390/inorganics13010009

[11] Thomas M, Zdebik D. Treatment of Real Textile Wastewater by Using Potassium Ferrate(VI) and Fe(III)/H_2O_2. Application of Aliivibrio Fischeri and Brachionus plicatilis. Tests for Toxicity Assessment. *Fibr and Text East Europe*. 2019; 27(3): 78-84. https://doi.org/10.5604/01.3001.0013.0746

[12] Thomas M, Kozik V, Barbusiński K, Sochanik A, Jampilek J, Bak A. Potassium Ferrate (VI) as the Multifunctional Agent in the Treatment of Landfill Leachate. *Materials.* 2020; 13 (21): 5017. https://doi.org/10.3390/ma13215017

[13] Yu J, Zhang SK, Zhu Q, Wu C, Huang S, Zhang Y, Yao S, Pang W. A Review of Research Progress in the Preparation and Application of Ferrate (VI). *Water*. 2023; 15: 699. https://doi.org/10.3390/ma13215017

[14] Talaiekhozani A, Talaei MR, Rezania SN. An overview on production and application of ferrate (VI) for chemical oxidation, coagulation and disinfection of water and wastewater. *J Envir Chem Eng*. 2017; 5(2): 1828-1842. https://doi.org/10.1016/j.jece.2017.03.025

[15] Ghernaout D, Naceur MW. Ferrate (VI): In situ generation and water treatment. *Desalin Water Treat*. 2011; 30(1-3): 1-14. https://doi.org/10.5004/dwt.2011.2217

[16] Munyengabe A, Zvinowanda C. Production, characterization and application of Ferrate(VI) in water and wastewater treatments. *Brazilian Journal of Analytical Chemistry*. 2019; 6(25): 40-57. https://doi.org/10.30744/brjac.2179-3425.RV-19-2019

[17] Nyzhnyk T. High efficiency titanium coagulants for water treatment. *TT: PhE.* 2017; 1: 54-56. http://dx.doi.org/10.21303/2585-6847.2017.00486

[18] Zhao YX, Li XY. Polymerized titanium salts for municipal wastewater preliminary treatment followed by further purification via crossflow filtration for water reuse. *Sep Purif Technol*. *2019;* 211: 207-217. https://doi.org/10.1016/j.seppur.2018.09.078

[19] Men Y, Wang X, Cheng S, Zhu L, Li Z. Pre-coagulation with novel titanium coagulants for mitigating membrane fouling in direct membrane filtration of municipal wastewater. *Chem Eng J.* 2024; 495: 153156. https://doi.org/10.1016/j.cej.2024.153156

[20] Gan Y, Zhang L, Zhang S. The suitability of titanium salts in coagulation removal of micropollutants and in alleviation of membrane fouling. *Water Res. 2021;* 205: 117692. https://doi.org/10.1016/j.watres.2021.117692

[21] Calderón AJ, González I. Some Hardware and Instrumentation Aspects of the Development of an Automation System for Jar Tests in Drinking Water Treatment. *Sensors.* 2017; 17: 2305. https://doi.org/10.3390/s17102305

[22] Sarantseva AA, Ivantsova NA, Kuzin EN. Investigation of the Process of Oxidative Degradation of Phenol by Sodium Ferrate Solutions. Russ J Gen Chem. 2023; 93(13): 3454-3459. https://doi.org/10.1134/S1070363223130273

[23] ISO 15705:2002. Water Quality—Determination of the Chemical Oxygen Demand Index (ST-COD)-SMALL-Scale Sealed-Tube Method; *ISO: Geneva, Switzerland*. 2002. https://www.iso.org/standard/28778.html

[24] Bain R, Bartram J, Elliott M, Matthews R, McMahan L, Tung R, Chuang P, Gundry S. A summary catalogue of microbial drinking water tests for low and medium resource settings. *Int J Environ Res Public Health*. 2012; 9: 1609-1625. https://doi.org/10.3390/ijerph9051609

[25] Collivignarelli MC, Abbà A, Benigna I, Sorlini S, Torretta V. Overview of the Main Disinfection Processes for Wastewater and Drinking Water Treatment Plants. *Sustainability.* 2018; *10*(1): 86. https://doi.org/10.3390/su10010086

[26] Kuzin EN, Kruchinina NE. Titanium-containing coagulants. for foundry wastewater treatment. *CIS Iron and Steel Review. 2020;* 20(2): 66-69. https://doi.org/10.17580/cisisr.2020.02.14

[27] Wang TH, Navarrete-López AM, Li S, Dixon DA, Gole JL. Hydrolysis of $TiCl_4$: initial steps in the production of TiO_2. *J Phys Chem A.* 2010; 114: 7561-7570. http://dx.doi.org/10.1021/jp102020h

[28] Chekli L, Eripret C, Park S, Tabatabai S, Vronska O, Tamburic B, Kim J, Shon HK. Coagulation performance and floc characteristics of polytitanium tetrachloride (PTC) compared with titanium tetrachloride ($TiCl_4$) and ferric chloride ($FeCl_3$) in algal turbid water. *Sep Purif Technol*. 2017; 175: 99-106. https://doi.org/10.1016/j.seppur.2016.11.019.

[29] Michael Berg J., Romoser A., Banerjee N. Zebda R., Sayes C. M. The relationship between pH and zeta potential of ~30 nm metal oxide nanoparticle suspensions relevant to *in vitro* toxicological evaluations. *Nanotoxicology.* 2009; 3-4: 276-283. https://doi.org/10.3109/17435390903276941

Procena efikasnosti inovativnog reagensa za prečišćavanje vode iz reke Save (Beograd)

Evgenii Nikolaevich Kuzin

Department of Industrial Ecology, D. Mendeleev University of Chemical Technology of Russia, Moscow, Russia

(Naučni rad)

Izvod

U Srbiji se sve više pažnje posvećuje unapređenju ekološke bezbednosti. Razvoj tehnologija za zaštitu hidrosfere predstavlja jedan od prioritetnih zadataka, čije će rešavanje značajno poboljšati kvalitet života stanovništva i približiti zemlju standardima Evropske unije. Reka Sava je jedan od najvećih vodotokova koji protiču kroz Beograd i predstavlja važan resurs koji zahteva efikasno upravljanje kvalitetom vode. U ovom radu je pokazano da primena kompleksnih koagulanata koji sadrže titanijum omogućava ne samo efikasno uklanjanje dispergovanih čestica iz vode i smanjenje sadržaja organskih jedinjenja za 70 %, već i smanjenje nivoa mikrobiološke kontaminacije za 66 %. Upotreba natrijum-ferata, koji deluje i kao koagulant i kao baktericid, omogućava značajno smanjenje sadržaja zagađujućih materija u vodi, kao i potpunu dekontaminaciju vode. Takođe je pokazano da kompleksni koagulacioni reagens koji sadrži titanijum značajno povećava brzinu sedimentacije koagulacionog mulja za 20 do 30 % i brzinu filtracije za 10 do 20 %.

Ključne reči: Tretman vode; koagulant sa titanijumom; natrijum-ferat.

Nettle fibre for technical applications

Parmeshwar Bobade, Vivek Jaiswal, Chandra Jeet Singh and Samrat Mukhopadhyay

Department of Textile and Fibre Engineering, Indian Institute of Technology Delhi, Delhi, India

Abstract

Due to greater awareness of environmental and social issues, as well as stricter environmental regulations, there is a rising demand for green materials to replace fossil-based resources and raw materials. With its excellent mechanical properties, biodegradability, and low cost, nettle fibre has the potential to become a sustainable fibre for technical applications. Dyeability, antimicrobial properties, renewability, and wrinkle resistance make this fibre suitable for textile applications. Due to its low density, it may be used in a wide array of applications such as woven and non-woven fabrics, blends, and composite materials. This paper aims to critically review nettle fibre in various textile applications and provide directions for future research.

Keywords: Alkali treatment; building material; non-woven textiles; textile composite; sound absorption; sustainability.

Available on-line at the Journal web address: http://www.ache.org.rs/HI/

TECHNICAL REVIEW PAPER

UDC 677.152-049.8

Hem. Ind. **80(1)** 29-49 (2026)

1. INTRODUCTION

Nettle (*Girardinia diversifolia*) fibre is derived from the stems of the nettle plant, a herbaceous plant that belongs to the *Urticaceae* family. The plant is grown as a wild shrub in Asia, Europe, North Africa and North America [1]. The *Urticaceae* family, which includes the nettle genus, comprises approximately 500 species [2-4]. It is a perennial grass species that does not require pesticides and can grow up to 3.6 to 5.5 m. It provides the longest natural fibre and is amenable to yarn formation and fabric manufacturing [5]. When conventional raw materials were less abundant and diverse, nettle played a critical role in the field of textiles. In Europe, people have been using nettle plants to extract fibres since the 12th century, mainly for domestic handicrafts [6]. During the 16th and 17th centuries, Scottish households favoured nettle fibre as their preferred textile for linens [2,7]. Germany was the first country to commercialize the production of nettle fibre. Attempts were made at the cultivation of nettle and the process of extracting fibres from the plant was established at the beginning of the 18th century. Europeans and Americans used nettle plant fibres to make sail cloths, sacks, cordages, and fishing nets [8-10]. Till 1860, nettle fibre was used to make sturdy, durable cloth in Great Britain, but it was discontinued due to low-cost imported materials [7]. During World War I, nettle fibre was used as a substitute for cotton. The German uniforms constituted of 85 % nettle fibre at the beginning of World War II. The British government used 100 tons of nettle plants to extract green dye for camouflage [11-13]. Due to limited scientific research and reliance on extraction traditional methods, the potential of nettle fibre for development into textile-grade products has not been fully explored [14].

2. COMPOSITION, MORPHOLOGY AND PROPERTIES OF NETTLE FIBRE

2. 1. Composition and morphology

The fibres are found in the plant's bast or skin, as shown in Figures 1a, 1b and 1c, and are highly oriented along the fibre axis with a small helix angle [5].

Corresponding authors: Chandra Jeet Singh E-mail: chandrajeettz@gmail.com; https://orcid.org/0000-0003-3841-3655 and Samrat Mukhopadhyay samrat.mukhopadhyay@iitd.ac.in; https://orcid.org/0000-0002-2978-9565 - Department of Textile and Fibre Engineering, Indian Institute of Technology Delhi, Delhi, India
Co-authors: Parmeshwar Bobade https://orcid.org/0009-0007-8252-9512 and Vivek Jaiswal https://orcid.org/0009-0000-6572-5377

Paper received: 9 June 2025; Paper accepted: 31 March 2026; Paper published: 8 April 2026.
https://doi.org/10.2298/HEMIND250609004B

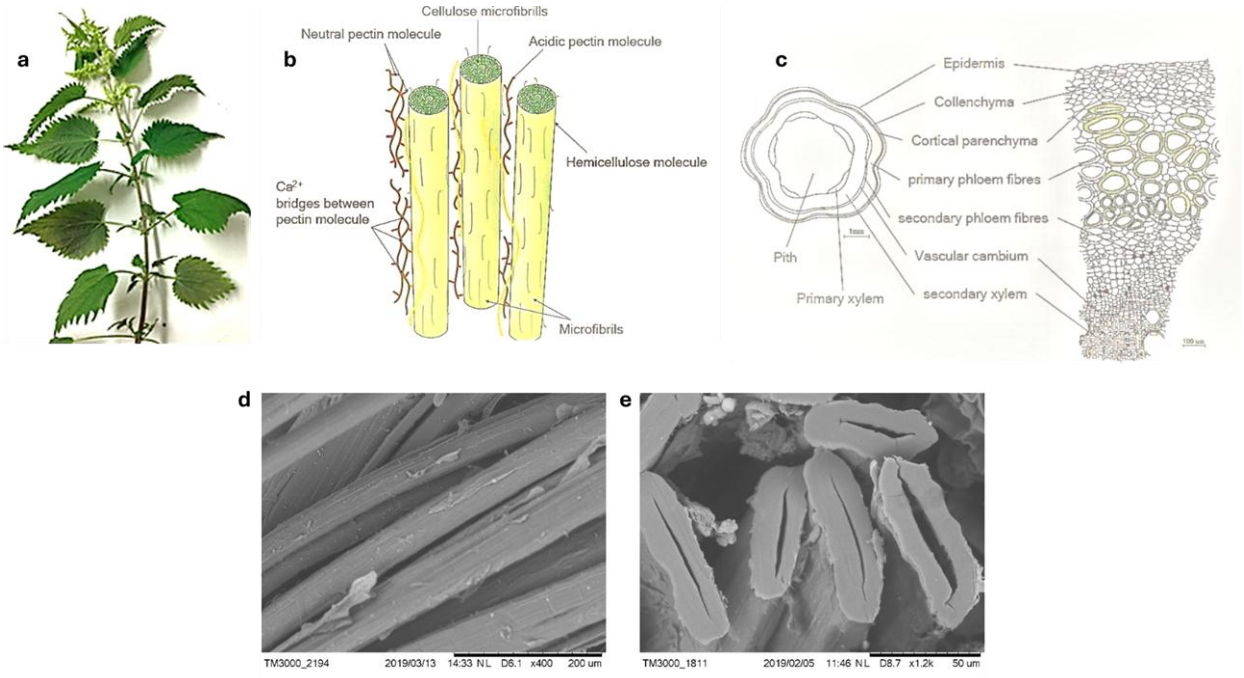

Figure 1. *Nettle fibre: a - photograph of nettle plants; b and c - schematic presentation of the structure of bast fibres in nettle stem, adapted with permission from [5,15] © IJHS 2018; scanning electron micrographs of d - longitudinal and e - cross-sectional view of nettle fibres, reprinted with permission from [16]*

Chemical composition of the nettle plant was reported to vary with the age of the plant with a mean fibre content reported as 11 % [17]. The middle portion of the plant had the highest fibre yield (13 %), with fibres containing the lowest cellulose content (79 ± 2 %) and the highest hemicellulose content (12.5 ± 3 %), compared to the top and bottom portions. Lignin content (4.4±0.4 to 3.5±0.2 %) and fibre diameter (47 to 19µm) decreased from the bottom to the top of the plant, with the longest fibres found at the top. Variability in the diameter, length, and lignin content affects the characteristics of the extracted fibre. The composition of nettle fibre might differ depending on the specific clone variation. Scanning electron microscopy of nettle fibres shows surface characteristics similar to other bast fibres. The longitudinal image of nettle fibres in Figures 1d and e shows a clean surface, free from impurities, voids, and scratch marks. The cross-section of nettle fibre (Figures 1d and e) is annular and has an elliptical rather than circular shape.

2. 2. Physical and mechanical properties

The physical properties of nettle fibre vary depending on the species. Fibre diameter ranges from 20 to 80 µm and varies along its length, while density ranges from 1.4-1.5 g cm^{-3}. The average length of the fibre for *Goirardinia diversifolia*, reported as 478 ± 21 mm, was considerably longer than that reported for *Urtica dioica* (52 ± 2 mm) and other common bast fibres. The moisture content of fibre was reported as 6 % for *Girardinia diversifolia* and 9.4 % for *Urtica dioica* [8,14,18]. The tensile strength of nettle fibre has been reported as 4451 ± 13 MPa, surpassing that of glass fibre. Its Young's modulus was 73 ± 22 GPa with an elongation at break of 6.2 ± 1.3 % [14]. As shown in Table 1, these values are the highest among all bast fibres and even exceed those of some industrial fibres, including glass. Due to their hollow structure and resulting low density, nettle fibres possess superior characteristics compared to most other fibres. However, these properties can vary depending on the plant species and the fibre extraction technique employed [19].

Table 1. *Mechanical and physical characteristics of different fibres**

Fibres	Length, mm	Average diameter, µm	Young's modulus, GPa	Tensile strength, MPa	Strain to failure, %	Density, g cm^{-3}	Ref.
Nettle	478±21	-	73±22	4451±131	6.2±1.3	1.4 to 1.5	[14]
Stinging nettle	52±2	19.9±4.4	87±28	1594±640	2.11±0.81	-	[20]
Flax	207±3	17.8±5.8	58±15	1339±486	3.27±0.4	1.53	[21]
Hemp	20±5	31.2±4.9	19.1±4.3	270±40	0.8±0.1	1.48	[22]

Fibres	Length, mm	Average diameter, μm	Young's modulus, GPa	Tensile strength, MPa	Strain to failure, %	Density, g cm^{-3}	Ref.
Coir	150 to 280	100 to 500	3 to 5	140-225	-	1.2	[23,24]
Jute	-	70-80	26.5	393-723	3.5-4.5	1.3	[25]
Ramie	135±15	34	24.5	560	2.5	1.51	[26]
E-Glass	-	5 to 25	76 to 78	3100-3800	3.4	2.55	[27]

*Among the references, some report values as means with standard deviations (mean ± SD), whereas others present data as ranges to reflect higher variability

In a study of fibre tensile properties [20], a positive association between Young's modulus and the fibre diameter was shown (Figure 2), with the measured values being widely spread. One possible explanation is that as the fibre's diameter increases, the lumen that is the hollow portion, also becomes larger. For this specific nettle, the average diameter was 20±2 μm, and the mean Young's modulus was 87 ±28 GPa [20]. There have been reports of similar effects with flax fibre [28].

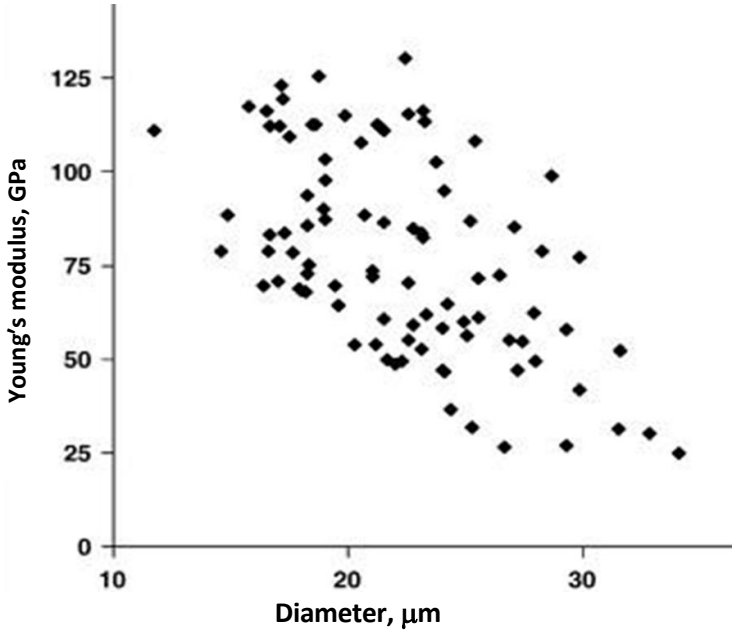

Figure 2. *The relationship between the Young's modulus and the diameter of stinging nettle fibre. Adapted from [29] © 2007 Elsevier*

3. CHARACTERISTICS OF NETTLE FIBRE

Fibres extracted from the nettle plant are pliable, the longest natural fibre known to humans. They are suitable for a variety of spinning techniques in fabric manufacturing. Moreover, this fibre type is stronger and lighter than cotton, the world's most widely used natural fibre [30,31]. Fabric made from nettle fibres is stronger and stiffer than linen and has also shown antimicrobial activity against nine different microorganisms due to compounds such as catechins and epitheca [32]. The fibre has also shown good resistance to wrinkling and pilling, resulting in improved durability and aesthetic properties of the fabric [33]. These properties are dependent on the processes used for fibre extraction [34]. Due to the fibre's hollow core structure, nettle fibre fabric can be tailor-made for both winter and summer seasons. In winter, the hollow core of the nettle fibre entraps air inside, providing the necessary insulation. It helps in keeping the body warm by preventing the transfer of body heat to the environment. In summer fabrics, thermal insulation can be reduced by increasing the twist in the yarn [35]. In addition, the fabric made from this fibre is dyeable yet cost-effective, like other cellulosic fabrics. These properties have increased the acceptability of the nettle fibre in textile applications [36]. From a sustainability point of view, this fibre could be used as a source of cellulose feedstock for regenerated cellulosic products and can also be reused [30,31]. The plant only needs a source of water and can survive a contaminated soil environment [37]. However, the use of nettle fibre is currently restricted to handmade textile

products due to its rigid and inextensible characteristics, as shown in Figure 3. Once these drawbacks are overcome through chemical treatments as with other bast fibres, they can be rendered useful in technical applications [13,38,39].

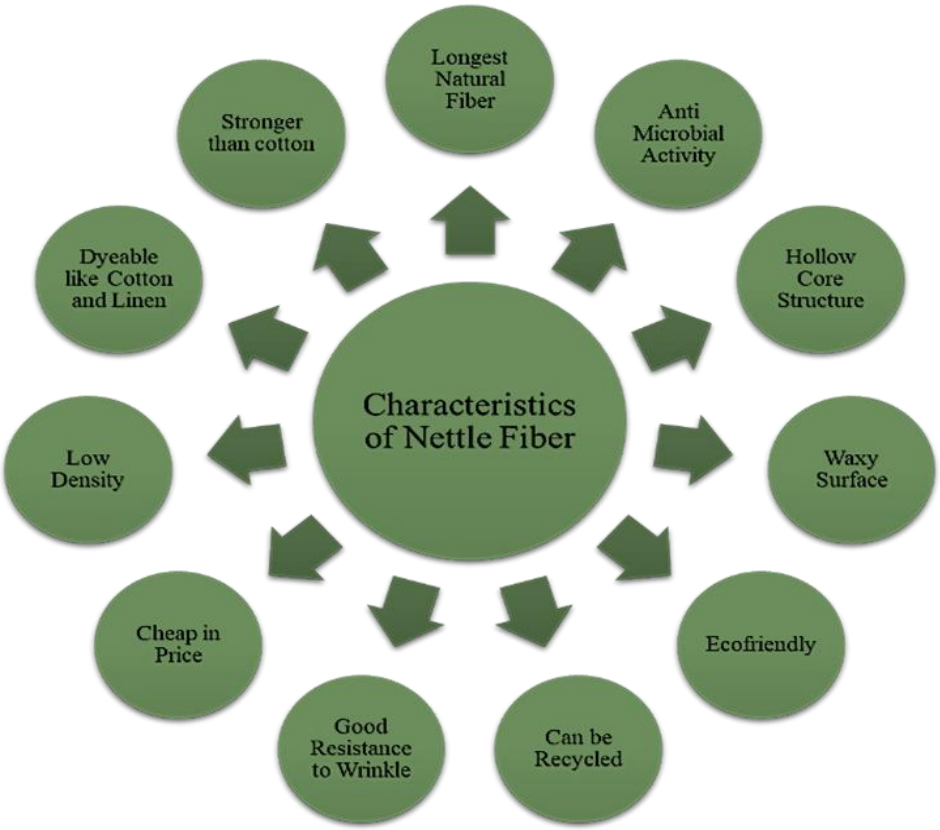

Figure 3. *Technical characteristics of nettle fibre*

4. PROCESSING OF NETTLE FIBRES

Processing of nettle fibre from the plant to the fabric stage consists of various steps. The nettle plant is a perennial crop (life of 10-15 years) and can produce fibres suitable for textile applications for 4-5 years [14,42]. Although the plant is typically ready to harvest in August, the exact timing is determined by various factors such as plant height, the seed-forming stage, and the emergence of new branches from the roots. Nettle plants are harvested with a sharp knife and then retted to extract the fibres. After cleaning and opening by specialized equipment, the fibres may be blended as needed for specific applications. The resulting blend is then carded to produce slivers, preparing it for further textile processing. Alignment and uniformity of the sliver are ensured during the drawing stages. Through opening and twisting, the sliver is converted into roving and then into yarn *via* the spinning process, following the required parameters. Subsequently, the yarn must go through the warping process to prepare a series of parallel yarns ready for weaving. Sizing is applied to the warp sheet to increase its strength, which helps reduce breakages during the weaving stage. Then the fabric is then manufactured on a loom by interlacing the warp and weft yarns perpendicularly. The aesthetic appearance of the fabric can be enhanced through dyeing, if required. Additionally, it can be treated with various chemicals at the finishing stage to add value, if necessary [43].

5. EXTRACTION METHOD

Fibres are separated by removing the gummy substance that binds them together, with a detailed process shown in Figure 4 [44,45]. Various methods can be used to extract fibres from the stem, and their respective advantages and disadvantages are discussed in the following section.

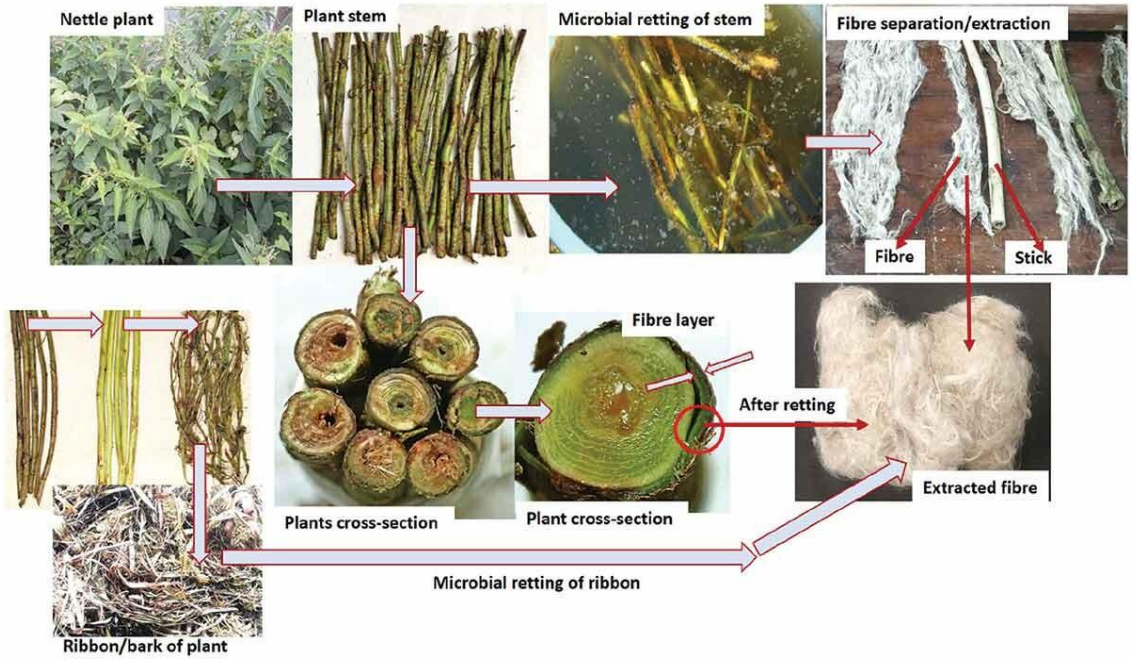

Figure 4*. Extraction process of nettle fibre. Adapted from [46].*

5. 1. Microbiological retting

5. 1. 1 Dew retting

Dew retting, also known as field retting, involves spreading the stalks widely in an open field for up to 10 weeks. During this period, microorganisms present in the soil and on the plants break down non-cellulosic contents, resulting in the removal of pectin and hemicellulose, while leaving the cellulosic fibres intact [44].

5. 1. 2. Water retting

After harvesting, the plant stalks are immersed in water for 2 to 3 weeks, allowing microorganisms to degrade the gummy substances binding the fibres together. This process is cheap but time-consuming [44].

5. 2. Enzymatic retting

Enzymatic retting, also known as the scouring process, is less time-consuming and requires less water. It uses enzymes to degrade the gummy part of the stem at a specific temperature. In terms of time-saving, eco-friendliness and convenience characteristics, this method has shown that it can be a promising substitute for conventional retting techniques [44].

5. 3. Mechanical separation

Mechanical separation is the most conventional method, where fibres are mechanically decorticated to separate them from the woody stem, followed by scutching and hackling. This process is similar to the extraction of banana fibres, as reported previously [47].

Although the process has become automated, the basic steps remain the same and include the following stages:

- Breaking: Extracted stalks are passed through rollers to crush and split the woody core.
- Scutching: Bundles are fed between rollers and beaten by mechanical blades to separate the fibres from the woody stem material.
- Hackling: The fibres are passed through a set of pins to disentangle and align them.

5. 4. Physical retting

5. 4. 1. Steam explosion

The steam explosion procedure utilizes high-pressure saturated steam, followed by rapid depressurization. This sudden change causes the breakdown of lignocellulose, hydrolysis of hemicellulose, depolymerisation of lignin, and separation of the fibres (defibrillation).

5. 4. 2. Hydrothermal methods

In the hydrothermal method, water at high temperature and pressure is used to degrade hemicellulose and lignin.

5. 4. 3. Osmotic degumming

In the osmotic degumming method, degumming occurs through the diffusion of water into the material within the stem. When the tension generated by water penetration exceeds the longitudinal strength of the stem, the epidermis fractures along its length without damaging the fibres. Once pectins get dissolved in water, the fibres can be separated out by filtration. These fibres exhibit high strength and a soft texture [48].

5. 4. 4. Plasma treatment

Plasma treatment involves various forms of gases at atmospheric and high pressures, while generally, oxygen and argon are used [49]. This is a surface modification technique that uses ionized gases under atmospheric or low-pressure conditions to alter the surface properties of materials without affecting their bulk characteristics. In this process, various gases can be used, but oxygen and argon plasmas are most commonly applied to activate and clean the material surface [50]. The energetic plasma species interact with the surface, removing contaminants and introducing functional groups, which improves properties such as wettability, adhesion, and dyeability. Due to its environmentally friendly nature and minimal chemical usage, plasma treatment is widely used in textile processing, polymer modification, and advanced material engineering applications [51].

5. 5. Chemical retting

In chemical retting, chemicals are used to degrade the gummy substances binding the fibres together. This method is often preferred since it yields fibres of uniform quality in a shorter time regardless of weather conditions. Common chemical treatments include alkalization, ammonia treatment, acidic retting, and oxidative delignification [52]. After extraction, the fibres can be processed into different forms, such as yarns, fabrics, or composites, depending on the intended application and specific requirements [53]. Comparison of different methods of retting is given in Table 2.

Table 2*. Comparison of different retting methods [44,49,54].*

Retting method	Description	Advantage	Disadvantage
Mechanical separation	Fibres are separated mechanically; then post-cleaning and further impurities are filtered.	A high amount of short fibres can be produced in less time.	Low quality of fibre
Water retting	Plant stems are immersed in water. They are regularly tested to check the extent of retting.	Provides highly uniform and high-quality retted fibres.	Severe pollution problem resulting from anaerobic fermentation of bacteria and high cost. Requires intensive wastewater treatment.
Enzymatic retting	Gum and pectins are hydrolysed by enzymes. To optimize retting efficiency, controllable retting conditions are allowed.	Specific properties for various applications can be achieved by adjusting the retting time and the type of enzyme used. It is a cleaner and faster process.	Low strength of fibre
Chemical retting	Hydrogen peroxide, sodium benzoate or sodium hydroxide are commonly used.	Possibility to obtain a smooth and clean surface. Consistency cannot be achieved in less time.	Deterioration in fibre quality for higher chemical concentration, high cost of processing, and adverse colour.

6. NETTLE FIBRES EXPLORED IN VARIOUS TECHNICAL APPLICATIONS

The textile sector has been increasingly focusing on sustainable fibres, as the use of conventional fibres results in excessive waste generation and pollution [55]. Nettle fibre has the potential to replace technical fibres that contribute to environmental pollution [56,57]. It is biodegradable, low-cost and exhibits good mechanical properties including high strength, making it ideal for technical textile applications. In addition, nettle fibre is renewable, abundantly available, and has low density allowing for its use in a broad range of applications [58]. However, its inextensibility has restricted its application primarily to handmade textile products [59]. This characteristic makes it difficult to process nettle fibres on conventional textile machines and converting them into yarn and fabrics for a variety of products has proven to be challenging. Some research studies focused on improving the processability of nettle fibres, introducing modifications to reduce their limitations [40,59]. It was reported that mild alkali treatment (0.5 % NaOH, 30 °C for 30 min) led to improved tensile strength (~36 %) and elongation at break (~40 %) with a slight reduction in initial modulus. In the case of concentrated alkali treatment (10 % conc., 100 °C for 6 h), strength and modulus decreased by ~14 and 21 %, respectively, with a ~8 % gain in elongation. An increase in tensile strength up to 5.5 g den^{-1} was also observed for the treatment with 4 % sodium chlorite for 4 h [60]. However, the treatment optimization has not been done yet for nettle fibres. The summary of fabrication methodologies for different materials, such as composites, woven, non-woven, and blended fabrics, along with the main observations by the researchers, is presented in Table 3.

Several attempts have been made to introduce nettle fibre to textile applications. A detailed review of those attempts is discussed below.

Table 3. *A summary of the reported work of nettle fibre used in various applications.*

Applications	Material	Main observations	Ref.
Composite	Nettle and polypropylene	PP composites reinforced with nettle fibre have comparable mechanical qualities to other lignocellulosic composites. Strong qualities of nettle fibre nucleate crystalline structure formation in the PP matrix.	[61]
	Nettle and poly (lactic acid) fibres	Properties were originally enhanced to 50/50 nettle/PLA fibres. ● Tensile strength - 14.93 times increased ● Elongation at break - 1.45 times increased ● Young's modulus - 48 % decreased ● Flexural strength - 2.05 times increased ● Impact strength - 14 times increased. Properties decreased from nettle/PLA 50/50 to 90/10 ● Tensile strength - 2.15 times decreased ● Elongation at break - 1.2 times decreased ● Young's modulus - 51 % decreased ● Flexural strength - 12.2 times decreased ● Impact strength - 6.2 times decreased	[59]
Hybridized composite	Nettle/wool and polyethylene	Tensile strength increased by 21 % up to 20 % fibre loading, then decreased by 4 % up to 25 % fibre loading. Tensile modulus increased by 161 % from 0 to 25 % fibre loading. Fibre loading enhanced flexural stiffness by 24 % at 20 % fibre loading, then reduced it by 6 % at 25 % fibre loading. With 25 % fibre loading, the tensile modulus rose by 33 %. The NaOH treatment improved mechanical characteristics.	[62]
	Nettle fibre, bauhinia-vahlii fibre and epoxy	Increasing dietary fibre increased the void fraction. The water absorption rate increased with fibre content. Tensile strength improved with composite fibre content. Nettle/epoxy composite is weaker than Bauhinia/epoxy composite. Composite hybrids are stronger than mono-fibre composites.	[63]
Woven fabric	Nettle, cotton, polyester, modal	The highest values of moisture loss of 23 % at 4 h and 47 % at 24 h were observed with nettle fibre. Softness values are not reduced with the utilization of nettle fibre in the production of towels. The towel's hydrophilicity was not adversely affected using nettle fibres.	[41]

Non-woven fabric	Nettle poly (lactic acid) fibres	Alkali treatment • Increased tensile strength by 27 % • Increased elongation at break by 68 % • Decreased initial modulus by 9 % • Increased coefficient of fibre-to-fibre friction by 9 %. Tensile strength decreased as the proportion of nettle fibre increased. Nettle fibres exhibited superior biodegradability compared to Poly (lactic acid) fibres.	[64]
	Nettle and polypropylene	Needle-punched non-woven fabric absorbs crude and diesel oil best. The highest sorption was found in a 30/70 nettle/PP with lower weight (GSM) and needle punch density. Needle-punched non-woven fabric with 30/70 nettle/PP demonstrates outstanding potential for reusability. It can be effective for oil spill cleaning.	[38]
	Nettle	Nettle non-woven fabric demonstrated comfort properties. 494 % water absorbency and 79 $cm^3/cm^2/s$ air permeability. The thermal conductivity reaches a minimum value of 0.0251 W/m K at a needle penetration depth of 8 mm. Fabric weight - 150 g/m^2 Needle density - 75	[65]
Blended fabric	Nettle and acrylic	As blended fabric contains more nettle fibre, moisture absorption rises. Higher-nettle content fabric offered better thermal insulation.	[65,66]
	Nettle, organic cotton and bamboo	The tensile strength of nettle fabric increased by 14.21 % with organic cotton and 10.23 % with bamboo fibre in the warp direction. The tensile strength of nettle fabric increased by 11.1 % with organic cotton and 10.1 % with bamboo fibre in the weft direction. Elongation at break of nettle fabric increased by 8.26 % with organic cotton and 7.53 % with bamboo fibre in the warp direction. Elongation at break of nettle fabric increased by 28.39 % with organic cotton and 7.25 % with bamboo fibre in the weft direction. Abrasion resistance of nettle fabric increased by 3.1 % with organic cotton and 4.23 % with bamboo fibre.	[67]

6. 1. Composite materials

Nettle fibres can be incorporated into bio-composites as a sustainable reinforcement material for automotive, aerospace, and construction industries.

Utilization of stinging nettle (*Urtica dioca*) in reinforcement of polymers was investigated confirming the usability of these fibres in manufacturing polymer composites [29]. To use nettle fiber for composite reinforcement [61], polypropylene was used as a matrix and nettle (10 wt.%) as a filler. The composite was manufactured through extrusion and subsequently by injection moulding. The properties of the obtained composite were compared with those of other composites containing different fillers. It was found that with the addition of nettle fibre to polypropylene resulted in a slight rise in Young's modulus, but a decrease in other properties such as tensile strength (23 %), elongation at break (12 %), impact strength (20 kJ m^{-2}) and hardness (18 %).

Figure 5 shows tensile strength values for different polypropylene composites with addition of 30 wt.% nettle and other natural fibres. It could be seen that the composites containing banana and kenaf fibres have significantly higher strength than the composite containing nettle fibres. The inherent stiffness of the fibre has been the key reason for such observation [68]. Since different researchers have attempted to work with these various organic fibres, it would be intriguing to understand the reasons behind the observed results in a comparative study.

In another research, a bio composite was manufactured for vehicle dashboard panels by carding and compression moulding process [59]. Significant breakage of nettle fibres was observed upon feeding them to the carding machine. The authors commented that the reason was in high stiffness and low elasticity of the fibres. To improve the processability of the fibres, nettle fibres were treated with a 10% NaOH solution (liquor ratio 1:50) at 61.5 °C for 30 min. The treatment resulted in increased fineness (denier), tensile strength, MPa and elongation at break of 0.4, 30 and 70 %, respectively, but the initial modulus decreased by 6.7 %. After the treatment, nettle and poly (lactic acid) (PLA) fibres were fed to a carding machine and slivers of different proportions were obtained: 10/90, 25/75, 50/50, 75/25, and 90/10 [59].

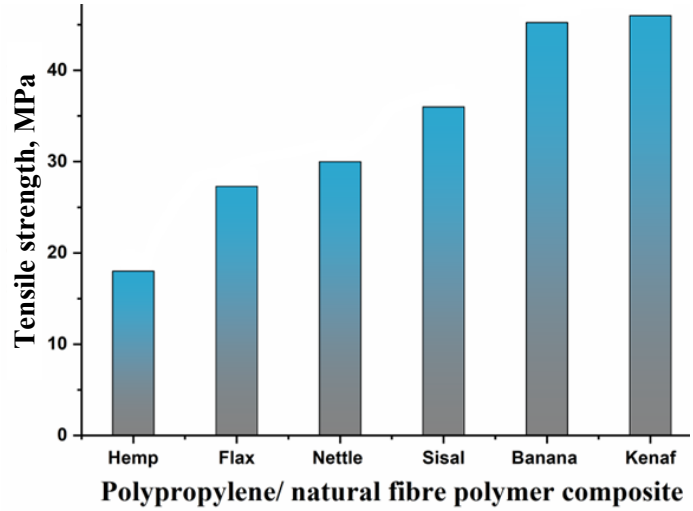

Figure 5. *Tensile strength of polypropylene composites with 30 wt.% fibre. The data is based on studies conducted by [68-70]*

Comparison of the bio composites showed that increasing the proportion of nettle fibre led to a decrease in overall density, owing to the fibre's lower density. As the nettle content is increased, mechanical properties such as tensile strength, elongation at break, Young's modulus, flexural strength, and impact strength improved up to the point where PLA and nettle fibres were present in equal proportions. Beyond this proportion, there was a significant decline in these properties. These results indicate that incorporating nettle fibre as reinforcement can enhance mechanical properties, but only up to an optimal proportion. When the nettle fibre content exceeded 50 % a decrease in mechanical properties was observed as a result of inadequate adhesion between the nettle fibres and the matrix, which led to fibre slippage within the composite [71]. This also caused a reduction in flexural strength. In the case of storage modulus, representing the energy stored in the composite, the nettle/PLA composite with a 50/50 mass ratio showed the highest storage modulus of 4024 MPa, while that of the neat PLA material was 2427 MPa at 35 °C. As shown in Figure 6, the storage modulus of the composite decreased with an increase in temperature. A sudden drop in storage modulus was observed at approximately 70 °C, corresponding to the glass transition temperature of PLA [72].

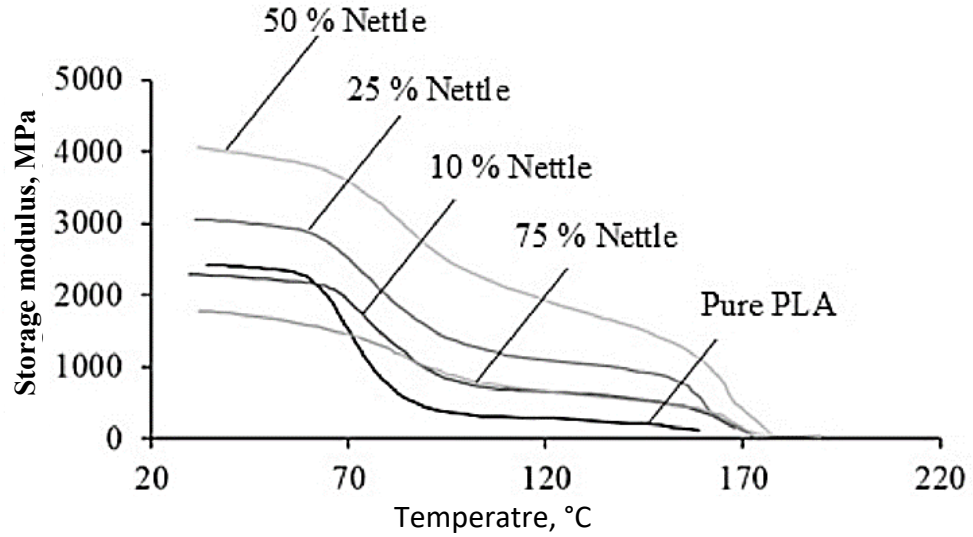

Figure 6. *Variation of storage modulus of nettle/PLA composite. Adapted from [59].*

This composition (nettle/PLA: 50/50) exhibited the best properties among PLA/nettle composites. In comparison to composites with other fibres, the kenaf/PLA composite initially exhibited higher tensile strength than the nettle/PLA composite. However, at higher fibre loadings, the nettle composite subsequently surpassed it due to its superior tensile properties. On the other hand, the nettle/PLA composite showed poorer properties compared to banana/PLA and

glass/PLA composites [73]. However, as the fibre loading increases, nettle/PLA composites can surpass kenaf/PLA in tensile properties due to better reinforcement effects at optimal ratios. This trend where mechanical properties increase with fibre content up to an optimum point and then decrease is common among natural fibre-reinforced PLA systems [63,74]. For instance, hybrid PLA composites containing banana or glass fibres have been reported to achieve even greater tensile strengths (up to 79 MPa for PLA/banana/sisal hybrids), attributed largely to superior interfacial bonding and compatibility especially when silane coupling agents are used.

Another study investigated the use of Himalayan nettle (*Girardinia Diversifolia*) as a filler in polyester composites [10,75], examining the influence of fibre loading on physical and mechanical properties. Composite samples with 5, 10, 15 and 20 wt.% fibre were produced using the conventional hand layup method. The results showed that as the fibre loading increased, void fraction and micro spaces within the composite increased up to 75 % when compared to that of the neat polyester sample. The incorporation of natural fibre also increased the hydrophilicity of the composite. Water absorption rose from 0.58 % in neat polyester to 7.04 % in composites with 20 wt.% fibre. Tensile strength improved from 18 MPa in neat polyester to 31 MPa at 15 wt.% fibre loading but decreased to 29 MPa (a 6.45 % reduction) at 20 % fibre content. The authors argued that up to 15 wt.% fibre loading, stress was transferred uniformly throughout the composite. However, beyond this point, the polyester matrix was insufficient to effectively transfer the load, leading to non-uniform stress distribution and a decrease in tensile strength. In terms of hardness, the sample with the highest fibre loading (20 wt.%) exhibited the highest value of 24.91 Hv, whereas the 100 % polyester sample had the lowest value of 17.24 Hv. This indicates that composite hardness increases with the increase in the nettle fibre content, as hardness depends on both the relative weight and the Young's modulus of the fibres. Similarly, impact strength increased with fibre loading up to 15 wt.%, likely because stronger coupling between interlaced fibre bundles requires more energy to break the composite. Beyond 15 wt % fibre loading, impact strength decreased slightly either because of fibre slippage or fiber/matrix pull out [75].

6.1. 1. Hybridized composites

Research has been conducted on hybridized composites [62] utilizing low-density polyethylene (LDPE) as the matrix (density 0.94 g cm^{-3}) with a hybridized woven fabric of wool and nettle serving as a filler. The plain hybridized woven fabric was manufactured by placing alternate wool and nettle fibres in the warp direction and using nettle as the weft. As LDPE is a non-polar substance and the nettle/wool hybridized fabric is a polar material, the resulting composite showed poor interfacial adhesion [10]. To improve the interphase, chemical modification of the hybridized fabric was performed by adding 2 % NaOH, which modified the surface topography resulting in the increase of the fibre's surface roughness. This also resulted in enhanced mechanical interlocking, or the physical connection between the fibres and the matrix material. The treatment further removed surface impurities from the fibre, showing a clean fibre surface. The fibre loading for the composite was kept at 15, 2 and 25 wt.% for both chemically treated and untreated samples. Comparison of the mechanical properties revealed that the tensile strength of the composites increased with fibre loading up to 20 wt.%. This improvement may be due to the higher proportion of the hybridized fabric in the composite. Additionally, a reduction in tensile strength was observed at higher fibre loadings: 4 % in the untreated sample and 5 % in the treated sample. The value of the resultant composite exceeded that of the clean LDPE sample. The decrease in strength with increased fibre loading may be due to weak adhesion between fibre and matrix at higher weight percentages. Higher fibre loading also resulted in interface microcrack formation and non-uniform stress transfer due to matrix-fibre agglomeration [76,77].

Besides, the modulus of the composite and proportion of nettle/wool fibre increased simultaneously. According to the authors, this occurred due to increased rigidity of the composite caused by a greater amount of the total nettle/wool component in the hybridized composite. The increase in the nettle/wool component proportion restricted the matrix mobility in the composite. A group of researchers reported a similar increase in hardness with an increase in fibre loading [78,79]. A comparison of chemical treatment performance showed that at a fibre loading of 20 wt.%, the modulus of the chemically treated sample increased by 1.6 %. Chemical treatment enhanced fibre uniformity and reduced the surface impurities. An analogous pattern was noted for flexural strength, which was found to increase with

nettle/wool fibre content up to 20 wt.%, similarly to tensile strength. However, increasing the proportion beyond 20% weakened the composite, leading to a reduction in flexural strength. The researchers considered that this observation may have been due to defects caused by tensile and compressive stresses generated during flexural tests. High stress intensity at the ends of the fibre led to poor matrix adhesion with the nettle/wool hybridized fibre. Still, the flexural strength values were greater than those determined for a neat LDPE sample. Finally, it was concluded that reinforcing with 20 % hybridized fibre resulted in optimal properties of the composite [62].

In one of the studies on hybridized epoxy composites, samples were manufactured using nettle and Bauhinia-vahlii fibres [63]. Mono and hybridized epoxy composites were produced with fibre weight percentages of 2, 4 and 6 %. Both fibre types were treated with a 5 % NaOH solution at room temperature for 6 h. resulting in improved mechanical properties. After the treatment, bidirectional mats were prepared manually. The composites were then fabricated using the hand layup method by alternating layering the fibres and a mixture of epoxy and a hardener (10:1) in a mold. The mold was subsequently kept under a pressure of 12 kg at room temperature for 24 h. Examination of the physical and mechanical characteristics revealed that the void fraction of the composite increased with the increase in the fibre content, which was attributed to the hollow structure of the fibres. However, the water absorption capacities also increased due to the hydrophilic in nature of the fibres. The tensile strength of the composites also increased with the increase in the fibre content. In all three composite types (nettle/epoxy, bauhinia/epoxy, and hybridized composite), the composite with the maximum fibre content exhibited the highest tensile properties. This can be attributed to improved adhesion between the fibre and matrix as the fibre content increases. Bauhinia/epoxy composite was reported to be stronger than nettle/epoxy composite due to the higher surface roughness of the bauhinia fibre. Furthermore, the hybridized (nettle/bauhinia) composite showed higher tensile strength than the mono-fibre composites. The highest tensile strength, 34.04 MPa, was exhibited by the 6% hybridized composite, which was ~55, 33 and 8 % greater than that of neat epoxy, nettle/epoxy and bauhinia/epoxy composites at the same fibre content. A similar trend was observed in the flexural characteristics of the composites [63].

6. 2. TEXTILE INDUSTRY

Nettle fibre can be used to produce eco-friendly fabrics for clothing, upholstery, and other textiles due to its strength, durability, and breathability [80]. Nettle fibre is gaining recognition in the textile industry as a sustainable and eco-friendly alternative to synthetic fibres and conventional natural fibres, such as cotton or flax. Harvested from the stems of the nettle plant (*Urtica dioica*), this fibre has been used historically in fabric production but has seen a resurgence due to its environmental benefits and favourable properties, making it an ideal candidate for a range of textile applications. Fabrics made from nettle fibre are resilient and can withstand wear and tear, making them suitable for long-lasting garments and household items. Upholstery fabrics made from nettle fibre are not only strong but also offer a unique aesthetic and tactile quality, which is ideal for furniture coverings, curtains, and other interior textiles. In addition to its durability, nettle fibre is breathable and thermoregulatory, which makes it particularly suitable for clothing. It allows for good airflow, keeping the wearer cool in warmer conditions and warm in cooler climates. This breathability also contributes to the fabric's ability to wick away moisture, making nettle fibre clothing comfortable for all-day wear [65,66]. Moreover, the production of nettle fibre is inherently sustainable. Furthermore, nettle fibre possesses natural antibacterial properties, making it beneficial for use in textiles that come into direct contact with the skin, such as undergarments and activewear. Its hypoallergenic nature is an added advantage, particularly for sensitive skin [80].

6. 2. 1. Woven fabrics

Nettle fibres have long been incorporated into woven textile materials. Woven fabrics are created by intertwining at least two sets of threads (warp and weft) perpendicular to each other. One notable attempt involved using nettle fibres for towel production, which requires specific characteristics [41]. Fibres intended for towels should ideally possess excellent water absorbency, quick drying, softness, and antibacterial properties. While cotton fibre meets most of these requirements, its slower drying rate can promote microbial growth on the towel. It was reported that blending nettle

with cotton fibres can overcome this problem and also provide the benefit of antimicrobial properties [81], as nettle fibre possesses inherent antimicrobial properties [32]. In the study, nettle was blended with cotton in a 70/30 cotton/nettle mass ratio in two different pile yarns (100 % cotton, 50 % cotton + 50 % modal), and the results were compared with samples made of 100 % cotton and polyester/cotton blend. It was observed that samples with nettle blend dried faster compared to the rest of the samples, possibly due to the hollow structure of nettle fibre, which can act as a natural insulator [82,83]. In addition, although nettle fibre is known for its firm texture, the softness values of the fabric were not decreased when the nettle was used in the weft direction. This could be attributed to the pile warp yarns, composed of either 100 % cotton or 50 % cotton + 50 % modal, which enveloped the relatively coarse nettle yarns and maintained a soft feel. The softness of samples made with modal fibre was significantly lower than that of other samples. On the other hand, the towel hydrophilicity was slightly reduced. After 5 washing cycles, a decrease in antibacterial activity was observed against *Staphylococcus aureus* and *Escherichia coli*. The antibacterial activity is probably due to constituents such as neuphytadiene, an antibacterial compound, and flavonoids, which can form complexes with bacterial cell walls, soluble proteins and extracellular proteins [84,92]. In particular, nettle's strong activity against *S. aureus* may be attributed to its rich content of phenolic compounds, including chlorogenic acid, caffeic acid, rosmarinic acid, and rutin [85].

6. 2. 2. Non-woven fabrics

Nettle fibres have also been explored for use non-woven materials. Nonwovens are engineered fibre structures, often flat, that achieve strength and stability through physical and/or chemical processes, without the use of weaving, knitting, or paper-making techniques. In this context, Kumar and Das [86] investigated the use of nettle fibres in non-woven geotextiles for slope stabilization in combination with poly (lactic acid) fibres. They produced the non-woven geotextile fabric by first creating parallel fibre webs using a carding machine, which were then processed into a non-woven fabric through needle-punching. Before the blending stage on the carding machine, the nettle fibre underwent alkali treatment. The untreated nettle fibre surface was uneven, with the presence of impurities, while the alkali treatment cleaned the outer layer of the fibre (Figure 7). The treatment also improved the processability of the fibre and reduced breakages on the carding machine by increasing the fineness, tensile strength, and elongation at break of the nettle fibre. The nettle and PLA fibres were blended in different proportions (0/100, 25/75, 50/50, 75/25 and 100/0).

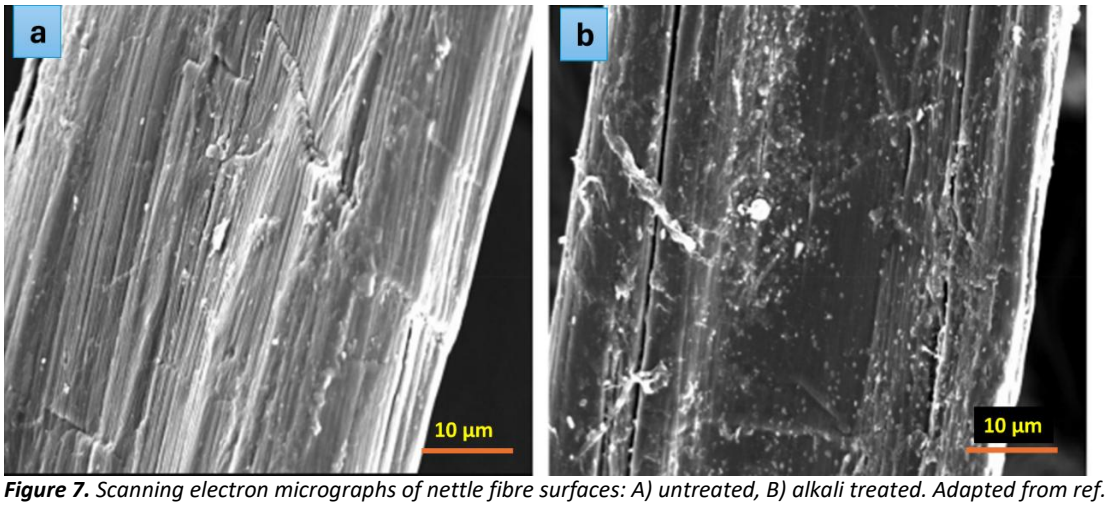

Figure 7. *Scanning electron micrographs of nettle fibre surfaces: A) untreated, B) alkali treated. Adapted from ref. [87] © 2022 Taylor & Francis Group, LLC*

The obtained non-woven geotextiles exhibited a decrease in the tensile strength as the nettle fibre content increased, with the lowest value observed with the 100 % nettle fibre fabric. This is due to the nettle fibre-to-fibre slippage, which increased with the nettle fibre proportion. The resulting fibre-matrix debonding led to the lower tensile strength of the material. Nettle fibre has also shown higher biodegradability than PLA fibres. Also, as the proportion of nettle fibre increased, the residual strength in the non-woven material decreased. For a 100 % nettle sample, only about

11 % of the original strength remained after 40 days and this diminished further after 120 days in the soil burial test. By contrast, 100 % PLA samples retained 70 % of their strength after 40 days and 59 % after 120 days. These results indicate that nettle fibre is significantly more biodegradable than PLA fibres. Overall, the prepared non-woven geotextile showed potential for use in slope stabilization.

Researchers have also developed nettle/polypropylene blended needle-punched non-woven fabrics for oil spill clean-up applications [38]. The study tested these fabrics with crude oil and diesel engine oil of specified viscosities and densities. Nettle fibres were trimmed to a 65 mm staple length, opened and then blended with 60 mm polypropylene fibres using a carding machine; the resulting webs were further needle-punched to produce the non-woven fabric. The study included 15 different samples prepared under varying process parameters: fabric weight (200, 300 and 400 g m^{-2}), punch density (150, 250,and 350 punches cm^{-2}) and nettle/polypropylene blend mass ratio (30:70, 50:50, and 70:30). It was shown that the fabric sorption capacity was affected by density, functional groups, and buoyancy characteristics (fabric's ability to float on a liquid surface) [88]. For both crude and diesel oil, it was found that the nonwoven fabric can be reused multiple times; however, a significant decrease in oil sorption capacity was observed after eight cycles.

In another study, an eco-friendly nettle non-woven sorbent for oil was developed [65]. Nettle fibres were treated with 2 % NaOH at room temperature, aligned on a carding machine and then processed by needle punching to form the non-woven fabric. Samples were prepared with varying needle punch densities (50, 75, 100 punches cm^{-2}), penetration depths (8, 10, 12 mm), and fabric weights (150, 250, 350 g m^{-2}) and were characterised for weight, thickness, and porosity. Results indicated that porosity and thickness were key factors determining the thermal characteristics of the fabric. With an increase in porosity, the volume of the air pocket increased with a consequent increase in thermal insulation. Thus, this led to a reduction in heat and moisture transfer of the clothing system. The water absorption capacity of the non-woven fabric increased with porosity, as greater pore volume allows more water to penetrate the material. Similarly, air permeability rose with an increasing porosity, since permeability is directly related to the amount of open space within the fabric. Among all the samples tested, the highest water absorbency (494 %) and air permeability (79 (cm^3 s^{-1}) cm^{-2}) were obtained with a needle punch density of 75 punches cm^{-2}, penetration depth of 8 mm, and an aerial weight of 150 g m^{-2}. This sample had also shown the highest porosity (0.97) and the lowest thermal conductivity (0.0251 W m^{-1} K^{-1}) [89].

6. 2. 3 Blended fabrics

Researchers have introduced nettle fibre into winter wear clothing [90]. Presently, the market is dominated by wool, an expensive natural fibre. To reduce costs and offer a more affordable solution, acrylic is commonly blended with wool. Replacing these fibres with a sustainable alternative that offers similar properties, such as nettle, presents an attractive option [90,91]. In this study, blends of nettle and acrylic fibres were prepared in different proportions (30/70, 50/50, and 70/30), and yarns of 16^s Ne and 24^s Ne were produced and further characterized for essential properties of winter wear (air permeability, moisture absorption, and thermal insulation). The results showed that increasing the proportion of nettle fibre led to higher air permeability in the blended fabric, as nettle fibre is less bulky than acrylic fibre.

Other researchers [67] have also explored the use of nettle fibre (*Girardina diversifolia*) and its blends. In this study, the extracted fibres were bio-scoured and bio-softened using Scour Zyme L and Celluso ft L enzymes to remove waxes and pectins, thereby making the textile material more hydrophilic. The softening process reduced the flexural rigidity of the fibres by 11 %. The fibres and their blends of a similar count were spun using open-end spinning technology into yarns: 100 % organic cotton, 100 % bamboo, 50/50 nettle/organic cotton, 50/50 nettle/bamboo, which were then used to produce textile fabrics utilizing a handloom. An increase in tensile properties was observed for both nettle/organic cotton (abrasion resistance 3 %, warp strength 4 %, weft strength 11 %, warp elongation 8 %, weft elongation 19 %) and nettle/bamboo blends (abrasion resistance 4 %, warp strength 10 %, weft strength 10 %, warp elongation 7.5 %, weft elongation 7 %). These improvements can be attributed to the higher tensile strength of nettle fibre compared to organic cotton and bamboo fibres [92], while bio-softening of nettles fibre could be the reason for the increase in elongation. The nettle fibre length contributed to the good abrasion resistance of the blended fabric. Based on the observed properties, it was concluded that nettle fibre can be successfully blended with various other fibres and spun in 10^s Ne

yarn. Fabrics produced from this yarn are suitable for home textiles and show potential as candidates for technical textile applications.

6. 2. 4. Geotextiles

In environmental applications, nettle fibre can be used to manufacture geotextiles for erosion control, soil stabilization, and plant growth [93]. Geotextiles made from nettle fibre provide natural alternatives to synthetic geotextiles, which are often derived from petroleum-based materials and pose environmental challenges after disposal. One of the main advantages of nettle fibre geotextiles is their biodegradability, which is especially beneficial in temporary applications, such as erosion control during re-vegetation projects. After fulfilling their role, these geotextiles naturally decompose, reducing long-term environmental impact. Their natural strength enables the formation of durable mats that effectively prevent topsoil displacement by wind, rain, or runoff on slopes, riverbanks, and construction sites. The open structure of nettle geotextiles allows water to permeate through while still providing sufficient reinforcement to stabilize soil, thereby reducing the risk of landslides or soil degradation [64,93]. In addition to erosion control, nettle geotextiles provide a robust and permeable layer that reinforces soil structure, making them suitable for applications such as road construction, embankments, and landscaping where controlling soil movement is critical for structural stability. The fibres' natural durability ensures effective performance during the operational period, offering reliable necessary support until vegetation or other long-term reinforcements become established. Additionally, nettle fibre geotextiles can play a significant role in supporting plant growth. Their porous structure allows roots to penetrate easily, facilitating plant establishment and promoting healthy root systems. The fibres also help retain the soil moisture, creating a more favourable environment for seedlings and vegetation. In reclamation projects or areas requiring reforestation or revegetation, nettle geotextiles can increase the success of planting efforts by shielding young plants from erosion while promoting natural growth. Due to their permeability, nettle fibres allow proper drainage of water, reducing the risk of waterlogging or pooling in the soil. This is critical in geotechnical applications where managing water flow is essential for maintaining soil integrity. The ability of nettle geotextiles to filter, allowing water to pass while preventing soil erosion, makes them highly effective in drainage systems, wetland restoration, and stormwater management. These geotextiles also align with sustainability goals in construction and environmental management [64]. Their use in ecological restoration and civil engineering projects supports the growing demand for green solutions that prioritize environmental responsibility.

6. 2. 5. Medical textiles

Natural antimicrobial properties of nettle fibre make it a valuable and sustainable option for use in medical textiles, including wound dressings, bandages, and other healthcare-related fabrics. Its natural ingredients, such as phenolics and flavonoids, which can inhibit the growth of bacteria, fungi, and other pathogens support hygiene, sterility, and patient comfort in medical settings [3]. Antimicrobial activity can lead to improved healing outcomes and fewer complications during patient recovery. Nettle fibre is also breathable and moisture-wicking, which enhances its suitability for wound care. Its ability to allow airflow while absorbing excess moisture creates an optimal environment for healing, helping to keep wounds optimally moist and reducing the risk of bacterial growth. At the same time, its breathability ensures patient comfort by allowing the skin to remain cool and dry, which is especially important for bandages that are worn for extended periods. In addition to its antimicrobial and moisture-wicking properties, nettle fibre is hypoallergenic, making it safe for use on sensitive or damaged skin. Traditional materials such as polyester or nylon used in medical textiles are not biodegradable, contributing to medical waste and environmental pollution. In contrast, nettle-based textiles can decompose naturally after disposal, reducing their ecological footprint. This characteristic aligns with the growing demand for sustainable solutions in healthcare, especially in reducing the environmental impact of disposable medical products [94]. In terms of durability, nettle fibres are strong and long-lasting, ensuring that nettle-based medical textiles maintain their integrity during use. This is crucial for bandages and dressings that must endure movement and regular handling without tearing or losing their effectiveness. Moreover, nettle fibres can be processed into various forms to suit different medical applications, from soft, absorbent fabrics for

wound dressings to more durable, woven fabrics for support bandages or compression wraps. This versatility makes nettle fibre a flexible and valuable resource for a wide range of medical textiles [94].

6. 3. Ropes and cords

Due to its natural strength and resilience, nettle fibre is suitable for creating ropes, cords, and twine, especially in applications requiring biodegradable materials [98]. Historically, nettle fibres were used for rope-making in various cultures. Today, with an increasing focus on sustainable materials, nettle fibre is regaining attention as an environmentally friendly alternative to synthetic and non-biodegradable fibres. Unlike synthetic ropes made from plastic-based fibres (such as nylon or polypropylene), which contribute to pollution when discarded, nettle fibre ropes naturally decompose over time, reducing their environmental impact. This makes nettle fibre especially valuable in outdoor applications where ropes might be exposed to the elements and left in nature, such as in forestry, hiking, or conservation efforts. One of the advantages of using nettle fibre in ropes and cords is its durability. The fibres are long, strong, and have a high tensile strength, allowing them to withstand significant stresses and strains. This makes nettle fibre ropes suitable for various demanding applications, such as agricultural use, gardening, marine activities, and construction, where robust and reliable materials are essential. Nettle ropes and twines are also lightweight, which makes them easier to handle, and transport compared to some traditional materials [91],[95]. They are also resistant to damage from UV light and water to a degree, further enhancing their versatility in outdoor settings. Furthermore, nettle fibre's natural resistance to mold and microbial growth is beneficial in humid or wet conditions, where ropes are often prone to degradation. This antimicrobial property helps extend the lifespan of nettle-based ropes, particularly in farming, fishing, or other industries that involve moisture [91].

6. 4. Insulation materials

Nettle fibre can be processed into insulation materials for buildings, providing a renewable, non-toxic and eco-friendly alternative to synthetic products such as fibreglass or mineral wool. Its excellent thermal efficiency helps maintain consistent indoor temperatures by reducing heat loss in winter and minimizing heat gain in summer. This improves energy efficiency lowers heating and cooling costs and supports sustainable construction and green building practices by reducing the building’s carbon footprints [91].

In addition to thermal insulation, nettle fibre also provides sound insulation [95]. Its dense structure can effectively absorb sound, making it ideal for use in interior walls, floors, and ceilings to reduce noise transmission between rooms or from outside sources. This dual functionality, thermal and acoustic insulation, adds to the versatility of nettle fibre in building applications. Affirmative sustainability aspects of nettle fibre make it a more sustainable option than many traditional insulation materials, which often rely on non-renewable resources or energy-intensive manufacturing processes. Nettle fibre insulation is therefore ideal for builders and architects looking to minimize environmental impact and promote sustainable construction practices.

Another important feature of nettle panels is their non-toxicity and absence of harmful chemicals. In contrast, many synthetic insulation products contain substances that can release volatile organic compounds (VOCs) or pose health risks to installers and building occupants. Nettle fibre, as naturally safe, is thus, a healthier choice for indoor environments, particularly for people with sensitivities or allergies. Moreover, nettle fibre naturally regulates moisture, adding valuable functionality as an insulation material. It can absorb and release moisture without compromising its insulation properties, helping to maintain indoor air quality and prevent mold growth. This moisture control contributes to a more comfortable and healthier indoor environment [6].

6. 5. Paper production

Nettle fibres are an excellent resource for producing high-quality paper, particularly for specialty applications such as artistic and archival papers. offering an eco-friendly and sustainable alternative to traditional wood-based paper. The long, strong fibres from the nettle plant (*Urtica dioica*) impart durability, a smooth texture and a fine finish to the final product. This makes nettle paper highly suitable for artistic applications, such as fine art prints, handmade stationery,

calligraphy, and bookbinding. The paper's strength also lends itself well to various printing techniques, from screen printing to letterpress, providing a versatile surface for artists and designers [58,96]. Additionally, nettle fibre paper has a distinctive aesthetic, often featuring a natural, slightly textured surface with a pleasant organic appearance, which is especially valued in handmade and specialty papers. The subtle texture and unique look make it a preferred choice for creating high-end products such as luxury packaging, greeting cards, or decorative papers, where a tactile, artisanal quality is desired. Nettle fibre paper is also archivally stable, meaning it resists degradation over time. The fibres are naturally resistant to yellowing and brittleness, making nettle paper suitable for archival purposes, such as preserving documents, artwork, or photographs that need to withstand long-term storage without deteriorating. From an environmental perspective, nettle fibre paper is an appealing option for eco-conscious consumers and industries, looking to reduce the ecological footprint of paper production. Moreover, nettle fibres can be blended with other natural fibres, such as cotton or hemp, to create a range of paper types with different weights, textures, and finishes. This flexibility in processing allows for a wide variety of applications, from delicate, translucent papers for fine art to sturdy, thick papers for packaging or industrial use [6].

6. 6. Sustainable packaging

Nettle fibres offer a promising solution for sustainable packaging, providing a biodegradable and eco-friendly alternative to traditional plastic-based materials [3]. As a demand for environmentally responsible packaging grows [97], nettle fibres are emerging as a versatile renewable resource that can reduce the ecological impact of packaging waste. One of the key advantages of incorporating nettle fibres into packaging materials is their biodegradability. Unlike conventional plastics, which take hundreds of years to decompose and contribute significantly to environmental pollution, nettle-based packaging breaks down naturally over time. This makes it an ideal choice for industries aiming to reduce their reliance on single-use plastics and minimize packaging waste that ends up in landfills or oceans. This makes nettle fibre a more sustainable option compared to packaging materials derived from fossil fuels or intensive agricultural processes. In terms of performance, nettle fibres are known for their strength and durability, which are crucial attributes for packaging materials. Nettle fibre-based packaging can effectively protect products, resisting wear and tear during shipping and handling, while maintaining structural integrity [18]. This makes it suitable for a wide range of applications, from protective packaging for fragile items to flexible wraps for food or consumer goods. Nettle fibre's natural moisture resistance and breathability make it well-suited for packaging applications that require protection from humidity, such as food packaging. These properties help reduce condensation and spoilage, thereby extending the shelf life of perishable goods and providing a natural sustainable solution for the food industry. Furthermore, nettle fibre packaging can be combined with other sustainable materials, such as recycled paper or bio-based films, to create composite packaging solutions that meet specific needs. Whether for rigid containers, flexible wraps, or cushioning materials, nettle fibres can be integrated into various packaging forms, providing versatility and adaptability across sectors [97]. Another advantage of nettle-based packaging is its lightweight nature, which can reduce shipping costs and energy use during transportation. Lightweight yet strong, nettle fibre packaging minimizes the environmental footprint associated with logistics, particularly for companies aiming to optimize their supply chains and reduce carbon emissions. In addition to its practical benefits, nettle fibre packaging is also appealing from a consumer perspective. As awareness of environmental issues grows, consumers are increasingly seeking eco-friendly products and packaging solutions. Packaging made from natural fibres such as nettle not only aligns with consumer preferences for sustainability but also conveys a brand's commitment to reducing its environmental impact.

7. CONCLUSIONS AND FUTURE PERSPECTIVES

This manuscript reviewed the use of nettle fibre in different textile industry sectors. Nettle fibre is notable for its high strength and is a promising material for both apparel and technical textiles. Significant research has demonstrated its potential in woven and non-woven fabrics, as well as composite materials Its combination of length, high tensile strength, and Young's modulus make it suitable for a wide range of applications. Additionally, nettle fibres are relatively

inexpensive, derived from renewable resources, and fully biodegradable. However, challenges remain due to inherent rigidity and variability of these fibres, which are influenced by growth conditions and plant maturity.

Further research is needed to expand the applications and improve the properties of nettle fibres. Investigations into fibre treatments could make them softer and more suitable for apparel use. One of the most promising directions is the reinforcement of polymeric composites, particularly through hybridization, which may overcome current limitations and enable high-end applications. Detailed studies of surface modifications could improve interfacial properties in fibre-reinforced composites, while comparative analysis with other natural fibres using the same matrix would be valuable. In addition to mechanical performance, research should also address damping, tribological, and machining properties, as well as biodegradability and thermal insulation. Finally, the potential of nettle fibres as biomaterials for adsorption warrants further exploration.

Conflicts of Interest: *The authors whose names are listed immediately below certify that they have no conflict of interest with anyone in the subject matter or materials discussed in this manuscript.*

Acknowledgments: *We wish to express our gratitude for the technical assistance provided by the Central Research Facility (CRF) at the Indian Institute of Technology Delhi, India.*

Data availability: *Data sharing is not applicable to this article as no new data were created or analysed in this study.*

REFERENCES

[1] Agus Suryawan IGP, Suardana NPG, Suprapta Winaya IN, Budiarsa Suyasa IW, Tirta Nindhia TG. Study of stinging nettle (Urtica dioica l.) Fibers reinforced green composite materials. *IOP Conf Ser: Mater Sc. Eng.* 2017; 201 012001. https://doi.org/10.1088/1757-899X/201/1/012001

[2] Srivastava N, Rastogi D, Fibers Uttarakhand: A State Rich in Plant Fibers. *J Nat Fibers.* 2020; 17(6): 861-876. https://doi.org/10.1080/15440478.2018.1534193

[3] Angel M, Subramanian G, Muthu S. Great potential of stinging nettle for sustainable textile and fashion. In: Gardetti MA, Muthu SS, eds. Handbook of Sustainable Luxury Textiles and Fashion: Volume 1, Springer Singapore, 2015: 43–57. https://doi.org/10.1007/978-981-287-633-1_3

[4] Yu C, Franck RR. Pineapple, curauá, craua (caroá), macambira, nettle, sunn hemp, Mauritius hemp and fique. In: Franck RE, ed. Bast and Other Plant Fibres, Woodhead Publishing, 2005: 322-344. https://doi.org/10.1533/9781845690618.322

[5] Srivastava N, Rastogi D. Nettle fiber: Himalayan wonder with extraordinary textile properties. *IJHS* 2018; 4(1): 281-285, https://www.homesciencejournal.com/archives/2018/vol4issue1/PartE/4-1-57-662.pdf

[6] Vogl CR, Hartl A. Production and processing of organically grown fiber nettle (*Urtica dioica* L.) and its potential use in the natural textile industry. AJAA. 2003; 18(3): 119-128. https://doi.org/10.1079/AJAA200242

[7] Harwood J, Edom G. Nettle fibre: its prospects, uses and problems in historical perspective. *Text Hist.* 2012; 43(1): 107–19. https://doi.org/10.1179/174329512X13284471321244

[8] Lanzilao G. Properties and Applications of Himalayan Nettle Fibre. PhD Thesis, University of Leeds, 2015

[9] Samanta KK. Applications of nettle fibre in textile: a brief review. *Int J Bioresour Sci.* 2021;8(1). https://doi.org/10.30954/2347-9655.01.2021.6

[10] Pokhriyal M, Prasad L, Raturi HP. An experimental investigation on mechanical and tribological properties of Himalayan nettle fiber composite. *J Nat Fiber.* 2018; 15(5): 752-761. https://doi.org/10.1080/15440478.2017.1364202

[11] Di Virgilio N, Papazoglou EG, Jankauskiene Z, Di Lonardo S, Praczyk M, Wielgusz K. The potential of stinging nettle (*Urtica dioica* L.) as a crop with multiple uses. *Ind Crops Prod.* 2015; 68(1-2): 42-49. https://doi.org/10.1016/j.indcrop.2014.08.012

[12] Bacci L, Di Lonardo S, Albanese L, Mastromei G, Perito B. Effect of different extraction methods on fiber quality of nettle (*Urtica dioica* L.). *Text Res J.* 2011; 81(8): 827-837. https://doi.org/10.1177/0040517510391698

[13] Mahendrakumar N, Ramaswamy TP, Venkatachalam PM, Sabareeswaran A, Biswal RM, Srivatsan S. Mechanical and dynamic properties of nettle-polyester composite. *Mater Express.* 2015; 5(6): 505-517. https://doi.org/10.1166/mex.2015.1263

[14] Lanzilao G, Goswami P, Blackburn RS. Study of the morphological characteristics and physical properties of Himalayan giant nettle (*Girardinia diversifolia* L.) fibre in comparison with European nettle (*Urtica dioica* L.) fibre. *Mater Lett.* 2016; 181(11): 200203. https://doi.org/10.1016/j.matlet.2016.06.044

[15] Viotti C, Albrecht K, Amaducci S, Bardos P, Bertheau C, Blaudez D, Bothe L, Cazaux D, Ferrarini A, Govilas J, Gusovius HJ, Jeannin T, Lühr C, Müssig J, Pilla M, Placet V, Puschenreiter M, Tognacchini A, Yung L, Chalot M. Nettle, a Long-Known Fiber Plant with New Perspectives. *Materials.* 2022;.15(12):.4288. https://doi.org/10.3390/ma15124288.

[16] Raj M, Fatima S, Tandon N. An experimental and theoretical study on environment-friendly sound absorber sourced from nettle fibers. *J Build Eng.* 2020;.31:.101395. https://doi.org/10.1016/j.jobe.2020.101395

[17] Hartl A, Vogl CR. Fiber yield and quality of fiber nettle (*Urtica dioica* L.) cultivated in Italy. *Ind Crops Prod.* 2009;.29(2-3): 480-484. https://doi.org/10.1079/ajaa200226

[18] Thyavihalli Girijappa YG, Mavinkere Rangappa S, Parameswaranpillai J, Siengchin S. Natural Fibers as Sustainable and Renewable Resource for Development of Eco-Friendly Composites: A Comprehensive Review. *Front Mater.* 2019; 6: 481024. https://doi.org/10.3389/fmats.2019.00226

[19] Mahendrakumar N, Thyla PR, Mohanram PV, Sabareeswaran A, Manas RB, Srivatsan S. Mechanical and dynamic properties of nettle-polyester composite. *Mater Express.* 2015;.5(6):.505-517. https://doi.org/10.1166/mex.2015.1263

[20] Rigneault H, Kumar NG, Cossart R, Septier D, Brévalle-Waslilewki G, Kudlinski A, Kaszas A. Investigation of the use of stinging nettle fibres (Urtica Dioica) for polymer reinforcement: Study of single fibre tensile properties. *Focus on Microscopy* 2008; (1): 255. https://doi.org/10.34894/VQ1DJA

[21] Baley C. Analysis of the flax fibres tensile behaviour and analysis of the tensile stiffness increase. *Compos Part A Appl Sci Manuf* .2002; 33(7): 939-948. https://doi.org/10.1016/S1359-835X(02)00040-4

[22] Eichhorn SJ, Young RJ. Composite micromechanics of hemp fibres and epoxy resin microdroplets. *Compos Sci Technol.* 2004; 64(5): 767-772. https://doi.org/10.1016/j.compscitech.2003.08.002

[23] Brahmakumar M, Pavithran C, Pillai RM. Coconut fibre reinforced polyethylene composites: effect of natural waxy surface layer of the fibre on fibre/matrix interfacial bonding and strength of composites. *Compos Sci Technol.* 2005; 65(3-4):563-569. https://doi.org/10.1016/j.compscitech.2004.09.020

[24] Suresh Kumar SM, Duraibabu D, Subramanian K. Studies on mechanical, thermal and dynamic mechanical properties of untreated (raw) and treated coconut sheath fiber reinforced epoxy composites. *Mater Des.* 2014; 59(1): 63-69. https://doi.org/10.1016/j.matdes.2014.02.013

[25] Shahinur S, Hasan M, Ahsan Q, Saha DK, Islam MS. Characterization on the Properties of Jute Fiber at Different Portions. *Int J Polym Sci.* 2015; 2015(1): 262348. https://doi.org/10.1155/2015/262348

[26] Goda K, Sreekala MS, Gomes A, Kaji T, Ohgi J. Improvement of plant based natural fibers for toughening green composites-Effect of load application during mercerization of ramie fibers. *Compos A.* 2006; 37(12): 2213-2220. https://doi.org/10.1016/j.compositesa.2005.12.014

[27] Liu M, Thygesen A, Summerscales J, Meyer AS. Targeted pre-treatment of hemp bast fibres for optimal performance in biocomposite materials. *Ind Crops Prod.* 2017;.108(1):.660-683. https://doi.org/10.1016/j.indcrop.2017.07.027

[28] Charlet K, Eve S, Jernot JP, Gomina M, Breard J. Tensile deformation of a flax fiber. *Procedia Eng* .2009;.1(1):.233-236. https://doi.org/10.1016/j.proeng.2009.06.055

[29] Bodros E, Baley C. Study of the tensile properties of stinging nettle fibres (*Urtica dioica*). *Mater Lett.* 2008;.62(14):.2143-2145. https://doi.org/10.1016/j.matlet.2007.11.034

[30] Bergfjord C, Mannering U, Frei KM, Gleba M, Scharff AB, Skals I, Heinemeier J, Nosch ML, Holst B. Nettle as a distinct Bronze Age textile plant. *Sci Report.* 2012; 2(1): 664. https://doi.org/10.1038/srep00664

[31] Bergfjord C, Holst B. A procedure for identifying textile bast fibres using microscopy: Flax, nettle/ramie, hemp and jute. *Ultramicroscopy.* 2010; 110(9): 1192-1197. https://doi.org/10.1016/j.ultramic.2010.04.014

[32] Gülçin I, Küfrevioğlu ÖI, Oktay M, Büyükokuroğlu ME. Antioxidant, antimicrobial, antiulcer and analgesic activities of nettle (*Urtica dioica* L.). *J Ethnopharmacol.* 2004; 90(2-3): 205-215. https://doi.org/10.1016/j.jep.2003.09.028

[33] Arık B, Yavas A, Avinc O. Antibacterial and wrinkle resistance improvement of nettle biofiber using chitosan and BTCA. *Fibres Text East Eur.* 2017; 25(3): 106-111. https://doi.org/10.5604/12303666.1237245

[34] Zeković Z, Cvetanović A, Švarc-Gajić J, Gorjanović S, Sužnjević D, Mašković P, Savić S, Radojković M, Đurović S. Chemical and biological screening of stinging nettle leaves extracts obtained by modern extraction techniques. *Ind Crops Prod.* 2017; 108(5): 423-430. https://doi.org/10.1016/j.indcrop.2017.06.055

[35] Jussila K. Clothing Physiological Properties of Cold Protective Clothing and Their Effects on Human Experience, PhD Thesis, 2016. https://urn.fi/URN:ISBN:978-952-15-3708-0

[36] Yavas A, Avinc O, Gedik G. Ultrasound and microwave aided natural dyeing of nettle biofibre (*Urtica dioica* L.) with madder (*Rubia tinctorum* L.). *Fibres Text East Eur.* 2017; 25(4): 111-120. https://doi.org/10.5604/01.3001.0010.2855

[37] Jeannin T, Yung L, Evon P, Labonne L, Ouagne P, Lecourt M, Cazaux D, Chalot M, Placet V. Are nettle fibers produced on metal-contaminated lands suitable for composite applications? *Mater Today Proc.* 2020; 31(6414): S291-S295. https://doi.org/10.1016/j.matpr.2020.01.365

[38] Brindha R, Thilagavathi G, Viju S. Development of Nettle-Polypropylene-Blended Needle-Punched Nonwoven Fabrics for Oil Spill Cleanup Applications. *J Nat Fiber.* 2020; 17(10): 1439-1453. https://doi.org/10.1080/15440478.2019.1578717

[39] Samanta KK, Roy AN, Baite H, Debnath S, Ammayappan L, Nayak LK, Singha A, Kundu TK. Properties of Himalayan Nettle Fiber and Development of Nettle/Viscose Blended Apparel Textiles. *J Nat Fiber.* 2023; 20(1) 2183924. https://doi.org/10.1080/15440478.2023.2183924

[40] Kumar N, Das D. Alkali treatment on nettle fibers: Part I: investigation of chemical, structural, physical, and mechanical characteristics of alkali-treated nettle fibers. *J Text Inst.* 2017; 108(8): 1461-1467. https://doi.org/10.1080/00405000.2016.1257346

[41] Sabir EC, Zervent Ünal B. The Using of Nettle Fiber in Towel Production and Investigation of the Performance Properties. *J Nat Fiber.* 2017; 14(6): 781-787. https://doi.org/10.1080/15440478.2017.1279102

[42] Vogl CR, Hartl A. Production and processing of organically grown fiber nettle (*Urtica dioica* L.) and its potential use in the natural textile industry. *AJAA* 2003; 18(3): 119-128. https://doi.org/10.1079/AJAA200242
[43] Ketema A, Worku A. Antibacterial Finishing of Cotton Fabric Using Stinging Nettle (*Urtica dioica* L.) Plant Leaf Extract. *J Chem.* 2020: 4049273. https://doi.org/10.1155/2020/4049273
[44] Md. Tahir P, Ahmed AB, SaifulAzry SOA, Ahmed Z. Retting process of some bast plant fibres and its effect on fibre quality: A review. *Bioresources* 2011; 6(4): 5260-5281. https://doi.org/10.15376/biores.6.4.5260-5281
[45] Lee CH, Khalina A, Lee SH, Liu M. A Comprehensive Review on Bast Fibre Retting Process for Optimal Performance in Fibre-Reinforced Polymer Composites. *Adv Mater Sci Eng.*2020: 6074063. https://doi.org/10.1155/2020/6074063
[46] Samanta KK, Roy AN, Baite H, Debnath S, Ammayappan L, Nayak LK, Singha A, Kundu TK. Properties of Himalayan Nettle Fiber and Development of Nettle/Viscose Blended Apparel Textiles. *J Nat Fiber.* 2023; 20(1): 2183924. https://doi.org/10.1080/15440478.2023.2183924
[47] Mukhopadhyay S, Fangueiro R, Shivankar V. Variability of Tensile Properties of Fibers from Pseudostem of Banana Plant. *Text Res J.* 2009; 79(5): 387-393. https://doi.org/10.1177/0040517508090479
[48] Banerjee PK. Environmental textiles from jute and coir. In: Kozłowski RM, ed. *Handbook of Natural Fibres: Vol 2*, Woodhead Publishing, 2012, 401-427. https://doi.org/10.1533/9780857095510.2.401
[49] Sisti L, Totaro G, Vannini M, Celli A. Retting Process as a Pretreatment of Natural Fibers for the Development of Polymer Composites. In: Kalia S, ed. *Lignocellulosic Composite Materials. Springer Series on Polymer and Composite Materials*. Springer, 2018: 97-135. https://doi.org/10.1007/978-3-319-68696-7_2
[50] Šimončicová J, Kryštofová S, Medvecká V, Ďurišová K, Kaliňáková B. Technical applications of plasma treatments: current state and perspectives. *Appl Microbiol Biotechnol.* 2019; 103(13): 5117-5129. https://doi.org/10.1007/s00253-019-09877-x
[51] Tabares FL, Junkar I. Cold plasma systems and their application in surface treatments for medicine. *Molecules.* 2021; 26(7): 1903. https://doi.org/10.3390/molecules26071903
[52] Tadele GA. Separation and characterization of Ethiopian origin nettle fiber. *IJERT* 2016; 5(3): 259-262. https://www.ijert.org/research/separation-and-characterization-of-ethiopian-origin-nettle-fiber-IJERTV5IS030301.pdf
[53] Bacci L, Di Lonardo S, Albanese L, Mastromei G, Perito B. Effect of different extraction methods on fiber quality of nettle (*Urtica dioica* L.). *Text Res J.* 2011; 81(8): 827-837. https://doi.org/10.1177/0040517510391698
[54] Lee CH, Khalina A, Lee SH, Liu M. A Comprehensive Review on Bast Fibre Retting Process for Optimal Performance in Fibre-Reinforced Polymer Composites. *Advance Mat Sci Eng.* 2020; (1): 6074063. https://doi.org/10.1155/2020/6074063
[55] Bajpai PK, Meena D, Vatsa S, Singh I. Tensile Behavior of Nettle Fiber Composites Exposed to Various Environments. *J Nat Fibe.r* 2013; 10(3): 244-256. https://doi.org/10.1080/15440478.2013.791912
[56] Hayles CS. Environmentally sustainable interior design: A snapshot of current supply of and demand for green, sustainable or Fair Trade products for interior design practice. *IJSBE* 2015; 4(1): 100-108. https://doi.org/10.1016/j.ijsbe.2015.03.006
[57] Summerscales J, Dissanayake NPJ, Virk AS, Hall W. A review of bast fibres and their composites. Part 1 – Fibres as reinforcements. *Compos Part A Appl Sci Manuf.* 2010; 41(10): 1329-1335. https://doi.org/10.1016/j.compositesa.2010.06.001
[58] Zimniewska M, Wladyka-Przybylak M, Mankowski J. Cellulosic Bast Fibers, Their Structure and Properties Suitable for Composite Applications. In: Kalia S, Kaith BS, Kaur I, eds. *Cellulose Fibers: Bio- and Nano-Polymer Composites, 1st edition,* Springer, Berlin, Heidelberg, 2011: 97-119. https://doi.org/10.1007/978-3-642-17370-7_4
[59] Kumar N, Das D. Fibrous biocomposites from nettle (Girardinia diversifolia) and poly(lactic acid) fibers for automotive dashboard panel application. *Compos B.* 2017; 130: 54–63. https://doi.org/10.1016/j.compositesb.2017.07.059
[60] Beenu Singh MG. Chemical treatment of nettle ribbons and its effect on tensile property of extracted fiber. *Int J Chem Stud.* 2020; 8(4): 1440-1443. https://doi.org/10.22271/chemi.2020.v8.i4m.9817
[61] Paukszta D, Mańkowski J, Kołodziej J, Szostak M. Polypropylene (PP) Composites Reinforced with Stinging Nettle (*Utrica dioica* L.) Fiber. *J Nat Fibe.r* 2013; 10(2): 147-158. https://doi.org/10.1080/15440478.2013.789287
[62] Yallew TB, Kumar P, Singh I. Mechanical Behavior of Nettle/Wool Fabric Reinforced Polyethylene Composites. *J Nat Fiber.* 2016; 13(5): 610-618. https://doi.org/10.1080/15440478.2015.1093576
[63] Kumar S, Mer KKS, Gangil B, Patel VK. Synergistic effect of hybrid Himalayan Nettle/Bauhinia-vahlii fibers on physico-mechanical and sliding wear properties of epoxy composites. *Def Technol.* 2020; 16(4): 762-776. https://doi.org/10.1016/j.dt.2019.08.006
[64] Kumar N, Das D. Nonwoven geotextiles from nettle and poly(lactic acid) fibers for slope stabilization using bioengineering approach. *Geotext Geomembr.* 2018; 46(2): 206-213. https://doi.org/10.1016/j.geotexmem.2017.11.007
[65] Viju S, Fibers GT-J of N, 2022 undefined. Comfort characteristics of nettle nonwoven fabrics. *J Nat Fiber.* 2022; 19(4): 1490-1497. https://doi.org/10.1080/15440478.2020.1779899
[66] Dastjerdi R. New features of silver/zinc loaded nanocomposite textiles; dyeability, abrasion resistance and comfort. *J Eng Fiber Fabr.* 2014; 9(4): 39-44. https://doi.org/10.1177/155892501400900405
[67] Radhakrishnan S. Development of Fabric from Girardina Diversifolia Stem Fibres and its Blends. *IJIRSET*. 2007; 49(11): 10499-15006. https://doi.org/10.15680/IJIRSET.2015.0411023
[68] Samal SK, Mohanty S, Nayak SK. Banana/glass fiber-reinforced polypropylene hybrid composites: Fabrication and performance evaluation. *PPTEn.* 2009; 48(4): 397-414. https://doi.org/10.1080/03602550902725407

[69] Arbelaiz A, Fernández B, Cantero G, Llano-Ponte R, Valea A, Mondragon I. Mechanical properties of flax fibre/polypropylene composites. Influence of fibre/matrix modification and glass fibre hybridization. *Compos A.* 2005; 36(12): 1637-1644. https://doi.org/10.1016/j.compositesa.2005.03.021

[70] Zampaloni M, Pourboghrat F, Yankovich SA, Rodgers BN, Moore J, Drzal LT, Mohanty AK, Misra M. Kenaf natural fiber reinforced polypropylene composites: A discussion on manufacturing problems and solutions. *Compos Part A Appl Sci Manuf.* 2007; 38(6): 1569-1580. https://doi.org/10.1016/j.compositesa.2007.01.001

[71] Fischer H, Werwein E, Graupner N. Nettle fibre (*Urtica dioica* L.) reinforced poly(lactic acid): A first approach. *J Compos Mater.* 2012; 46(24): 3077-3087. https://doi.org/10.1177/0021998311435676

[72] Vouyiouka SN, Papaspyrides CD. Mechanistic Aspects of Solid-State Polycondensation. *Polymer Science A.* 2012; 4: 857-874. https://doi.org/10.1016/B978-0-444-53349-4.00126-6

[73] Wang W, Lowe A, Kalyanasundaram S. Effect of Chemical Treatments on Flax Fibre Reinforced Polypropylene Composites on Tensile and Dome Forming Behaviour. *Int J Mol Sci.* 2015; 16(3): 6202-6216. https://doi.org/10.3390/ijms16036202

[74] Dabi GG, Wakjira YT, Feysa HE, Abebe wondwossen M. Development and characterization of laminated fiber reinforced bio-Composite From nettle and poly lactic acid fiber. *J Ind Text.* 2022: 52. https://doi.org/10.1177/15280837221118064

[75] Getme AS, Patel B. A Review: Bio-fiber's as reinforcement in composites of polylactic acid (PLA). *Mater Today Proc.* 2020; 26: 2116-2122. https://doi.org/10.1016/j.matpr.2020.02.457

[76] Senthil Kumar J, Thamizhvalavan P, Balasubramanian M, Rajkumar S. Enhanced mechanical performance and failure mechanisms of woven glass fiber-reinforced polymer composites with optimized multi-walled carbon nanotube reinforcement. *Polym Compos*. 2025; 46(S3): S743-5754. https://doi.org/10.1002/pc.29995

[77] Saravanakumar K, Arumugam V, Souhith R, Santulli C. Influence of milled glass fiber fillers on mode I & mode II interlaminar fracture toughness of epoxy resin for fabrication of glass/epoxy composites. *Fibers.* 2020; 8(6): 36. https://doi.org/10.3390/FIB8060036

[78] Atuanya CU, Edokpia RO, Aigbodion VS. The physio-mechanical properties of recycled low density polyethylene (RLDPE)/bean pod ash particulate composites. *Res Phys.* 2014; 4: 88-95. https://doi.org/10.1016/j.rinp.2014.05.003

[79] Atuanya CU, Nwaigbo SC, Igbokwe PK. Effects of Breadfruit Seed Hull Ash Particles on Microstructures and Properties of Recycled Low Density Polyethylene/Breadfruit Seed Hull Ash Composites. *J Mat Sci Eng.* 2013; 2(1): 792-802. https://doi.org/10.4172/2169-0022.1000116

[80] Li X, Panigrahi S, Tabil LG. A study on flax fiber-reinforced polyethylene biocomposites. *Appl Eng Agric.* 25(4): 525-531. https://doi.org/10.13031/2013.27454

[81] Ketema A, Worku A. Antibacterial Finishing of Cotton Fabric Using Stinging Nettle (*Urtica dioica* L.) Plant Leaf Extract. *J Chem.* 2020: 4049273. https://doi.org/10.1155/2020/4049273

[82] Sinha SK, Sharma A, Maity S. Thermal Resistance and Moisture Management Behaviour of Nettle/Polyester Nonwoven Fabrics. *Tekstilec.* 2009; 62(4): 258-268. https://doi.org/10.14502/tekstilec2019.62.258-268

[83] Vishwajeet, Majumdar A, Gupta D, Majumdar A. Structure and properties of fibres extracted from Himalayan nettle (*Girardinia diversifolia*). *J Ind Crop.* 2024; 222(5) 120091, *https://doi.org/10.1016/j.indcrop.2024.120091*

[84] Salih NA. Antibacterial effect of nettle (*Urtica dioica*). *Al-Qadisiyah J Vet Med Sci.* 2014; 13(1): 1. https://doi.org/10.29079/vol13iss1art270

[85] Zenão S, Aires A, Dias C, Saavedra MJ, Fernandes C. Antibacterial potential of Urtica dioica and Lavandula angustifolia extracts against methicillin resistant Staphylococcus aureus isolated from diabetic foot ulcers. *J Herb Med.* 2017; 10(2): 53-58. https://doi.org/10.1016/j.hermed.2017.05.003

[86] Kumar N, Das D. Nonwoven geotextiles from nettle and poly(lactic acid) fibers for slope stabilization using bioengineering approach. *Geotext Geomembranes.* 2018; 46(2): 206-213. https://doi.org/10.1016/j.geotexmem.2017.11.007

[87] Pankaj, Jawalkar C, Kant S. Study on Mechanical Properties and Delamination Factor Evaluation of Chemically Treated Nettle Fiber Reinforced Polymer Composites. *J Nat Fiber.* 2023; 20(1): 2135053. https://doi.org/10.1080/15440478.2022.2135053

[88] Wei QF, Mather RR, Fotheringham AF, Yang RD. Evaluation of nonwoven polypropylene oil sorbents in marine oil-spill recovery. *Mar Pollut Bull.* 2003; 46(6): 780-783. https://doi.org/10.1016/S0025-326X(03)00042-0

[89] Viju S, Thilagavathi G. Hot Water Treatment on Nettle Fibers: An Environment-Friendly/Economical Process for the Production of Oil Sorbent. *J Nat Fiber.* 2022; 19(2): 761-769. https://doi.org/10.1080/15440478.2020.1761929

[90] Viju S, Thilagavathi G. Comfort Characteristics of Nettle Nonwoven Fabrics. *J Nat Fiber.* 2022; 19(4): 1490-1497. https://doi.org/10.1080/15440478.2020.1779899

[91] Samanta KK, Roy AN, Baite H, Debnath S, Ammayappan L, Nayak LK, Singha A, Kundu T. Development of Nettle Fibre Blended Apparel Textiles. In: Gupta D, Majumdar A, Gupta S, eds.) *Functional Textiles and Clothing 2023*. *ICFTC Springer Proceedings in Materials*, *Vol 42,* Springer, Singapore. https://doi.org/10.1007/978-981-99-9983-5_15

[92] Rao KMM, Rao KM. Extraction and tensile properties of natural fibers : Vakka, date and bamboo. *Compos Struct.* 2007; 77(3): 288-295. https://doi.org/10.1016/j.compstruct.2005.07.023

[93] Horrocks AR, Anand SC. *Handbook of Technical Textiles*. Woodhead Publishing Ltd; 2000, ISBN: 978-1-85573-385-5

[94] Islam MM, Haque MI, Mondal MIH. Biomedical textiles for orthopaedic and surgical applications. In: Mondal IH ed. *Medical Textiles from Natural Resources,* Woodhead Publishing, 2022: 213-253. https://doi.org/10.1016/C2020-0-03263-9

[95] Maitra S, Sahni S, Gupta D. Nonwoven acoustic panels from Himalayan nettle (*Girardinia diversifolia* L.) fibre. *Ind Crops Prod.* 2024; 216(4): 118746. https://doi.org/10.1016/j.indcrop.2024.118746

[96] Kozlowski R, Muzyczek M. Hemp, flax and other plant fibres. In: Nayak R ed. *Sustainable Fibres for Fashion and Textile Manufacturing, Woodhead Publishing* 2023: 75-93. https://doi.org/10.1016/B978-0-12-824052-6.00017-2

[97] Shahid-ul-Islam, Jaiswal V, Butola BS, Majumdar A. Production of PVA-chitosan films using green synthesized ZnO NPs enriched with dragon fruit extract envisaging food packaging applications. *Int J Biol Macromol.* 2023; 252: 126457-126457. https://doi.org/10.1016/J.IJBIOMAC.2023.126457

Vlakna koprive za tehničke primene

Parmeshwar Bobade, Vivek Jaiswal, Chandra Jeet Singh and Samrat Mukhopadhyay

Department of Textile and Fibre Engineering, Indian Institute of Technology Delhi, Delhi, India

(Stručni pregledni rad)

Izvod

Zbog sve veće svesti o ekološkim i društvenim problemima, kao i strožih ekoloških propisa, raste potražnja za zelenim materijalima koji bi zamenili resurse i sirovine na bazi fosilnih goriva. Sa svojim odličnim mehaničkim svojstvima, biorazgradivošću i niskom cenom, vlakna koprive imaju potencijal da postanu održiva vlakna za tehničke primene. Sposobnost bojenja, antimikrobna svojstva, obnovljivost i otpornost na gužvanje čine ova vlakna pogodnim za tekstilne primene. Zbog svoje niske gustine, mogu se koristiti u širokom spektru primena kao što su tkane i netkane tkanine, mešani i kompozitni materijali. Ovaj rad ima za cilj da kritički razmotri primenu vlakna koprive u različitim oblastima tekstilne industrije i da pruži smernice za buduća istraživanja.

Ključne reči: Tretman alkalijama; građevinski materijal; netkani tekstil; tekstilni kompoziti; apsorpcija zvuka; održivost.

Thermal conductivity measurements of liquids: challenges and a novel solution

Andrej M. Stanimirović[1], Divna M. Majstorović[2] and Emila M. Živković[2]

[1]*Electric Power Industry of Serbia, Belgrade, Serbia*
[2]*University of Belgrade, Faculty of Technology and Metallurgy, Belgrade, Serbia*

Abstract

This paper provides a concise and accessible overview of commonly used methods for measuring the thermal conductivity of liquids. Both steady-state and transient techniques are briefly outlined, including guarded hot plate methods, laser flash analysis, and approaches based on time-dependent thermal response. Particular focus is placed on the transient hot wire method, recognized for its simplicity, versatility, and its proven suitability for liquid samples. In addition, a recently developed patented approach based on the transient hot wire technique is presented in a more illustrative manner. The concept relies on improvements in sensor design and data interpretation, aimed at enhancing measurement stability and reducing typical sources of error in liquid measurements. Rather than a detailed technical validation, the emphasis is on explaining the idea and its potential benefits in practical applications.

Keywords: Transport property; experimental method; transient hot wire technique; new setup.

Available on-line at the Journal web address: http://www.ache.org.rs/HI/

TECHNICAL PAPER

UDC 52-334.6:550.34.016

Hem. Ind. **80(1)** 51-59 (2026)

1. INTRODUCTION

Accurate determination of the thermal conductivity of liquids plays a crucial role in a wide range of scientific and engineering applications, including energy systems, chemical processing, and thermal management technologies. As modern industries increasingly rely on precise thermophysical property data for modelling, simulation, and optimization, the demand for reliable and efficient measurement techniques continues to grow.

Over the past decades, numerous experimental methods have been developed to measure the thermal conductivity of liquids, broadly categorized into steady-state, transient and periodic techniques. While steady-state methods are conceptually straightforward, they are often limited by long measurement times and susceptibility to parasitic heat losses. In contrast, transient methods, *e.g.* the transient hot wire technique, have gained prominence due to their rapid response, reduced influence of convection, and high precision.

This paper provides a comprehensive review of existing methods for measuring the thermal conductivity of liquids, with particular emphasis on the principles, advantages, and limitations of transient techniques. In addition, a novel experimental setup based on the transient hot wire method is presented. Patented in 2021 [1], the setup demonstrates both originality and potential for applications in research and industry [2,3].

2. OVERVIEW OF METHODS FOR MEASURING THERMAL CONDUCTIVITY OF LIQUIDS

Measurement of the thermal conductivity of liquids is more challenging than for solids due to the onset of natural convection. While a non-uniform temperature field is required to induce heat transfer, temperature-dependent density variations and molecular mobility in liquids lead to spontaneous fluid motion, which distorts the temperature field and affects measurement accuracy.

To address this, various methods have been developed and are generally classified as steady-state, transient, and periodic. In steady-state methods, convection effects can be minimized through appropriate sample geometry, enabling simpler experimental setups and reduced data requirements. Transient methods rely on short-duration measurements

Corresponding author: Emila M. Živković, University of Belgrade, Faculty of Technology and Metallurgy, Karnegijeva 4, 11120 Belgrade, Serbia
E-mail: emila@tmf.bg.ac.rs; https://orcid.org/0000-0001-5843-8230
Co-authors: Andrej M. Stanimirović https://orcid.org/0009-0000-4181-3030 and Divna M. Majstorović https://orcid.org/0000-0002-0294-1352

Paper received: 1 March 2026; Paper accepted: 3 April 2026; Paper published: 8 April 2026.
https://doi.org/10.2298/HEMIND260301005S

following a rapid thermal perturbation, before convection significantly develops. These methods simplify experimental design but typically require fast data acquisition and dedicated processing. Periodic methods introduce small harmonic temperature oscillations around a steady or quasi-steady state. Although they combine challenges of both steady and transient approaches, their main advantage is the use of very small sample volumes.

2. 1. Steady-state methods

The steady-state parallel-plate method [4] is based on one-dimensional heat conduction in a suitably designed measurement cell. To ensure predominantly unidirectional heat transfer, configurations with parallel plates or concentric cylinders are typically employed. In the parallel-plate setup, shown in Figure 1, a small volume of liquid is confined between two metal plates, and accurate measurement of a small temperature difference is required, usually using high-sensitivity thermocouples placed at positions where the temperatures are nearly identical.

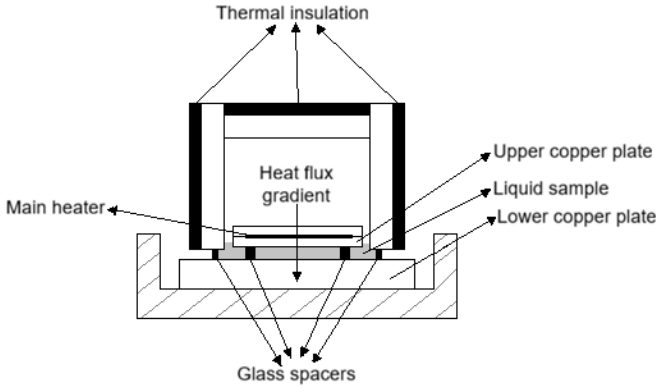

Figure 1. Apparatus for the steady-state measurement method with parallel plates

Assuming that the total heat generated by the main heater is transferred through the liquid layer, the effective thermal conductivity of the system (including separators effects) is given by Equation (1):

$$k = \frac{PL_g}{S\Delta T} \tag{1}$$

where P is the heater power, ΔT the temperature difference between the plates, L_g the thickness of the liquid layer (defined by glass spacers) and S is the cross-sectional area. The thermal conductivity of the liquid is then presented by Equation (2):

$$k_e = \frac{kS - k_g S_g}{S - S_g} \tag{2}$$

where k_g and S_g denote the thermal conductivity and cross-sectional area of the spacers. To ensure measurement accuracy, heat losses must be minimized, typically by employing guard heaters that maintain isothermal conditions and eliminate radiative and parasitic heat fluxes.

The cylindrical cell method [5] is currently one of the most widely used steady-state techniques for measuring liquid thermal conductivity. In this configuration, the liquid fills the annular space between two concentric cylinders. The apparatus typically consists of a copper inner cylinder containing an electrical heater and an outer (*e.g.* galvanized) cylinder, with axial ends thermally insulated to reduce heat losses. Heat transfer occurs primarily in the radial direction through the liquid. Temperatures at the inner and outer boundaries (T_0 and T_i) are measured using calibrated thermocouples positioned near the centre of the cell, while the heat input P is determined from the voltage and current supplied to the heater. Based on the Fourier's law in cylindrical coordinates, the thermal conductivity is given by Equation (3):

$$k = \frac{\ln(r_2 / r_1)}{2\pi L\left[\frac{\Delta T}{P} - \frac{\ln(r_3 / r_2)}{2\pi L k_c}\right]} \tag{3}$$

where $\Delta T = T_i - T_0$, k_c is the thermal conductivity of the inner cylinder material (copper), L is the cylinder length, and r_1, r_2 and r_3 are the corresponding radii defining the geometry of the system.

2. 2. Periodic methods

The temperature oscillation technique [6] is based on monitoring temperature changes in a liquid induced by periodic variations of temperature or heat flux. The measured thermal response reflects the effective thermal conductivity of the liquid. The experimental setup requires a measurement cell whose ends are maintained at a constant temperature by fluid circulation from a thermostatic bath, while a Peltier element provides periodic thermal excitation. Temperature is measured at multiple positions, and the signals are continuously acquired, filtered and processed using data acquisition and analysis software. The thermal diffusivity of the liquid is determined from the attenuation of the temperature oscillation amplitude from the boundary toward the centre of the sample. The thermal conductivity is then calculated from thermal diffusivity based on known density and specific heat capacity at constant pressure.

The 3ω method [7] is commonly used for liquids whose thermal conductivity strongly depends on temperature. It is based on radial heat conduction from a thin conductive element that serves simultaneously as a heater and thermometer. A sinusoidal current of angular frequency ω produces periodic Joule heating, generating temperature oscillations at frequency 2ω, while the resulting voltage response at 3ω is used for thermal conductivity determination.

For an infinitely thin line heat source on the surface of a semi-infinite medium, the temperature rise at distance r is given by Equation (4):

$$\Delta T = \frac{P}{l\pi k} K_0 qr \tag{4}$$

where k is the thermal conductivity of the medium, P/l is the power per unit length at frequency 2ω, K_0 is the modified Bessel function of the second kind (zero order), r is the radial distance between the line heat source and any point in the surrounding medium where the temperature change is being evaluated, and $1/q$ is the thermal penetration depth. The sensing element is typically fabricated by sputtering a thin metal layer onto an insulating substrate and is immersed in the liquid sample within a temperature-controlled bath (thermostat or cryostat).

The thermal comparator method [8,9] is a rapid technique based on point contact between a heated probe and the test liquid. When two materials at different temperatures are brought into contact over a very small area, a transient equilibrium temperature is established, which depends on their thermal conductivities. The contact temperature is measured using thermocouples, providing a voltage proportional to the temperature difference between the probe tip and a reference point inside the probe. Calibration curves obtained using reference liquids with known thermal conductivities allow determination of the thermal conductivity of an unknown sample.

The apparatus, shown in Figure 2, consists of a Cu probe, a heating coil, a microvoltmeter and a stabilized power supply.

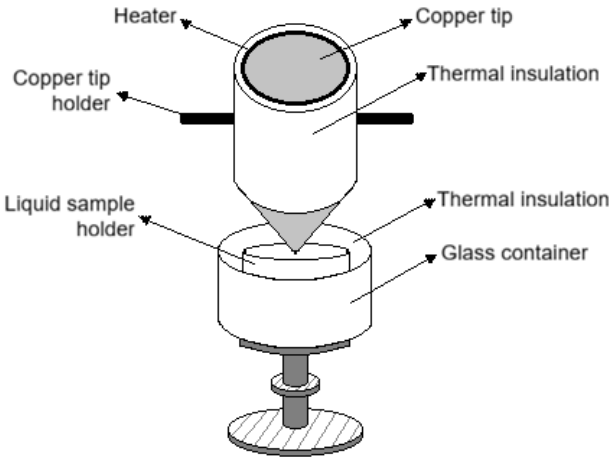

Figure 2. Apparatus for the thermal comparator method

The probe is the most critical component, as the measurement accuracy depends on heat transfer through a very small contact area. The heater maintains a controlled temperature difference between the probe and the sample, and the measurement is performed under near steady-state conditions, where the voltage signal correlates directly with thermal conductivity.

2. 3. Transient methods

Transient (impulse) methods are based on time-dependent thermal responses of a material following a short and well-defined thermal excitation. These methods are particularly advantageous for liquid thermal conductivity measurements due to their short measurement times, reduced sensitivity to convection, and high accuracy. Among them, the transient hot wire method remains the most reliable and widely used technique, while the transient plane source and laser flash methods provide valuable alternatives for specific experimental constraints.

The laser flash method, originally developed for solids, is also applicable to liquids [10]. The liquid sample is placed as a thin layer between two very thin metal disks, which act as sample holders in a sandwich configuration. A short laser pulse heats the upper disk, causing a rapid temperature increase. Heat is then conducted through the liquid layer to the lower disk, where the temperature rise is detected using a thermocouple, infrared detector, or a similar sensor. The thermal conductivity can be determined from the shape of the transient temperature response of the lower disk without the need for reference materials. Although highly accurate for solids, the method is less precise for liquids, with a typical uncertainty of about 2.6 % near room temperature. Its main advantages include (1) very small sample volume (thin layer, typically 1 to 2 mm thick), (2) relatively simple temperature control and uniform initial conditions, (3) small and easily estimated heat losses to the surrounding gas, (4) applicability as an absolute method for low-conductivity liquids without direct measurements of input energy or sample thickness, and (5) negligible radiative losses due to a small temperature rise (~2 K). Due to these characteristics, the method is particularly suitable for low-thermal-conductivity liquids such as molten salts at elevated temperatures.

The transient plane source method (TPS) is a fast and accurate technique for measuring thermal transport properties, including thermal conductivity, thermal diffusivity, and volumetric heat capacity, from a single non-destructive measurement [11,12]. The method is based on a planar heat source surrounded by the material under investigation. In practice, the sensor is fabricated as a double nickel spiral embedded between two thin layers of insulating material, commercially known as Kapton® polyimide film. The spiral functions simultaneously as a heater and temperature sensor. A concentric guard heater is often used to minimize radial heat losses. Electrical resistance of the nickel spiral serves as a temperature indicator due to its known temperature coefficient of resistance. During measurements, a current pulse is applied, causing a controlled temperature to increase in the sensor's temperature (typically from fractions of a degree to a few kelvin). The resulting changes in voltage and resistance are recorded as a function of time. A modified TPS configuration is also used for liquids, where the sample is placed on only one side of the planar sensor [13].

The transient hot wire (THW) method [14] is the most widely used and most accurate transient contact method for measuring the thermal conductivity of liquids. It is applicable to a broad range of fluids and is generally considered the reference technique. The method is based on transient radial heat conduction from a thin wire immersed in the liquid. Its implementation requires precise experimental control, high-sensitivity temperature measurement, and automated data acquisition and processing. Due to short measurement times and multiple influencing parameters, computer-controlled systems are essential. A key advantage of the THW method is the effective elimination of natural convection effects, which significantly improves accuracy compared to steady-state techniques. Modern systems achieve uncertainties around 1 %. Electrically insulated hot wires are used for conductive liquids, while bare wires are limited to non-conductive fluids. For electrically conductive or liquids at high-temperatures, modified configurations are used. In the liquid metal transient hot wire method [15], a glass capillary filled with mercury acts as an electrically isolated heating element. For highly corrosive melts (*e.g.* carbonates), maintaining large homogeneous samples is difficult. In such cases, the transient short hot wire method is applied [16], which uses smaller samples (up to ~10 cm) and is based on numerical solutions of two-dimensional heat conduction with realistic boundary conditions.

3. A NEW INSTRUMENT FOR MEASURING THE THERMAL CONDUCTIVITY OF LIQUIDS USING A NEEDLE-SHAPED SENSOR

A new instrument for measuring the thermal conductivity of liquids is based on the transient hot wire method and employs a needle-shaped sensor as the primary sensing element [1]. The system consists of a needle sensor, a liquid sample container, and a control system that governs electrical excitation and data acquisition. The liquid sample is placed in the container, preferably cylindrical with a vertical axis, to ensure symmetric radial heat propagation from the sensor. The needle sensor is immersed in the liquid and generates a transient temperature field due to controlled Joule heating. The thermal conductivity is determined from the time-dependent temperature response.

3. 1. Needle sensor

The needle sensor consists of a heating element, a temperature detection element, electrical conductors (current and voltage leads), electrical insulation, and a protective sheath. The heating element is a thin metallic wire of small cross-section that generates heat via the Joule effect when an electric current is applied. To maximize the measurement accuracy, low-resistance current leads are used so that most of the electrical power is dissipated in the heating element itself. The heating power is determined from the measured voltage and current. In a four-wire configuration, separate voltage leads are used to measure the voltage drop across the heating element more accurately, thereby minimizing the influence of lead resistance.

Electrical insulation separates all conductive components of the needle sensor and prevents electrical interference between the current paths, voltage measurement lines, and the sheath. Materials such as magnesium oxide (M_gO) powder or epoxy resin are used due to their high electrical resistivity and thermal stability. The needle sensor is enclosed in a protective sheath that provides mechanical support and thermal protection. The sheath material is selected to withstand temperatures higher than the operating temperature of the heating element; steel is a typical example. The sheath consists of two sections with different diameters. The narrow section contains the heating element, voltage lead, and electrical insulation. The fine wires are typically spot-welded at the sensor tip to ensure a stable electrical contact. The wider section accommodates the electrical connections, including current and voltage leads with appropriate insulation.

Temperature changes within the sensor are measured using either a thermocouple or a resistance thermometer. A thermocouple measures temperature variations based on the generated thermoelectric voltage, while a resistance thermometer determines temperature from changes in electrical resistance with temperature. In a simplified configuration, the heating element itself can serve as the resistance thermometer, allowing temperature to be obtained directly from its temperature-dependent resistance.

A longitudinal cross-section of the needle sensor is shown in Figure 3a. The sensor is immersed in a liquid sample (1) and connected to the control system (12) via current and voltage leads. The sensor consists of a small-diameter sheath (2) and a large-diameter sheath (11), a heating element (4), electrical insulation (5), low-resistance current leads (7, 8), and voltage leads (3, 9, 10). The heating element (4) is spot-welded at its tip (6) to the voltage lead (3) and to the small-diameter sheath (2), ensuring stable electrical and mechanical contact. The small-diameter sheath (2) contains the heating element (4), electrical insulation (5), and one voltage lead (3). The large-diameter sheath (11) accommodates the current leads (7, 8) and the remaining voltage leads (9, 10), which connect the sensor to the control system (12). The liquid sample (1) is in direct thermal contact with the external surface of the needle sensor, which includes both sheath sections and the active sensing region.

Figure 3b illustrates a representative configuration of the needle-shaped sensor and the sample container. The sensor sheath consists of two sections: a small-diameter portion (2) and a large-diameter portion (11). The needle sensor is mounted to a threaded coupling element (13), which enables secure attachment and positioning. The liquid sample container is designed as a test tube (14) and is equipped with a corresponding threaded coupling element (15) for integration with the sensor assembly. The assembled configuration of the sample container and the needle sensor is shown on the right side of Figure 3b.

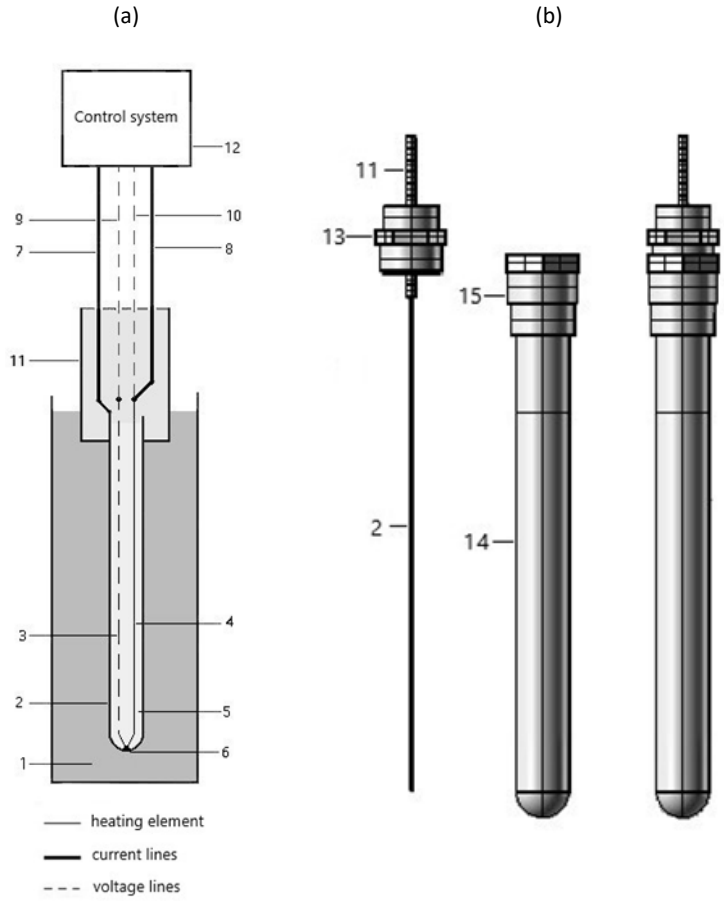

Fig3. Schematic representation of (a) needle sensor and (b) sample container with needle sensor: 1 - liquid sample, 2 - small diameter sheath, 3 - voltage line, 4 - heating element, 5 - electric insulation, 6 - welded connection, 7, 8 - current lines, 9, 10 - voltage lines, 11 - large diameter sheath, 12 - control system, 13 - threaded coupling element, 14 - sample reservoir, 15 - threaded coupling element

3. 2. Control System

The control system regulates the operation of the instrument and processes electrical signals related to current, voltage, temperature, and time. It controls the electrical excitation of the heating element, records measurement duration, and acquires sensor signals using a digital measurement system, typically based on an analog-to-digital converter (ADC). The system is implemented as a microcontroller, computer, or a combination of both, and provides real-time monitoring of current, voltage, and derived temperature values via an interactive user interface. It is programmable, enabling automated measurement control, data storage, and numerical processing.

Temperature is calculated based on the electrical characteristics of the sensing element. For thermocouples, temperature is derived from thermoelectric voltage, while for resistance thermometers it is obtained from resistance variation. When the heating element itself serves as the resistance thermometer, temperature is directly determined from its resistance change.

Figure 4 shows a schematic diagram of the control system and its connection to the needle sensor. The heating element (4) is powered by the source (19) through current leads (7, 8), with a standard resistor (16) connected in series to measure the current. One current lead (8) connects the power source to the resistor, while the other (7) is spot-welded to the small-diameter sheath (2) of the sensor.

The operation of the power source is controlled via digital control lines (21). Voltages across the heating element (4) and the standard resistor (16) are measured via voltage leads (9, 10, 17, 18) and recorded by the data acquisition system (20), which stores the data for further analysis.

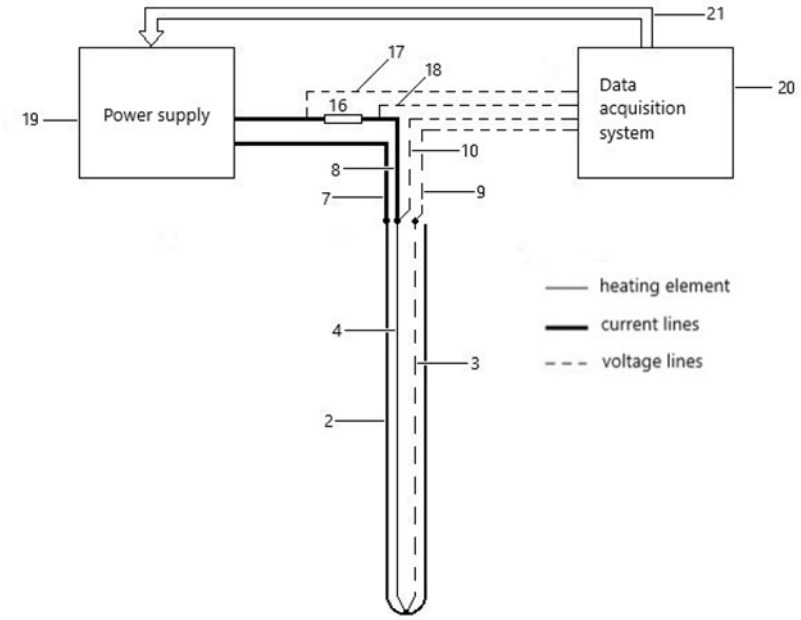

Fig4. Schematic representation of the control system: 2 - small diameter sheath, 3 - voltage line, 4 - heating element, 7, 8 - current lines, 9, 10 - voltage lines, 16 - standard resistor, 17, 18 - voltage lines, 19 - power supply, 20 - data acquisition system, 21 - digital signals

3. 3. Preferred configuration

In the preferred embodiment, the heating element is electrically connected to the control system via two pairs of conductors. The first pair consists of current leads with electrical resistance lower than that of the heating element, which supplies electric current for Joule heating. The second pair consist of voltage leads used for accurate measurements of the voltage drop across the heating element.

The electric current through the heating element is determined indirectly by measuring the voltage drop across a standard resistor connected in series with the heating element. The heating power per unit length and the electrical resistance of the heating element can be accurately calculated based on the measured current and the voltage drop across the heating element. Since the electrical resistance of the heating element changes with temperature, its resistance can be used to determine the sensor's temperature variation. The thermal conductivity of the liquid sample is calculated using the heating power and the temporal rate of temperature change of the needle sensor. In the preferred configuration, a coaxial type K (or J) thermocouple is employed, in which the Alumel (or iron) wire simultaneously functions as the heating element and as a resistance thermometer. Additionally, the instrument preferably consists of several needle sensors for the simultaneous determination of the thermal conductivity of multiple samples.

Thermal conductivity k is calculated using the transient hot-wire relation, Equation (5):

$$k = \frac{q}{4\pi \frac{\mathrm{d}\,\Delta T}{\mathrm{d}\ln t}} \tag{5}$$

where $\mathrm{d}\,\Delta T/\mathrm{d}\ln t$ is the slope of the linear dependence of temperature rise on the logarithm of time, and q is the heat input per unit length of the heating element.

The heat input is determined from electrical measurements using Equation (6):

$$q = \frac{V_\mathrm{w} I_\mathrm{w}}{L_\mathrm{w}} = \frac{V_\mathrm{s} V_\mathrm{w}}{R_\mathrm{s} L_\mathrm{w}} \tag{6}$$

where V_w, I_w and L_w are the voltage, current, and length of the heating element, respectively, while V_s and R_s refer to the reference measurement circuit used for current determination.

This configuration was tested on several standard fluids, the results were compared with literature values, and the measurement uncertainty was evaluated [17].

4. CONCLUSION

The presented patented approach highlights the potential for further improvement of the transient hot wire technique, primarily through sensor optimization and enhanced data processing. Such improvements contribute to reducing the influence of common sources of error, such as convection and unstable measurement conditions, thereby increasing the accuracy and repeatability of the results.

Although the paper is not focused on detailed experimental analysis, it clearly indicates current development trends and the potential benefits of new solutions. In this sense, the paper serves both as a useful refresher and as an encouragement for further research and advancement in methods for measuring the thermal properties of liquids. Therefore, the displayed apparatus is undergoing further testing and improvements, especially in terms of the software and measurement reliability.

Acknowledgements: The authors gratefully acknowledge the financial support received from the Research Fund of the Ministry of Science, Technological Development and Innovation of the Republic of Serbia and the Faculty of Technology and Metallurgy University of Belgrade (Contract No. 451-03-34/2026-03/200135).

REFERENCES

[1] Živković E, Stanimirović A, Majstorović D. Uređaj za merenje toplotne provodljivosti tečnosti primenom senzora u obliku igle, RS 61920, 2021
[2] Živković EM, Živković NV, Majstorović DM, Stanimirović AM, Kijevčanin MLj. Volumetric and transport properties of binary liquid mixtures with 1-ethyl-3-methylimidazolium ethyl sulfate as candidate solvents for regenerative flue gas desulfurization processes. *J Chem Thermodyn.* 2018; 119:135-154. https://doi.org/10.1016/j.jct.2017.12.023
[3] Stanimirović AM, Živković EM, Majstorović DM, Kijevčanin MLj. Transport properties of binary liquid mixtures - candidate solvents for optimized flue gas cleaning processes. *J Serb Chem Soc.* 2016; 81: 1427-1439. https://doi.org/10.2298/JSC160623083S
[4] Challoner AR, Powell RW. Thermal conductivity of liquids: new determinations for seven liquids and appraisal of existing values. *Proc A* 1956; 238: 90-106. https://doi.org/10.1098/rspa.1956.0205
[5] Kurt H, Kayfeci M. Prediction of thermal conductivity of ethylene glycol-water solutions by using artificial neural networks. *Appl Energy* 2009; 86: 2244-2248. https://doi.org/10.1016/j.apenergy.2008.12.020
[6] Czarnetzki W, Roetzel W. Temperature oscillation techniques for simultaneous measurement of thermal diffusivity and conductivity. *Int J Thermophys.* 1995; 16: 413-422. https://doi.org/10.1007/BF01441907
[7] Cahill DG. Thermal conductivity measurement from 30 to 750 K: the 3ω method. *Rev Sci Instrum.* 1990; 61: 802-808. https://doi.org/10.1063/1.1141498
[8] Clark WT, Powell RW. Measurement of thermal conduction by the thermal comparator. *J Sci Instrum.* 1962; 39: 545-551. https://doi.org/10.1088/0950-7671/39/11/303
[9] Powell RW. Experiments using a simple thermal comparator for measurement of thermal conductivity, surface roughness and thickness of foils or of surface deposits. *J Sci Instrum.* 1957; 34: 485-492. https://doi.org/10.1088/0950-7671/34/12/303
[10] Tada Y, Harada M, Tanigaki M, Eguchi W. Laser flash method for measuring thermal conductivity of liquids-application to low thermal conductivity liquids. *Rev Sci Instrum.* 1978; 49: 1305-1314. https://doi.org/10.1063/1.1135573
[11] Dixon C, Strong MR, Mark Zhang S. Transient Plane Source Technique for Measuring Thermal Properties of Silicone Materials Used in Electronic Assemblies. *Int J Microcircuits Electron Packag.* 2000; 23: 494-500
[12] Gustafsson SE. Transient plane source techniques for thermal conductivity and thermal diffusivity measurements of solid materials. *Rev Sci Instrum.* 1991; 62: 797-804. https://doi.org/10.1063/1.1142087
[13] C-Therm. http://www.ctherm.com/products/tci_thermal_conductivity/how_the_tci_works/ Accessed March 1, 2026.
[14] Nagasaka Y, Nagashima A. Absolute measurement of the thermal conductivity of electrically conducting liquids by the transient hot-wire method. *J Phys E Sci Instrum.* 1981; 14: 1435-1440. https://doi.org/10.1088/0022-3735/14/12/020
[15] Bleazard JG, Teja AS. Thermal conductivity of electrically conducting liquids by the transient hot-wire method. *J Chem Eng Data* 1995; 40: 732-737. https://doi.org/10.1021/je00020a003
[16] Xie H, Gu H, Fujii M, Zhang X. Short hot wire technique for measuring thermal diffusivity of various materials. *Meas Sci Technol.* 2006; 17: 208-214. https://doi.org/10.1088/0957-0233/17/1/032
[17] Stanimirović AM, Živković EM, Milošević ND, Kijevčanin MLj. Application and testing of a new simple experimental setup for thermal conductivity measurements of liquids. *Therm Sci.* 2017; 21: 1195-1202. https://doi.org/10.2298/TSCI160324219S

Merenje toplotne provodljivosti tečnosti: izazovi i novo rešenje

Andrej M. Stanimirović[1], Divna M. Majstorović[2] i Emila M. Živković[2]

[1]*Elektroprivreda Srbije, Beograd, Srbija*
[2]*Univerzitet u Beogradu, Tehnološko-metalurški fakultet, Beograd, Srbija*

(Stručni rad)

Izvod

Ovaj rad pruža sažet i pristupačan pregled najčešće korišćenih metoda za merenje toplotne provodljivosti tečnosti. Ukratko su prikazane stacionarne i nestacionarne tehnike, uključujući metode sa zaštićenom toplom pločom, laserski bljesak, kao i pristupi zasnovani na vremenski zavisnom toplotnom odzivu sistema. Poseban fokus stavljen je na metodu prelazne vruće žice, koja se izdvaja po svojoj jednostavnosti, fleksibilnosti i pogodnosti za merenja na tečnim uzorcima. Pored toga, predstavljen je na ilustrativan način i novorazvijeni patentirani pristup zasnovan na tehnici prelazne vruće žice. Koncept se zasniva na unapređenju dizajna senzora i interpretacije podataka, sa ciljem poboljšanja stabilnosti merenja i smanjenja tipičnih izvora grešaka kod merenja karakteristika tečnosti. Umesto detaljne tehničke validacije, naglasak je stavljen na objašnjenje same ideje i njenih potencijalnih prednosti u praktičnoj primeni.

Ključne reči: Transportno svojstvo; eksperimentalna metoda; tehnika prelazne vruće žice; nova konfiguracija

Članstvo Saveza hemijskih inženjera Srbije u European Young Engineers: Nove mogućnosti za mlade hemijske inženjere

Marija Vjetrović

Savez hemijskih inženjera Srbije, Beograd, Srbija

Savez hemijskih inženjera Srbije postao je član organizacije European Young Engineers (Evropski mladi inženjeri) 11. oktobra 2024. godine, čime je otvoreno novo poglavlje u međunarodnom delovanju i razvoju mladih inženjera u Srbiji. Odluka o pristupanju potvrđena je tokom online konferencije, održane u Luksemburgu, kada je SHI zvanično postao deo ove značajne evropske mreže.

Ključne reči: međunarodna saradnja, mladi inženjeri; konferencije; vebinari

Available on-line at the Journal web address: http://www.ache.org.rs/HI/

VESTI

Hem. Ind. **80(1)** 61-63 (2026)

Savez hemijskih inženjera Srbije (SHI) postao je član organizacije European Young Engineers - EYE (Evropski mladi inženjeri) 11. oktobra 2024. godine, čime je otvoreno novo poglavlje u međunarodnom delovanju i razvoju mladih inženjera u Srbiji. Odluka o pristupanju potvrđena je tokom online konferencije (Slika 1), održane u Luksemburgu, kada je SHI zvanično postao deo ove značajne evropske mreže.

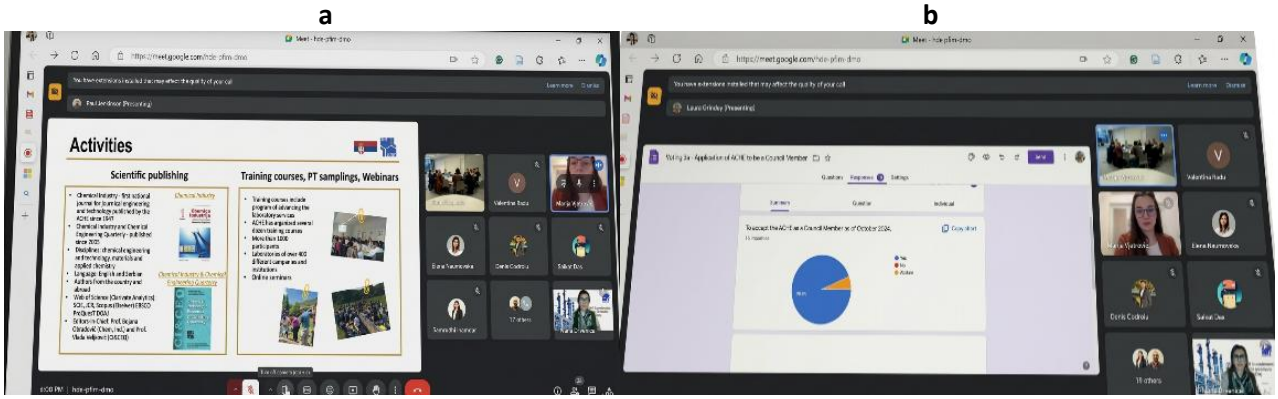

Slika 1. Online konferencija organizacije European Young Engineers oktobra 2024. godine, na kojoj je potvrđeno članstvo SHI (a) prezentacija o SHI i (b) glasanje o prijemu u članstvo

Saradnja sa organizacijom EYE donosi brojne koristi, pre svega kroz mogućnost direktnog povezivanja sa kolegama iz različitih evropskih zemalja, razmenu znanja i iskustava, kao i pristup savremenim praksama i inovacijama u inženjerstvu.

Predstavnik SHI u Upravnom odboru organizacije EYE je dipl. inž. Marija Vjetrović tehnički sekretar Saveza hemijskih inženjera Srbije, i njen zadatak je predstavljanje interesa mladih inženjera iz Srbije i učešće u donošenju odluka i kreiranju aktivnosti na nivou organizacije.

Ovo članstvo predstavlja važan korak ka jačanju prisustva domaće zajednice svih mladih inženjera na evropskoj sceni i omogućava aktivnije učešće u savremenim tokovima struke.

O ORGANIZACIJI EUROPEAN YOUNG ENGINEERS

Organizacija Evropski mladi inženjeri [1] je međunarodna, neprofitna organizacija osnovana 1994. godine, koja danas okuplja više od 100 hiljada mladih inženjera iz 22 evropske zemlje. Osnovana je sa ciljem da mladim inženjerima u Evropi obezbedi platformu za lakše povezivanje, razmenu ideja i iskustava, kao i zajedničko zastupanje stavova prema institucijama vlasti, industriji i akademskoj zajednici.

Jedna od najznačajnijih aktivnosti ove organizacije su konferencije koje se organizuju dva puta godišnje, u prolećnom i jesenjem terminu, u saradnji sa nekom od zemalja članica. Svaka konferencija održava se u drugom gradu, pružajući

učesnicima jedinstvenu priliku da posete lokalne kompanije, upoznaju industrijsku praksu, ali i istraže kulturu i specifičnosti zemlje domaćina. Ovi događaji ne doprinose samo profesionalnom razvoju i umrežavanju sa kolegama iz cele Evrope, već omogućavaju i sticanje novih iskustava kroz putovanja i međunarodnu saradnju.

Pored konferencija, organizacija EYE održava i različite radionice i vebinare. Radionice su osmišljene kao interaktivni programi usmereni na razvoj praktičnih veština, kroz rad na konkretnim zadacima i studijama slučaja, gde učesnici imaju priliku da primene teorijska znanja u realnim situacijama.

Vebinari predstavljaju potpuno drugačiju, savremenu i dinamičnu platformu za razmenu znanja (Slika 2). Oni su osmišljeni kao interaktivni virtuelni događaji, gde učesnici, posebno studenti i mladi istraživači, imaju priliku da predstave svoje projekte, radove i istraživačke panele, diskutuju o rezultatima i dobiju povratne informacije od kolega iz različitih zemalja i oblasti. Ovakav format podstiče aktivno učešće, razvija veštine prezentovanja i kritičkog razmišljanja, ali i omogućava lakše povezivanje sa potencijalnim saradnicima iz međunarodnog okruženja.

Slika 2. Prikaz platforme organizacije EYE za održavanje vebinara, kao savremeni format za prezentaciju projekata i diskusiju

UČEŠĆE SHI U AKTIVNOSTIMA ORGANIZACIJE EUROPEAN YOUNG ENGINEERS

Prvo učešće predstavnika Saveza hemijskih inženjera Srbije na konferenciji organizacije *EYE* uživo obeleženo je susretom sa kolegama iz različitih evropskih zemalja na Malti od 24. do 27. aprila 2025. godine [2]. Tokom konferencije, učesnici su imali priliku da se kroz stručne posete upoznaju sa radom industrije i akademskog sektora, uključujući kompanije *Methode Electronics* i *L-Università ta' Malta*, čime je omogućen neposredan uvid u savremene inženjerske prakse (slika 3). Tokom te konferencije, posebno su bili značajni sastanci Upravnog odbora EYE, gde su razmatrana ključna pitanja daljeg razvoja organizacije, budućih aktivnosti i saradnje među članicama. Donete su važne odluke u vezi sa članstvom novih organizacija i organizacijom narednih konferencija, uključujući izbor Gruzije, kao domaćina sledećeg okupljanja u Tbilisiju u septembru 2025. Ujedno je izabrano i novo rukovodstvo EYE, čime su postavljeni temelji za naredni period rada organizacije.

Pored zvaničnog dela programa, konferenciju su obeležili paneli, radionice i neformalna okupljanja, koja su dodatno doprinela razmeni iskustava i uspostavljanju kontakata SHI predstavnika sa kolegama iz Evrope. Boravak na Malti upotpunjen je upoznavanjem kulturnih znamenitosti, uključujući posetu ostrvu Gozo.

Predstavnici SHI učestvovali su i na narednoj EYE konferenciji u Gruziji kroz virtuelne sastanke. Tom prilikom razmatrana su pitanja prijema novih članica u organizaciju EYE i doneta je odluka o održavanju naredne konferencije tokom proleća 2026. godine.

Slika 3. Prvo učešće predstavnika SHI na EYE konferenciji na Malti –:(a) učesnici konferencije u stručnoj poseti, (b) zajednička fotografija učesnika i (c) sastanak Upravnog odbora

NAJAVA PROLEĆNE KONFERENCIJE ORGANIZACIJE EUROPEAN YOUNG ENGINEERS 2026

Prolećna EYE konferencija 2026. godine će se održati u Napulju, u periodu od 7. do 10. maja [3]. Ovim putem pozivamo sve zainteresovane članove SHI da se prijave i uzmu učešće na konferenciji u Napulju, kao i da prate dalje aktivnosti EYE i aktivno se uključe u rad te organizacije. Za sve dodatne informacije o radu i aktivnostima EYE može kontaktirati predstavnike SHI na adresu elektronske pošte: shi@ache.org.rs.

Pri tome posebno ističemo poziv organizacije EYE i predlog Upravnom odboru da SHI bude jedan od domaćina naredne *EYE* konferencije, što predstavlja veliko priznanje i potvrdu dosadašnjeg angažmana. Organizacija ovakvog događaja u Srbiji pružila bi jedinstvenu priliku mladim inženjerima, svih profila, da kroz direktnu razmenu iskustava sa kolegama iz cele Evrope unaprede svoja znanja, veštine i profesionalne perspektive.

Ovakav razvoj dodatno učvršćuje poziciju SHI kao aktivnog i relevantnog člana evropske inženjerske zajednice, uz otvaranje prostora za nove inicijative, projekte i dugoročnu međunarodnu saradnju u okviru organizacije *EYE*.

REFERENCE

[1] European Young Engineers, https://eyengineers.eu
[2] EYE konferencija na Malti, 24. do 27. aprila 2025. https://www.uesamalta.com/s-projects-basic
[3] Prijave za EYE konferenciju u Napulju, 7. do 10. Maja 2026. https://eyeconference2026.it

Membership of the Association of Chemical Engineers of Serbia in European Young Engineers: New opportunities for young chemical engineers

Marija Vjetrović

Association of Chemical Engineers of Serbia, Belgrade, Serbia

(News)

Abstract

The Association of Chemical Engineers of Serbia became a member of the European Young Engineers organization on October 11, 2024, which opened a new chapter in the international activity and development of young engineers in Serbia. The decision to join was confirmed during an online conference, held in Luxembourg, when SHI officially became part of this important European network.

Keywords: international cooperation, young engineers; conferences; webinars

ДОКТОРСКЕ ДИСЕРТАЦИЈЕ

Докторске дисертације хемијско–технолошке струке одбрањене на универзитетима у Србији у 2025. години

ТЕХНОЛОШКО -МЕТАЛУРШКИ ФАКУЛТЕТ, УНИВЕРЗИТЕТ У БЕОГРАДУ

	Име и презиме	Наслов	Ментор
1.	**Тамара Ђукић**	Стандардизација фотон корелационе спектроскопије као методе за одређивање величине имунокомплекса у дијагностичке сврхе	Верица Ђорђевић, Весна Илић
2.	**Невена Илић**	Производња лаказа гљивама беле трулежи на агроиндустријском отпаду и њихова примена у поступцима разградње ксенобиотика фенолне структуре	Сузана Димитријевић-Бранковић, Катарина Михајловски
3.	**Милош Тошић**	Побољшање фотокаталитичких својстава титан(IV)-оксида дејством зрачења импулсног ласера и процена токсичности производа фотокаталитичке разградње карбофурана	Сузана Димитријевић-Бранковић, Милош Момчиловић
4.	**Тамара Смољанић**	Утицај корозије на интегритет и век вештачког кука	Љубица Миловић
5.	**Јованка Пејић**	Синергетско дејство цистеина и његових деривата са лантаноидима као зеленим инхибиторима корозије алуминијумских легура	Јелена Бајат, Мирослав Павловић
6.	**Тамара Матић**	Биоактивни материјали на бази калцијум-фосфата и мезопорозног биостакла допираних јонима магнезијума и/или стронцијума: синтеза, процесирање, карактеризација и примена у биомедицини	Ђорђе Вељовић
7.	**Наташа Кнежевић**	Одржива технологија производње лигноцелулозних мембрана за уклањање анјонских и катјонских загађујућих материја из воде	Александар Маринковић, Милена Милошевић
8.	**Слађана Лакетић**	Модификација структуре и својстава легуре титана са високим садржајем ниобијума за биомедицинску примену	Бојан Међо, Ивана Цвијовић Алагић
9.	**Кристина Гак Симић**	Функционални течнокристални системи на бази азобензена и стилбена	Немања Тришовић
10.	**Милена Стевановић**	Електрофоретске композитне превлаке хидроксиапатита, хитозана и графена на титану са и без додатка гентамицина	Ђорђе Јанаћковић, Ана Јанковић
11.	**Ања Петров Иванковић**	Ензимски потпомогнута производња пребиотика за топикалну примену и одређивање њихових структурних и функционалних својстава	Дејан Безбрадица, Марија Ћоровић
12.	**Милица Вељковић**	Ензимска синтеза и мембранско пречишћавање фрукто-олигосахарида	Дејан Безбрадица, Милица Симовић
13.	**Јелена Ракић**	Утицај хемијских активатора на својства везива са високим уделом механички активираног електрофилтерског пепела	Весна Радојевић, Звездана Башчаревић
14.	**Стефан Бошковић**	Математичко моделовање процеса електростатичке екструзије	Весна Радојевић, Звездана Башчаревић
15.	**Наташа Младеновић Николић**	Оптимизација синтезе и примена алкално активираних материјала на бази отпада богатог алуминијумом	Радојица Пешић
16.	**Ксенија Милошевић**	Развој фотоактивних самопречишћавајућих g-C_3N_4/TiO_2/полимер композита за уклањање штетних материја из отпадних вода	Мелина Калагасидис Крушић, Јасмина Достанић

	Име и презиме	Наслов	Ментор
17.	**Ања Антанасковић**	Синтеза, карактеризација и примена мултифункционалних биочађи на бази отпадне лигноцелулозне биомасе	Милан Миливојевић, Зорица Лопичић
18.	**Иван Пешић**	Uticaj modifikacije površine ugljeničnih materijala na njihova svoj Синтеза и карактеризација композита с полимерном матрицом на бази максена stva i adsorpciju odabranih estrogenih hormona iz vode	Весна Радојевић, Милош Петровић
19.	**Милена Пијовић Радовановић**	Оптимизација процеса добијања високопорозних угљеничних материјала термохемијском конверзијом биомасе за примену у зеленим технологијама	Владимир Павићевић, Бојан Јанковић
20.	**Јована Буха Марковић**	Утицај на животну средину тешких метала и полицикличних ароматичних угљоводоника из процеса сагоревања угља и отпадног угља	Мирјана Ристић
21.	**Јелена Обрадовић**	Процена ризика по здравље ученика школе у урбаној средини услед присуства штетних хемијских супстанци на суспендованим честицама у ваздуху	Антоније Оњиа, Славица Ражић
22.	**Јелена Стојаковић**	Развој и примена LC-MS/MS методе за анализу органских UV филтера и процена ризика услед њиховог присуства у различитим матрицама	Татјана Ђуркић, Антоније Оњиа
23.	**Александра Јанићијевић**	Синтеза и карактеризација материјала за мултифункционалну активну амбалажу на бази наноцелулозе и поли(винилиден-флуорида) уз додатак пунилаца баријум-титаната и магнетита	Предраг Живковић, Сузана Филиповић
24.	**Милица Делић**	Микроталасно излуживање и дисперзивна микроекстракција лантаноида из летећег пепела	Антоније Оњиа, Маја Ђолић

ТЕХНИЧКИ ФАКУЛТЕТ У БОРУ, УНИВЕРЗИТЕТ У БЕОГРАДУ

	Име и презиме	Наслов	Ментор
1.	**Вања Трифуновић**	Валоризација цинка и других корисних компоненти из прашине електролучне пећи	Снежана Милић
2.	**Павле Стјепановић**	Стохастички модел управљања залихама као основа планирања набавке процесних материјала у припреми минералних сировина	Милан Трумић Марија Кузмановић

ТЕХНОЛОШКИ ФАКУЛТЕТ, УНИВЕРЗИТЕТ У НОВОМ САДУ

	Име и презиме	Наслов	Ментор
1.	**Сања Рацков**	Дизајнирање наноструктурних материјала на бази јонских течности	Бранка Пилић, Милан Вранеш
2.	**Ђурђица Карановић**	Примена хетерогених система на бази слојевитих хидроксида и мешовитих оксида за ефикасно уклањање полутаната из водених раствора: анализа фотокаталитичких и адсорпционих перформанси	Милица Хаднађев Костић
3.	**Марко Илић**	Развој и примена нових метода за одређивање аутентичности уља семена и плодова различитих биљних врста	Маријана Ачански, Кристиан Пастор
4.	**Марко Павловић**	Моделовање и оптимизација процеса производње фосфорне киселине	Предраг Којић, Јелена Лубура Стошић
5.	**Ведрана Пророк**	Интензификација процеса мембранске филтрације применом 3D штампаних промотора турбуленције	Светлана Поповић, Дејан Моврин
6.	**Бојана Радић**	Монилиформин у кукурузу: оптимизација методологије одређивања, анализа појаве и могућности редукције	Зорица Стојановић, Јована Кос
7.	**Милана Матић**	Функционални производи са додатом вредношћу на бази бундеве	Јелена Пејин

8.	**Бењамин Салаковић**	Компаративна хемометријска анализа хроматографске липофилности и микробиолошке активности алкил и циклоалкил деривата симетричних триазина	Страхиња Ковачевић
9.	**Дарио Балабан**	Симулација, анализа и оптимизација полигенеративног постројења за гасификацију комуналног отпада	Предраг Којић
10.	**Мило Мујовић**	Етарско уље и липофилни екстракти из одабраног зачинског биља као природни антиоксиданси и антимикробни агенси у полупроизводима од уситњеног меса	Бранислав Шојић

ТЕХНОЛОШКИ ФАКУЛТЕТ У ЛЕСКОВЦУ, УНИВЕРЗИТЕТ У НИШУ

	Име и презиме	Наслов	Ментор
1.	**Валентина Николић**	Оптимизација поступка ултразвучне екстракције биоактивних једињења из кичице (Centaurium erythraea Rafn) воденим растворима пропилен-гликола и етанола	Сандра Константиновић
2.	**Горан Амин**	Збрињавање отпадне воде после оптимизације бојења акрилних влакана поступком адсорпције на модификованом зеолиту	Драган Ђорђевић

SPISAK RECENZENATA

Spisak recenzenata radova čije je procesiranje završeno tokom 2025. godine

List of reviewers of papers whose processing has been completed during 2025

Izuzetno smo zahvalni naučnicima koji su velikodušno posvetili svoje vreme i stručnost recenziji rukopisa dostavljenih časopisu Hemijska industrija tokom 2025. godine. Njihove promišljene ocene i posvećenost izvrsnosti od neprocenjivog su značaja za očuvanje integriteta, rigoroznosti i naučnog kvaliteta časopisa. Stručna recenzija predstavlja jedan od temelja kvalitetnog naučnog izdavaštva i duboko cenimo njihov ključni doprinos ovom procesu.

We extend our sincere gratitude to the scholars who have generously dedicated their time and expertise to the peer review of manuscripts submitted to the journal Hemijska industrija in 2025. Their thoughtful evaluations and commitment are invaluable in upholding the integrity, rigor, and scientific quality of the journal. Rigorous peer review remains a cornerstone of high-quality scientific publishing, and we deeply appreciate reviewers' contributions to this process.

1. **Younes Amini,** *Nuclear Science and Technology Research Institute, Tehran, Iran*
2. **Zoran Anđić,** *Hemijski fakultet, Univerzitet u Beogradu, Srbija*
3. **Jelena Bajat***, Tehnološko-metalurški fakultet, Univerzitet u Beogradu, Srbija*
4. **Ivana Banković Ilić***, Tehnološki fakultet u Leskovcu, Univerzitet u Nišu, Srbija*
5. **Zvezdana Baščarević***, Institute for Multidisciplinary Research, Univerzitet u Beogradu, Srbija*
6. **Mateja Belovari,** *Institut Ruđer Bošković, Zagreb, Hrvatska*
7. **Grozdanka Bogdanović,** *Tehnički fakultet u Boru, Univerzitet u Beogradu, Srbija*
8. **Bryan Brummelhaus de Menezes,** *Federal University of Santa Maria, Rio Grande do Sul, Brazil, researcher*
9. **Dragana D. Božić,** *Farmaceutski fakultet, Univerzitet u Beogradu, Srbija*
10. **Nevenka Bošković-Vragolović,** *Tehnološko-metalurški fakultet, Univerzitet u Beogradu, Srbija, redovni profesor*
11. **Asma Boudaoud,** *Faculty of Technology, Amar Telidji University of Laghouat, Laghouat, Algeria, professor*
12. **Danijela Bursać Kovačević,** *Prehrambeno-biotehnološkom fakultetu, Univerzitet u Zagrebu, Hrvatska*
13. **Aleksandar Dekanski,** *Beograd, Srbija, naučni savetnik u penziji*
14. **Mohd Din,** *School of Chemical Engineering, Engineering Campus, Universiti Sains Malaysia, Penang, Malaysia*
15. **Milena Dojčinović,** *Institut za multidisciplinarna istraživanja, Univerzitet u Beogradu, Srbija*
16. **Ivana Drvenica**, *Institut za medicinska istraživanja, Univerzitet u Beogradu, Srbija*
17. **Pero Dugić,** *Tehnološki fakultet, Univerzitet u Banja Luci, Bosna i Hercegovina*
18. **Maja Đolić,** *Tehnološko-metalurški fakultet, Univerzitet u Beogradu, Srbija*
19. **Marijke Antonia Fagan-Endres,** *Department of Chemical Engineering, University of Cape Town, South Africa*
20. **Branimir Grgur,** *Tehnološko-metalurški fakultet, Univerzitet u Beogradu, Srbija*
21. **Ashwani Gupta,** *The Combustion Laboratory, Department of Mechanical Engineering, University of Maryland, USA*
22. **Siti Nurul Hidayah,** *Faculty of Pharmacy, Universitas Gadjah Mada, Bulaksumur Yogyakarta, Indonesia, professor*
23. **Gorica Ivaniš,** *Tehnološko-metalurški fakultet, Univerzitet u Beogradu, Srbija*
24. **Aleksandra Ivanovska,** *Inovacioni centar Tehnološko-metalurškog fakulteta, Univerzitet u Beogradu, Srbija*

25. **Darko Jaćimovski,** *Institut za hemiju, tehnologiju i metalurgiju, Univerzitet u Beogradu, Srbija*
26. **Anandkumar Jayapal,** *National Institute of Technology Raipur, Raipur, India*
27. **Anita Klaus,** *Poljoprivredni fakultet, Univerzitet u Beogradu, Srbija*
28. **Tibela Landeka Dragičević***, Prehrambeno-biotehnološki fakultet, Sveučilište u Zagrebu, Hrvatska*
29. **Divna Majstorović,** *Tehnološko-metalurški fakultet, Univerzitet u Beogradu, Srbija*
30. **Panya Maneechakr,** *Faculty of Science, Rangsit University, Pathumthani, Thailand*
31. **Zoran Mandić,** *Fakultet hemijskog inženjerstva tehnologije, Sveučilište u Zagrebu, Hrvatska*
32. **Dragana Medić,** *Tehnički fakultet u Boru, Univerzitet u Beogradu, Bor, Srbija*
33. **Nikola Milašinović,** *Kriminalističko-policijski univerzitet, Beograd, Srbija*
34. **Dušan Mijin***, Tehnološko-metalurški fakultet, Univerzitet u Beogradu, Srbija*
35. **Jelena Miladinović,** *Tehnološko-metalurški fakultet, Univerzitet u Beogradu, Srbija*
36. **Ana Milivojević,** *Tehnološko-metalurški fakultet, Univerzitet u Beogradu, Srbija*
37. **Ana Munoz-Labrador***, Instituto de Investigación en Ciencias de la Alimentación CIAL (CSIC-UAM), Madrid, Spain*
38. **Vesna Nikolić,** *Inovacioni centar Tehnološko-metalurškog fakulteta, Univerzitet u Beogradu, Srbija*
39. **Bojana Obradović,** *Tehnološko-metalurški fakultet, Univerzitet u Beogradu, Srbija*
40. **Murat Özen,** *Bursa Technical University, Department of Chemistry, Bursa, Turkey*
41. **Vladimir Pavkov,** *Institut za nuklearne nauke Vinča, Univerzitet u Beogradu, Srbija*
42. **Milica Pavlicevic,** *Connecticut Agricultural Experiment Station, New Haven, Connecticut, USA*
43. **Jovana Perendija,** *Institut za hemiju, tehnologiju i metalurgiju, Univerzitet u Beogradu, Srbija*
44. **Aleksandra Perić-Grujić,** *Tehnološko-metalurški fakultet, Univerzitet u Beogradu, Srbija*
45. **Vesna Radojević,** *Tehnološko-metalurški fakultet, Univerzitet u Beogradu, Srbija*
46. **Teodora Retegan Vollmer,** *Chalmers University of Technology, Gothenburg, Sweden*
47. **Dunja Sokolović,** *Fakultet tehničkih nauka, Univerzitet u Novom Sadu Srbija*
48. **Ana Sutulović,** *Tekstilno-tehnološki fakultet, Univerzitet u Zagrebu, Zagreb, Hrvatska*
49. **Jelena Tomić,** *Naučni institut za prehrambene tehnologije, Univerzitet u Novom Sadu, Srbija*
50. **Đenđi Vaštag,** *Prirodno-matematički fakultet, Univerzitet u Novom Sadu, Srbija, redovi profesor*
51. **Đorđe Veljović,** *Tehnološko-metalurški fakultet, Univerzitet u Beogradu, Srbija*
52. **Milica J Vujković,** *Fakultet za fizičku hemiju, Univerzitet u Beogradu, Srbija*
53. **Milana Zarić,** *Institut za hemiju, tehnologiju i metalurgiju, Univerzitet u Beogradu, Srbija*
54. **Nikola Živković,** *Institut za nuklearne nauke Vinča, Univerzitet u Beogradu, Srbija*
55. **Wenlei Xie,** *Henan University of Technology, Zhengzhou, PR China*